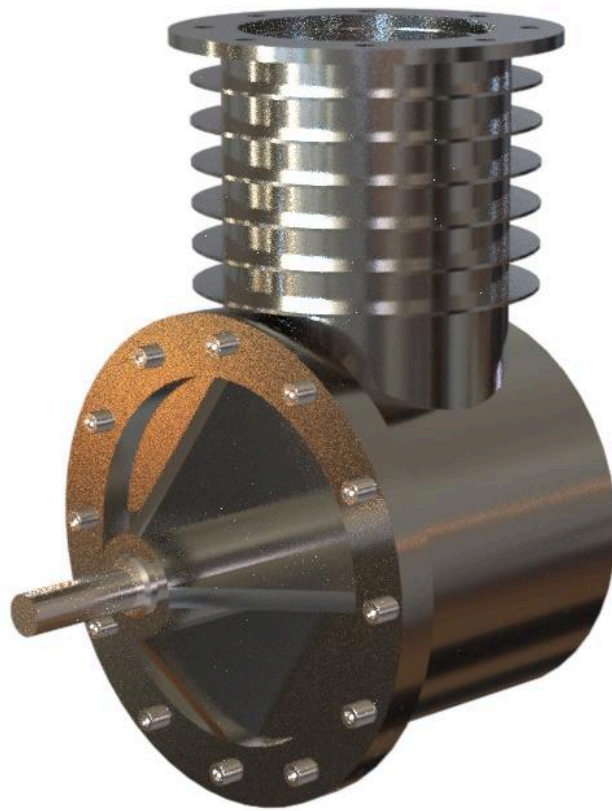


PROJECT FROM MECHANICAL TECHNOLOGY

FOUR-STROKE PETROL ENGINE

Giulia Rossi, Chiara Vestri



UNIVERSITÀ DI PISA

A.A. 2024/2025

C. d. L. in Industrial Design Engineering

TABLE OF CONTENTS

1. INTRODUCTION

- 1.1 Acknowledgements
- 1.2 Project Objectives
- 1.3 General Principles Adopted for the Assembly Design

2. GENERAL INFORMATION

- 2.1 Assembly Drawing
- 2.2 3D Rendering of the Components
- 2.3 Exploded View of the Assembly
- 2.4 Description of the Assembly
- 2.5 Operating Principle of the Four-Stroke Engine

3. ENGINE BLOCK – CASTING PROCESS

- 3.1 Description of the Component
- 3.2 Material Selection
- 3.3 Selection of the Manufacturing Process
 - 3.3.1 Selection of the Casting Technique
 - 3.3.2 Machining Allowances
 - 3.3.3 Hole Removal
 - 3.3.4 Selection of the Parting Plane
 - 3.3.5 Draft Angles
 - 3.3.6 Fillet Radii
 - 3.3.7 Pattern Oversizing (Shrinkage Allowance)
 - 3.3.8 Core Design
- 3.4 Solidification Analysis
 - 3.4.1 Solidification Modulus Calculation
 - 3.4.2 Solidification Simulation
 - 3.4.3 Riser Design
 - 3.4.3.1 Riser Sizing
 - 3.4.3.2 Riser Positioning
- 3.5 Gating System
 - 3.5.1 Total Mass and Pouring Time Calculation
 - 3.5.2 Choke Area Sizing
 - 3.5.3 Sprue Design
 - 3.5.4 Casting Simulation
 - 3.5.5 Time and Cost Analysis
- 3.6 Pattern Plates and Flasks

4. SHAFT – MACHINING PROCESS

- 4.1 Description of the Component
- 4.2 Material Selection
- 4.3 Choice of Manufacturing Process
- 4.4 Raw Material Selection
- 4.5 Machine Tool Selection

4.6 Cutting Tool Selection

4.7 Machining Cycle

4.8 Cutting Parameters

4.9 Time Analysis

4.10 Cost Analysis

5. PISTON – ADDITIVE MANUFACTURING

5.1 Description of the Component

5.2 Material Selection

5.3 Choice of Additive Manufacturing Process

5.4 Printer Selection

5.5 Printing Parameters

5.6 Slicing Settings

5.7 Printing Time and Cost Analysis

6. CONNECTING ROD – PLASTIC DEFORMATION

6.1 Description of the Component

6.2 Material Selection

6.3 Choice of Manufacturing Process

6.4 Forging Process Design

6.5 Die Design

6.6 Press Selection

6.7 Heat Treatment

6.8 Time and Cost Analysis

7. END CAP – WELDING PROCESS

7.1 Description of the Component

7.2 Selection of the Welding Process

7.3 Joint Design

7.4 Welding Procedure

7.5 Time and Cost Analysis

1. INTRODUCTION

1.1 Acknowledgements

The entire process of drafting the thesis was carried out with the invaluable collaboration of the students and professors of the ITI "Enrico Mattei" of Rosignano Solvay, who kindly made their technical expertise available to us, as well as their time for the practical construction of the mechanical components analyzed in the following sections.

We would like to thank the Professors in charge of the Mechanical Technology course of the C.d.L. in Industrial Design Engineering, for the various suggestions and advice provided during the preparation of this thesis.

Our most sincere and due thanks also go to Prof. Eng. Salvatore Armato, professor of mechanical and technological laboratory at the ITI Mattei in Rosignano Solvay, for his constant assistance during machine tool operations.

We also thank students Lorenzo Taffi and Lorenzo Domenici, who proved to be expert performers and collaborators throughout every phase of the piece's creation, sharing their experience and wisdom with us with absolute professionalism.

1.2 Purpose of the project

The aim of this project is to set up the production process of five components of an assembly of our choice. We will document this study is carried out through the following paper, assuming that this task was commissioned by a company.

We will then measure the dimensions of the individual components, previously separated from the assembly itself, to create a CAD model of each of them and of the final assembly, with attached technical drawings.

This constitutes the initial data to start the project, to which any requests will be added, such as the number of pieces to be produced, production times and costs.

The production processes to take into consideration are the following:

- fusion
- chip removal
- plastic deformation
- welding
- 3D stamp

As true designers, we will choose the most appropriate process based on specific parameters, such as production times and costs.

1.3 Principles adopted for the realization of the overall

As a whole we have chosen a **four-stroke petrol engine**, previously created in one of our exercises with the Solidworks software during the Geometric Modeling course.

During the Geometric Modeling course we were not provided with precise measurements of the various parts that made up the assembly.

Therefore, when creating the 3D model of the solid, since we did not have any previous information on the product or drawings with the respective dimensions, we decided to adapt all the measurements, both theoretical and technical, to the first piece that was produced in the workshop with the "Enrico Mattei" Industrial Technical Institute in Rosignano Solvay.

First, we redesigned each individual component using CAD, then created the final three-dimensional model in digital format.

We were able to satisfy the request to theoretically combine a process with each individual component.

Our ensemble has more than five pieces and we have not found ourselves forced to completely modify the starting composition, except for adapting some shapes in relation to the creation of the pieces in the workshop.

In this regard, since it would increase the complexity of construction and assembly operations, we decided with the Professor of the Higher Institute not to include in the project additional parts, present in reality, attached to the engine such as the flywheel, the spark plug, various sensors, injectors or intake/exhaust ducts, focusing only on the essential parts that we initially had.

In drafting the report, it was necessary to take into account some practical constraints arising from the need to produce the pieces with the machines and equipment available in the school workshop and in the areas of the "Enrico Mattei" ITI.

To measure the dimensions for choosing the rough piece and for the subsequent production of the finished piece, a twentieth vernier caliper was used.

As previously mentioned, the dimensions that we cannot measure have been estimated, deduced from other measurements, or hypothesized to be useful or credible (e.g. shaft-hub fits, dimensional tolerances, surface finishes), always within the limits of our expertise.

Structurally, the document is divided into five sections, each dedicated to the various processes required by the project. Below, we will see introductory paragraphs regarding the operation and description of each individual mechanical part and the overall system..

The number of pieces you set out to produce varies depending on the component.

2. GENERAL INFORMATION

2.1 Assembly drawing

The following assembly drawing has been produced to provide an overview of the assembly and to list the names, total quantities, and materials of its constituent elements.

Detailed dimensions will appear later in the drawings for each component.

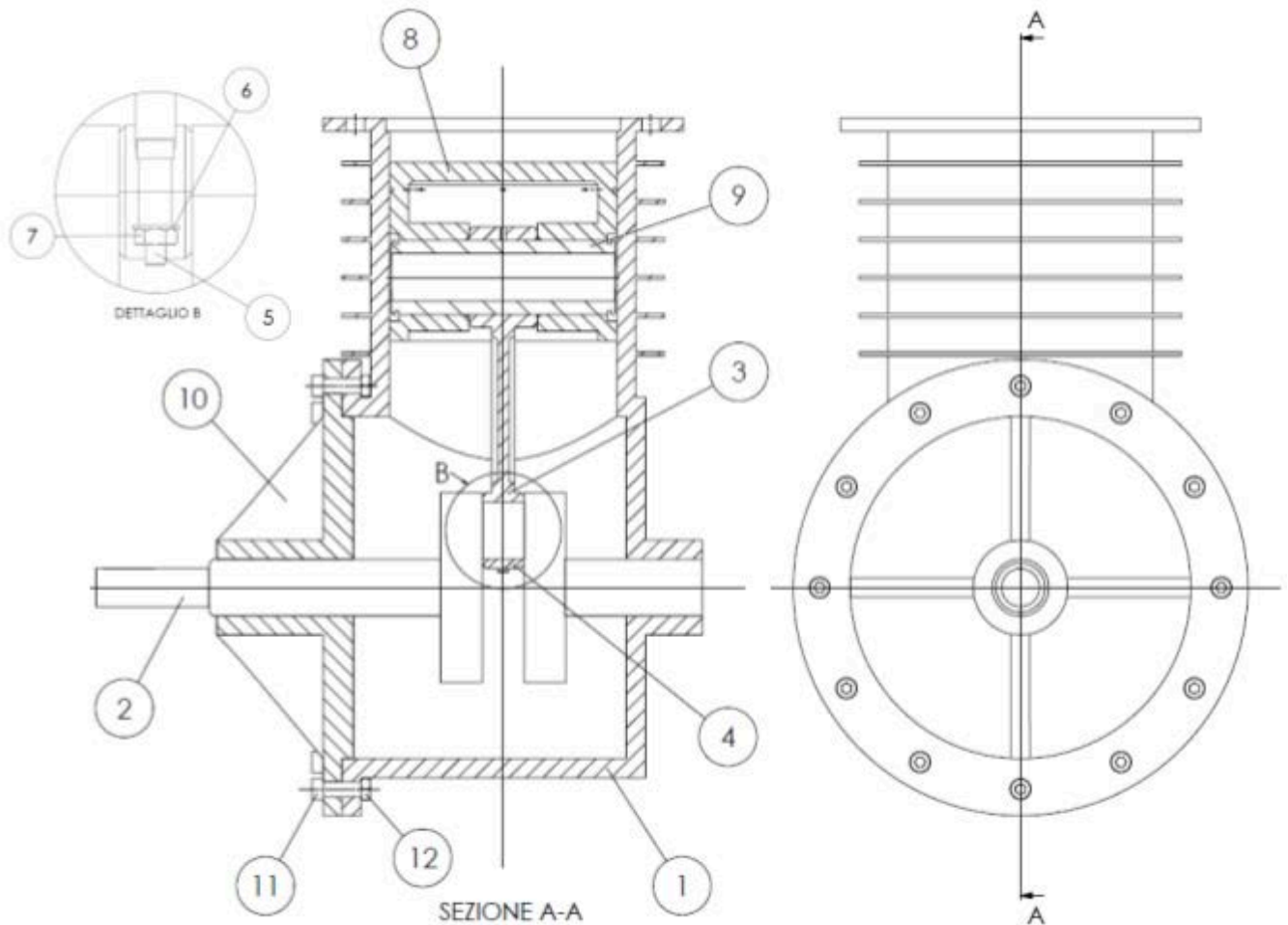
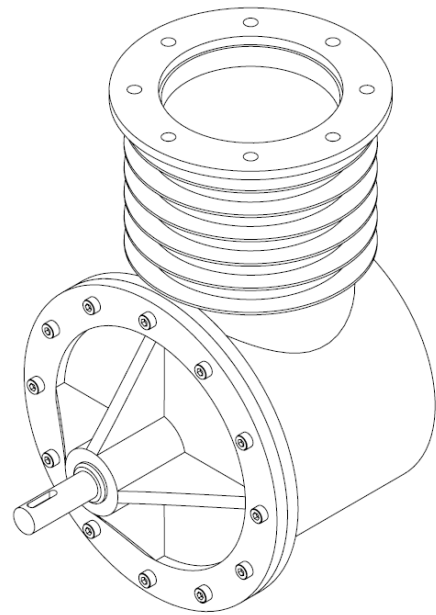
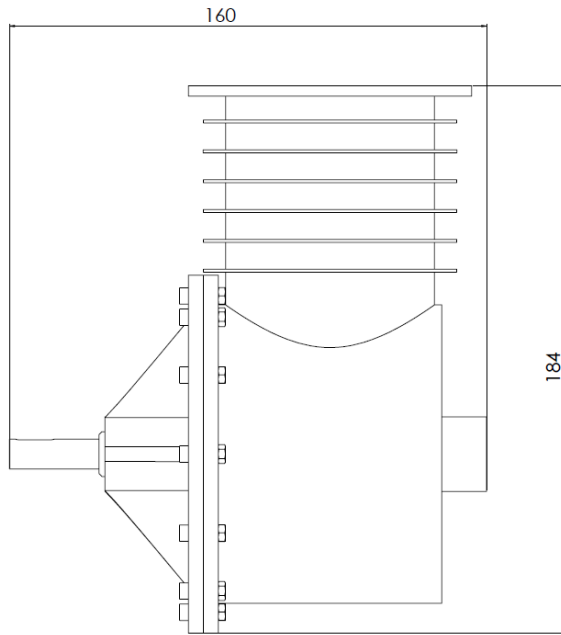


[Fig. 1] CAD drawing of the assembly.



No.	Name	Amount	Material
1	Engine block	1	Aluminum
2	Tree	1	Carbon alloy steel
3	Biella	1	Forged steel
4	Against Biella	1	Forged steel
5	ISO 4762 M3X16	2	Steel
6	ISO 7089 WASHER	2	Steel
7	ISO 4032 M3	2	Steel
8	Piston	1	Aluminum alloy
9	Pin	1	Hardened steel
10	Cork	1	Stainless steel
11	ISO 4762 M3X12	12	Steel
12	ISO 4032 M3	12	Steel

2.2 3D rendering of components

The following 3D renderings show the main components of the modeled assembly inSolidworks.



Component 1. Engine block



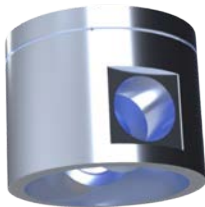
Component 2. Tree



Component 3. Biella



Component 4. Against Biella



Component 8. Piston



Component 9. Pin



Component 10. Cork

Components not listed: 5,6,7,11,12

2.3 Exploded view of the assembly

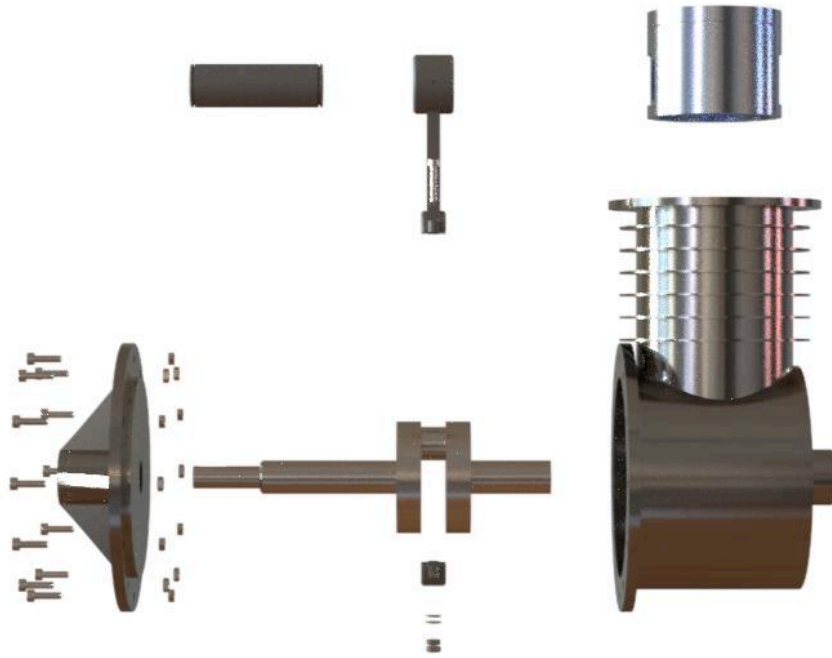


[Fig.2] Exploded view, side view.

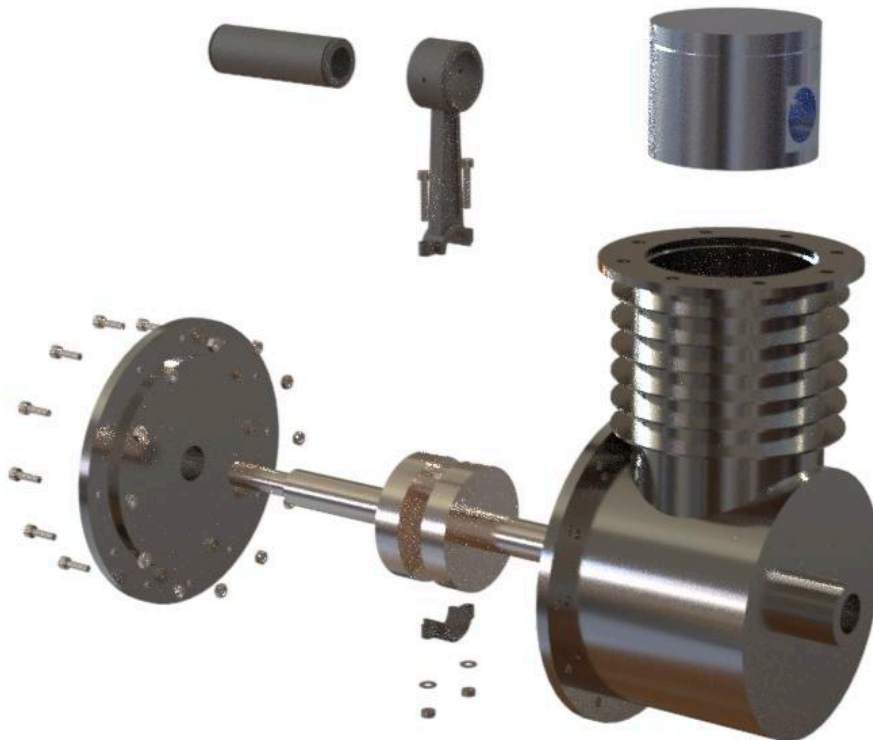


[Fig.3] Exploded view, perspective view.

2.4 Description of the assembly

The assembly under consideration is part of a four-stroke gasoline engine, also called an Otto cycle engine. It is a type of internal combustion engine used in private vehicles, such as cars, mopeds, motorcycles, racing cars, and some propeller-driven airplanes.

2.5 Purpose and operation

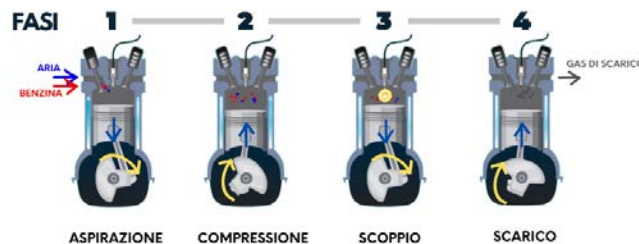
<https://www.tecnologiaduepuntozero.it/2017/01/15/motore-benzina/>



The four-stroke gasoline engine injects gasoline and mixes it with air to create an explosive gas. This gas enters a cylinder chamber, where it is compressed by a piston.

Next, a spark causes the gas to explode, pushing the piston backwards.

The kinetic energy of the piston, which moves in a rectilinear alternating motion, is converted into rotary motion of the crankshaft via the connecting rod and crank mechanism.



Spark-ignition internal combustion engines can be divided according to the way in which the operating cycle is carried out, that is, the sequence of phases that occur within them:

1. INTAKE: The piston descends, drawing the air-fuel mixture through the intake valve into the combustion chamber.
2. COMPRESSION: the piston rises, compressing the mixture inside the chamber.
3. OUTBREAK: A spark ignites the mixture, causing an explosion that causes the combustion gases to expand, pushing the piston downward.
4. EXHAUST: As the piston rises, it expels the burnt gases from the engine through the exhaust valve.

In 4-stroke engines, one combustion cycle is equivalent to two revolutions of the crankshaft.

3. INTRODUCTION OF THE COMPONENT: ENGINE BLOCK (N.1)

3.1 Description of the piece

The component examined is the engine block, the main element of the assembly, having the function of containing and supporting the internal mechanical parts, such as the piston, connecting rod, connecting rod, crankshaft and pin.

The engine block consists primarily of a hollow cylindrical body, which represents the component's load-bearing structure and houses the piston and moving parts. The upper section features overlapping cooling fins, which increase the heat exchange surface area and facilitate the dissipation of heat generated during operation.

The upper flange features eight equally spaced holes for attachment to any upper engine components. The front flange features twelve equally spaced holes for connection to the end cap. The main side hole allows for the passage and correct positioning of the crankshaft, enabling connection to the connecting rod and crankshaft system.

From a production standpoint, the presence of internal cavities, walls of different thicknesses, functional surfaces and small diameter holes requires careful design of the casting blank, with the addition of oversizes, draft angles, fillets and cores.

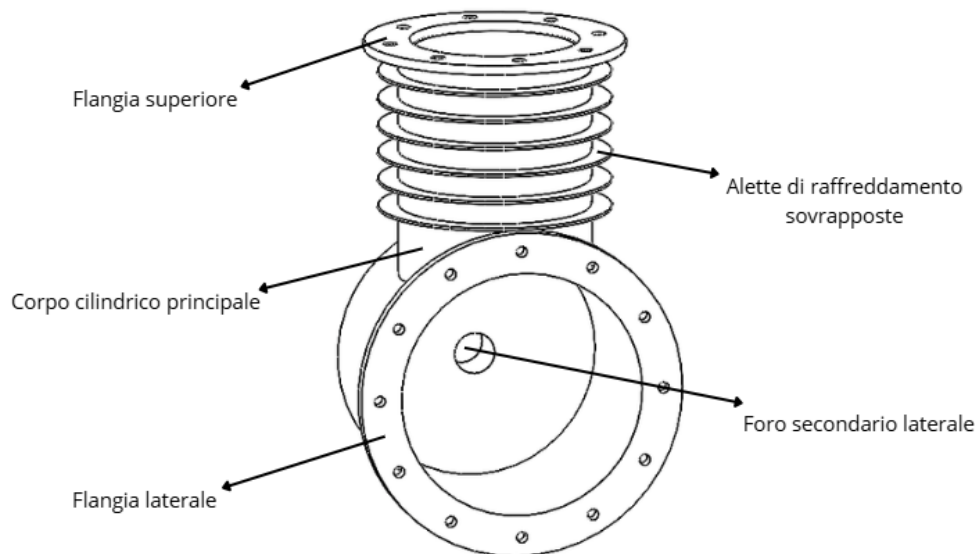


[Fig.4] Illustration of engine block parts.

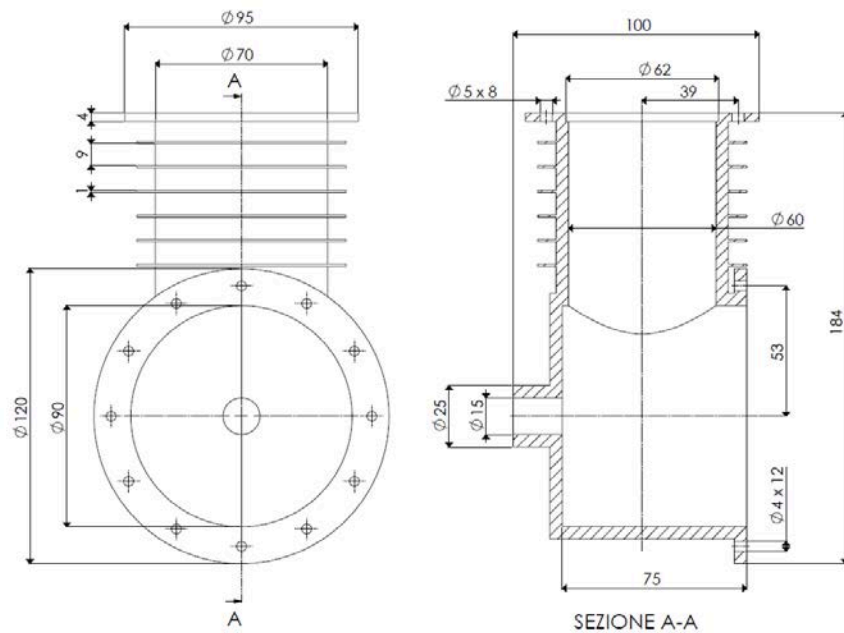


[Fig.5] CAD drawing of the engine block.

3.2 Choice of material

For the construction of the engine block, a foundry aluminum alloy was chosen, in particular the alloy **EN AC-AISi7Mg0.3**, also identified with the designation **42100**. This alloy is widely used for cast mechanical components, especially when good castability, lightness, mechanical strength, and heat dissipation capabilities are required.

The aluminum in question was chosen for its low weight, excellent thermal conductivity, good corrosion resistance, and high workability, making it ideal for small engines.

Physical properties:

- **Density:** 2.66 kg/dm³
- **Electrical conductivity:** 19 - 25 MS/m
- **Thermal conductivity:** 150 - 170 W/(m · K)
- **Elastic modulus:** 74 GPa
- **Coefficient of thermal expansion:** $22 \cdot 10^{-6} \text{ K}^{-1}$ (between 20°C and 100°C)
- **Specific heat (at 100°C):** 0.92 J/(kg · K)

Mechanical properties:

- **Tensile strength (at room temperature):** generally good.
- **Tensile strength (at 200°C):** acceptable.
- **Ductility:** excellent.
- **Fatigue resistance:** (between 80 and 110 N/mm².)

Famiglia: Al Si 7 Mg Denominazione EN : EN AB 42100 - Al Si 7 Mg 0,3 Denominazione UNI: Assente												
Rev. 0 del 01/09/02												
COMPOSIZIONE CHIMICA %												
LEGA	ELEMENTI											
	Cu	Mg	Si	Fe	Mn	Ni	Zn	Pb	Sn	Ti	Impurezze singole	Impurezze globali
EN AB 42100	min		0,30	6,5							0,10	
	max	0,03	0,45	7,5	0,15	0,10	0,03	0,07	0,03	0,03	0,18	0,10
Denominazione Assente UNI	min											
	max											
CARATTERISTICHE MECCANICHE												
Stato Fisico Colata	stato metallurgico	R		S		A	HB					
		Carico unitario di rottura Kg/mm2	N/mm2	Carico al limite snervamento Kg/mm2	N/mm2	Allungamento %	Durezza Brinell					
IN SABBIA (Grezzo) Parzialmente Invec.	F		140-220		80-140	2-6	45-60					
	T64		200-270		120-170	4-10	60-80					
	T6		240-320		220-280	3-6	80-110					
IN CONCHIGLIA Parzialmente invecchiato.	F		180-240		90-150	4-8	50-65					
	T64		220-270		120-180	6-12	65-85					
	T6		250-340		220-280	5-9	80-100					
SOTTOPRESSIONE (Grezzo)												
CARATTERISTICHE ED IMPIEGHI TIPICI												
Lega con ottime caratteristiche meccaniche; trova applicazione nelle costruzioni meccaniche, nell'industria dei trasporti ed aeronautica, costruzioni navali ecc.												
CARATTERISTICHE TECNOLOGICHE												
RESISTENZA MECCANICA A CALDO	SCARSA		FRAGILITA' DI RITIRO				PICCOLA					
RESISTENZA GENERALE ALLA CORROSIONE	BUONA		TENUTA A PRESSIONE				BUONA					
LAVORABILITA' ALL' UTENSILE	BUONA		SALDABILITA' (1)				OTTIMA					
COLABILITA'	BUONA		ATTITUDINE ALL'ANODIZZAZIONE DECORATIVA (2)				CATTIVA					
LUCIDABILITA'	MEDIA		ATTITUDINE ALL'ANODIZZAZIONE PROTETTIVA (2)				CATTIVA					
PROPRIETA' FISICHE												
PESO SPECIFICO	2,66 Kg/dm ³		CONDUTTIVITA' TERMICA a 20°C (4)				1,4 - 1,7 W/cmK					
INTERVALLO DI SOLIDIFICAZIONE E DI FUSIONE (3)	550 - 625 °C		DILATAZIONE TERMICA da 20 a 100°C									
CALORE SPECIFICO(a100)°	0,92 J/gK		DILATAZIONE TERMICA da 20 a 200°C				22,0x10-6/°C					
RITIRO LINEARE IN SABBIA	1,1-1,2 %		DILATAZIONE TERMICA da 20 a 300°C									
RITIRO LINEARE IN CONCHIGLIA	0,8-1,1 %		TEMPERATURA MASSIMA DI FUSIONE				780 °C					
RITIRO LINEARE IN PRESSOCOLATA			INTERVALLO OTTIMO DI COLATA									
CONDUTTIVITA' ELETTRICA(4)	21-27 M/O mm ²		- in sabbia				680-750 °C					
MODULO ELASTICO (4)	7400 m/mm ²		- in conchiglia				680-750 °C					
			- sottopressione									
COMPARAZIONE CON NORMATIVE ESTERE EQUIVALENTI O SIMILARI												
	ITALIA	GERMANIA (Din1725/5-86)	FRANCIA (NFA57-105)	G.B.R. (BS1490-88)	USA (ASTM B179-82)	ISO (3522-84)	GIAPPONE (JIS H2211-92)	SPAGNA (UNE38200)				
Equivalenti	UNI 8024	GALSI 7 MG	AS 7 G03	LM 25	A 356.2	Al Si 7 Mg	C 4 CV					
Similari												
TRATTAMENTI TERMICI												
Tempra in acqua 520-530 °C dopo preriscaldamento 4-10 ore a regime Invecchiamento artificiale completo a 155-165 °C per 6-8 ore. Invecchiamento parziale a 150-160 °C per 2-3 ore												

(List of family properties AISi7Mg0.3)

3.3 Choice of processing technique

The manufacturing technique chosen for the construction of the engine block is the **fusion**. This process is particularly suitable for the production of components with complex geometries, internal cavities and surfaces that are not easily obtainable through solid machining.

In the case of the engine block, casting allows the main body of the component to be obtained in a single casting, reducing the amount of material subsequently removed and limiting the number of mechanical operations required. The chosen aluminum alloy, EN AC-ALSi7Mg0.3, also has good castability and is suitable for producing castings with relatively thin walls and complex shapes.

Subsequent mechanical processing will still be necessary in functional areas, such as mating flanges, cylindrical seats and threaded holes, in order to ensure adequate dimensional accuracy and surface quality.

3.3.1 Choice of casting technique

Before proceeding with the design of the blank, it is necessary to identify the most suitable casting technique, since many subsequent decisions depend on this choice, such as the definition of the allowances, the choice of the parting plane, the design of the cores, the feeding system and the casting system.

The choice is made considering the component as part of a **small/medium series production**, not just as a single piece. This makes it possible to justify the use of a more precise and repeatable process than simple manual sand molding.

The main aspects evaluated are the following:

1) Geometric complexity of the piece

The engine block has a complex geometry, characterized by internal cavities, cylindrical surfaces, flanges, cooling fins, and areas with varying thicknesses. To achieve these shapes, it would be inconvenient to start from a solid and proceed solely by chip removal, as this would result in significant material waste and a large number of machining operations.

Casting is therefore the most suitable process, as it allows for the direct production of a rough shape that closely matches the final geometry of the component. Furthermore, thanks to the use of cores, it is possible to create the internal cavities and main seats of the engine block.

Permanent mold techniques, such as shell casting, are less suitable in this case, because they require expensive metal molds and are more convenient for high production runs and less complex geometries.

2) Chosen material

The component is made of foundry aluminum alloy **EN AC-AISI7Mg0.3**, a material suitable for the production of castings thanks to its good castability, lightness and ability to dissipate heat.

The chosen alloy allows for components with good mechanical strength and low mass, important characteristics for a small engine block. Furthermore, aluminum lends itself well to subsequent mechanical processing, necessary for finishing functional surfaces, such as flanges, cylindrical seats, and threaded holes.

3) Production volume and cost of equipment

The choice of process must also take into account the number of pieces to be produced. For a single-piece production, traditional sand molding would be more economical, while for very high production runs, the use of permanent molds might be justified.

In our case, we're considering small/medium series production. For this reason, it's essential to choose a technique that guarantees good casting quality, repeatability, and dimensional accuracy, without incurring the high costs typical of permanent metal molds.

4) Comparison of the main techniques in transient form

Among the transient processes, several solutions can be considered:

Technique	Advantages	Limits
Synthetic earth moulding	Economical, simple and suitable for pieces of different sizes.	Limited dimensional accuracy and surface finish.
Graduation at CO₂	Quick and fairly inexpensive process.	Decent surface quality and less precision than shell-molding.
Cold-box graduation	Very suitable for the production of precise and resistant cores.	More suitable for cores than for the entire external mold.
Shell-molding	Good dimensional accuracy, excellent surface finish and good repeatability.	Higher cost than traditional sand molding.
Lost-foam/Policast process	Allows for complex shapes and reduces some mold divisions.	More complex loss models and process control.

5) Final choice

After evaluating the various possibilities, the most suitable technique for the construction of the engine block appears to be the **formatura in shell-molding**, also called *shell forming*.

This technique represents a good compromise between quality, precision, and cost. Compared to traditional sand casting, it achieves a better surface finish and greater dimensional accuracy. Furthermore, it guarantees good repeatability, a useful feature for small to medium-sized production runs.

Shell molding is therefore suitable for the component in question because it allows for the creation of a complex casting in aluminum alloy, maintaining good surface quality and reducing the amount of subsequent mechanical processing.

3.3.2 Definition of overmetals

When designing the casting rough part, it is necessary to provide for machining allowances, i.e. additional thicknesses of material applied to the surfaces that will subsequently need to be finished through mechanical machining.

Dimensioni nominali (mm)	Sovrametalli di lavorazione (mm)	Tolleranze (mm)
≤ 50	0,5 + 1	± 0,1 + 0,25
50 + 175	0,5 + 1	± 0,16 + 0,42
175 + 300	1 + 2	± 0,29 + 0,67
300 + 450	1,3 + 2,5	± 0,71 + 0,83

Indicative average values of machining allowances and tolerances achievable on aluminium alloy castings using the Shell-molding process.

In the case of the engine block, allowances are essential because the casting process, while ensuring good reproduction of the geometry, does not directly achieve the dimensional tolerances and surface quality required in the functional areas. The mating surfaces, cylindrical seats, and mounting holes must therefore be machined after the casting has solidified.

Overmetals are mainly applied in the following areas:

Component area	Reason for adding the oversize	Planned subsequent processing
UPPER FLANGE	Mating surface with other components.	Face milling/milling
INTERNAL CYLINDRICAL SEAT	Requires geometric precision and good finishing.	Boring
FRONT FLANGE	Coupling with the closing cap.	Face milling/milling
SIDE HOLE FOR SHAFT	Need for correct positioning of the tree.	Drilling/reaming
THREADED HOLE AREAS	Small holes are removed from the blank.	Subsequent drilling and tapping

For the component under examination, being made of aluminium alloy and using a shell-molding process, an indicative over-metal can be assumed equal to approximately **1,5 mm** on surfaces intended for mechanical processing. This value allows for compensation for any surface irregularities in the casting and ensures sufficient material to achieve the final dimensions specified in the technical drawing.

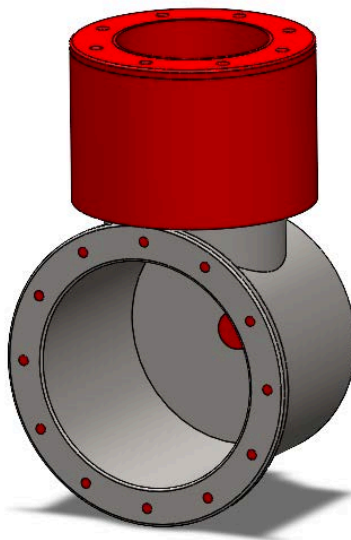
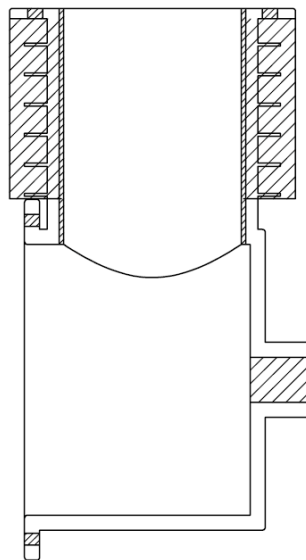
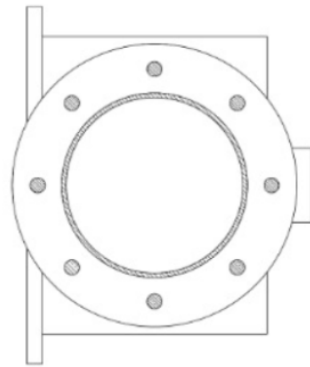


[Fig.6] 3D image with the addition of the overmetals highlighted in red.



SEZIONE A-A

[Fig.7] CAD drawing of the rough casting.

3.3.3 Hole Removal

In the model intended for casting, small diameter holes are eliminated, in particular *the twelve holes on the front flange* ($\varnothing 4$ mm) and *the eight holes on the upper flange* ($\varnothing 5$ mm).

This choice is necessary because directly producing small holes through casting would require the use of thin cores, which are difficult to position and subject to breakage during the forming phase or during the pouring of the liquid metal. Furthermore, the dimensional precision achievable through casting would not be sufficient for holes intended for mechanical couplings or subsequent threading.

For these reasons, the holes are removed from the casting model and subsequently created using mechanical processes, particularly drilling and, where necessary, tapping. This ensures greater precision, improved surface quality, and correct positioning of the fasteners.

3.3.4 Selecting the dividing surface

The choice of the parting surface is a fundamental phase in the design of the mould, since it influences the simplicity of opening of the shape, the demouldability of the model, the position of the burrs and the arrangement of the cores.

Several possible dividing planes were evaluated for the engine block: a horizontal plane, a frontal plane, and a vertical plane passing through the component's longitudinal axis. Among these, the main vertical plane proved to be the most suitable, as it divides the block into two half-shells that are as symmetrical as possible.

This solution simplifies the mold geometry, avoiding the use of movable inserts or overly complex divisions. Furthermore, it allows for better model extraction and concentrates the casting flash along an easily accessible centerline that can be removed through subsequent deburring.

The choice of the vertical plane is also advantageous for the arrangement of the cores, as it allows them to be positioned more stably within the mould and to better control the internal cavities of the component.

The chosen dividing surface is therefore the principal vertical plane indicated in the figure[Fig. 8].

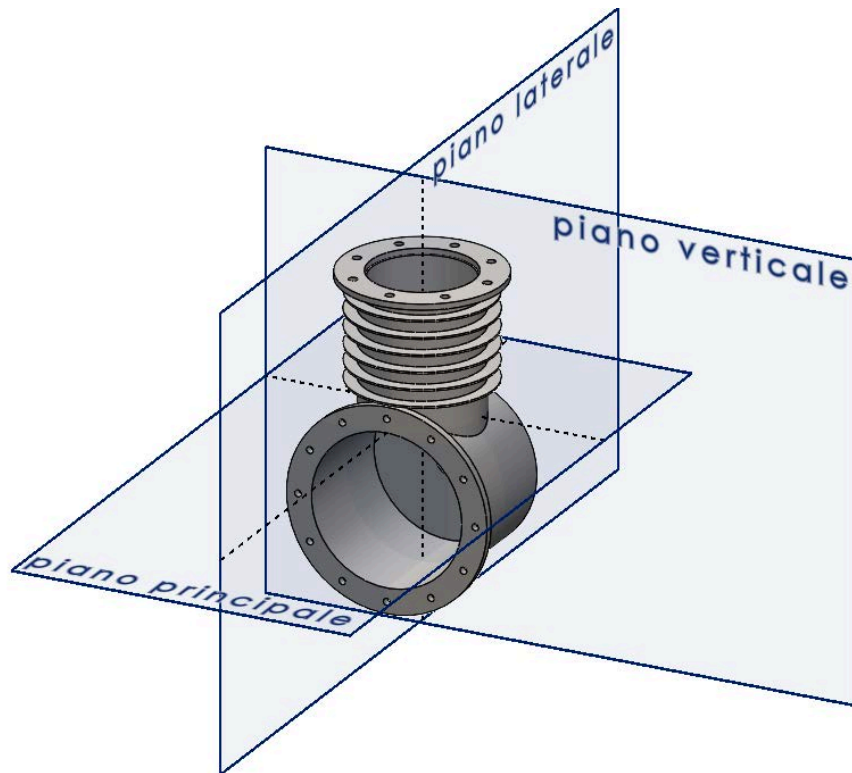
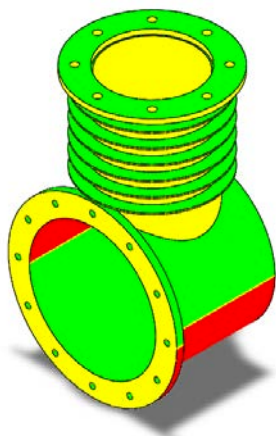


[Fig.8] Subdivision of the engine block with division planes.

The choice therefore falls on the main plan that can be seen in [Fig.8].

3.3.5 Draft angles



Draft angles are introduced on the model surfaces parallel to the extraction direction, so as to facilitate the detachment of the model from the mold without damaging the sand or altering the casting geometry.

In the case of the engine block, draft angles should be applied mainly to the vertical external surfaces, flange walls, external cylindrical surfaces and areas affected by oversizes.

Functional surfaces that will be subsequently machined can tolerate this modification, as they will be brought back to their final dimensions through mechanical processing.

VALORI DELLO SFORMO s in mm e in %
dell' ANGOLO di SFORMO β

ALTEZZA del MODELLO (mm)	SFORMO		Angolo di sformo β
	s (mm)	(%)	
fino a 40	0.5	1.25	1'30"
40 - 59	0.75	1.8 - 1.2	1'
60 - 119	1	1.7 - 0.8	40"
120 - 159	1.5	1.7 - 0.8	40"
160 - 199	1.75	1.1 - 0.9	40"
200 - 249	2	1.0 - 0.8	30"
250 - 299	2.5	1.0 - 0.8	30"
300 - 399	3	1.0 - 0.75	30"
400 - 499	3.5	0.9 - 0.8	30"
>= 500	4	<= 0.8	30"

Considering the overall height of the engine block, equal to approximately 184 mm , from the table of recommended values, a draft angle equal to $40''$.

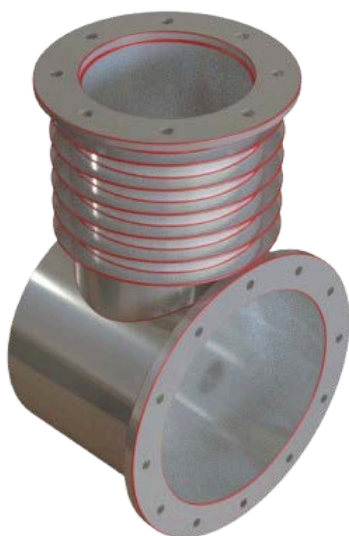
This tilt is applied along the direction of model extraction, causing the geometry to widen progressively moving away from the direction of parade.

This modification does not alter the functionality of the component, as it affects rough surfaces or surfaces intended for subsequent processing. On the contrary, it is necessary to ensure proper shaping and reduce the risk of breakage or sand entrainment during model extraction.

3.3.6 Fillet radius

When designing the casting blank, it's essential to eliminate, wherever possible, sharp edges on the model by introducing appropriate fillet radii. Sharp edges can hinder proper mold filling, promote stress concentrations, and cause sand erosion during the flow of the molten metal.

The fittings are mainly applied in the transition areas between the cylindrical body and the flanges, in correspondence with the surfaces with excess metal, along the edges of the internal cavities and in the areas affected by the presence of the cores.



For the **small edges** indicative connections are adopted equal to $0,5\text{ mm}$, while in the **most critical areas** and **most stressed** from the metal flow, upper connections can be foreseen, equal to approximately $1-2\text{ mm}$. This choice allows for improved cavity filling, reduced risk of surface defects, and increased casting strength.

The introduced fittings do not change the function of the component, but allow the original geometry to be adapted to the needs of the casting process.

3.3.7 Oversizing of the casting blank

During cooling and solidification, the metal undergoes dimensional shrinkage, resulting in a reduction in the final dimensions of the casting compared to those of the mold cavity. To compensate for this phenomenon, the model must be appropriately oversized.

In the case of the engine block, made of EN AC-ALSi7Mg0.3 aluminium alloy, an average linear shrinkage coefficient γ is assumed equal to:

$$\gamma = 1.2\%$$

The scale factor to be applied to the model is calculated using the relationship:

$$1 : (1 - \gamma) = s : 1$$

$$s = \frac{1}{1 - \gamma} = \frac{1}{1 - 0,012} = 1,012$$

The casting model is then scaled by a factor of 1.012, in order to compensate for the linear shrinkage of the material and obtain, after cooling, dimensions as close as possible to the nominal ones of the finished component.

This oversize is applied to the casting stock along with machining allowances, draft angles and fillet radii.

3.3.8 Forming and designing of cores

The presence of internal cavities in the engine block makes it necessary to use cores, i.e. sand elements positioned inside the mold before casting, with the aim of generating the internal voids of the casting.

The outer mold is made using the shell molding process, while the cores are made using the cold box process. This choice is motivated by the fact that the cold box process allows for cores with good dimensional accuracy, high strength during the casting phase, and good collapsibility during the subsequent stripping phase.

In the case of the component under consideration, the cores must allow for the creation of the main internal cavity, the piston housing area, and the lateral passage for the crankshaft. To simplify the process and avoid an excessive number of separate elements, a macro-core composed of two main elements was chosen.

The first element creates the main internal cavity of the engine block and is supported in the mold by appropriate core supports. The second element, predominantly cylindrical in shape, creates the lateral passage for the crankshaft and is secured to both the first core and the external form, ensuring correct positioning during mold closing and casting.

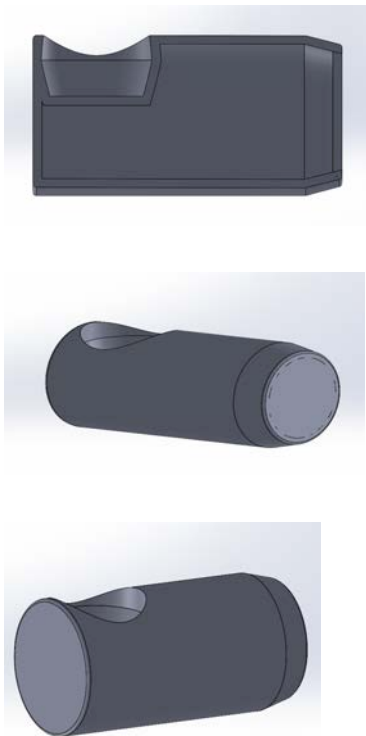
The two core elements can be joined using a male-female geometry, possibly integrated with a refractory adhesive specifically designed for foundries. This solution provides a sufficiently

rigid system during the casting of the liquid metal, limiting the risk of misalignment, metal infiltration, and internal burr formation.

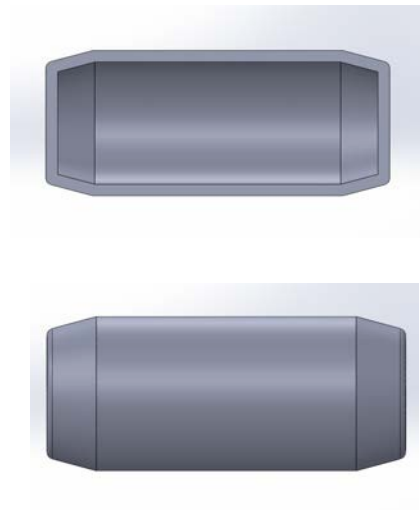
After the casting has solidified, the cores must be removable by de-coring. For this reason, it is important that the core material exhibits good collapsibility, so that it can break and escape from the component openings without damaging the internal surfaces of the engine block.

The expected sequence is therefore: creation of the two cores, assembly of the macro-core, positioning in the mold using the core holders, closing of the two half-shells of the mold, casting of the metal and subsequent removal of the core after the casting has cooled.

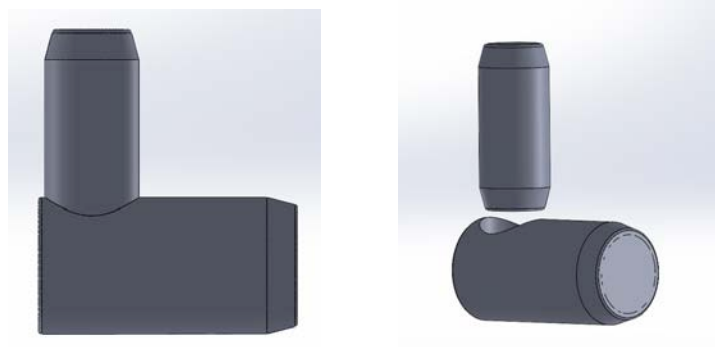
Soul number 1



Soul number 2



Final soul



3.4 Theoretical study of the aspects of solidification

After defining the geometry of the casting blank and the modifications needed to adapt the component to the production process, it is necessary to analyze the behavior of the metal during solidification.

This phase plays a fundamental role in the design of a casting, as it allows us to identify the areas that solidify last and are therefore most subject to the formation of shrinkage defects, such as internal cavities and porosity.

During cooling, the liquid metal undergoes volumetric contraction. If this contraction is not compensated for by an adequate power supply system, the component may develop internal defects that compromise its mechanical strength and final quality.

To predict the solidification behavior, both theoretical methods, based on the calculation of the solidification modulus, and numerical simulation tools are used, which allow verification of the solidification path of the casting and the correct design of the feeding system.

3.4.1 Calculation of the solidification modulus

In order to predict the solidification trend inside the mould and identify the areas most subject to the formation of shrinkage cavities, the solidification modulus criterion is applied with the *Chvorinov's rule*.

The solidification modulus is defined as the ratio between the volume of the portion considered and the effective surface through which the heat exchange with the mold occurs:

$$M = \frac{V}{S_{eff}}$$

Where:

- M is the solidification modulus [mm]
- V is the volume of the area considered [mm³]
- S_{eff} is the effective heat exchange surface [mm²]

The higher the modulus, the longer it will take for that area to solidify. Consequently, areas with higher modulus will tend to solidify last and must be fed correctly using sprues.

Since the engine block has a complex geometry, the component is simplified by dividing it into **three main areas**, each assimilated to an elementary geometry. For each zone, the volume, the effective heat exchange surface area, and the corresponding solidification modulus are manually calculated.

The areas considered are:

1. cylinder barrel;
2. cylinder choke;
3. crankcase/crankcase.

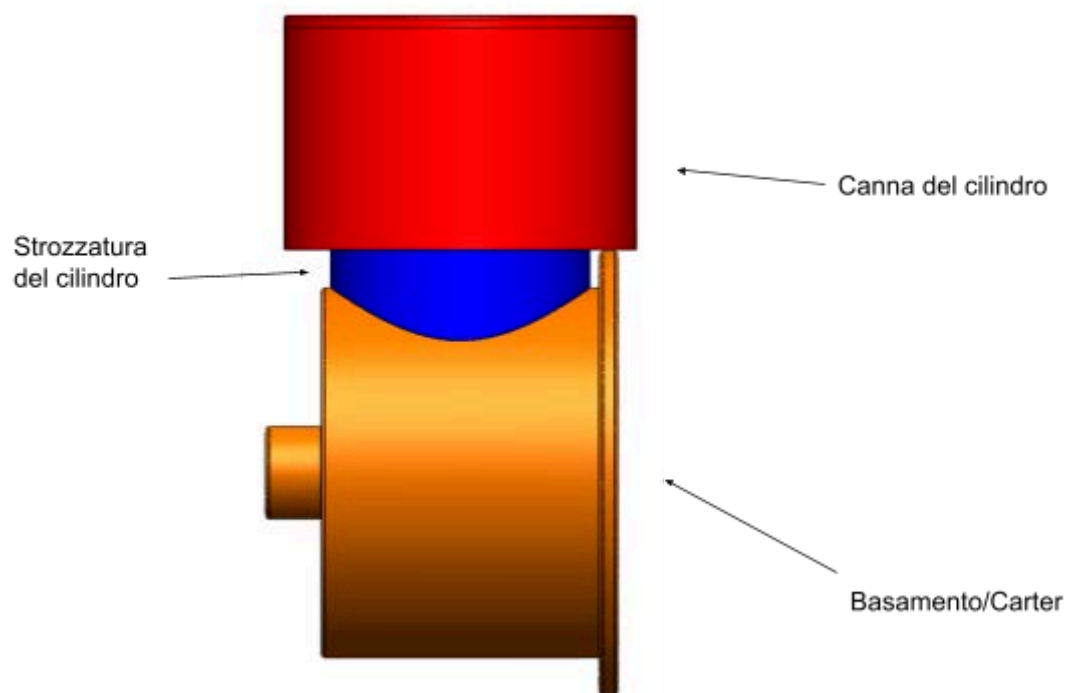


[Fig. 9] Division of areas.

- **Zone 1: Cylinder barrel**

$$V_1 = \frac{\pi}{4} (D_{half}^2 - d_{int}^2) \times h_1 = 131.253,8 \text{ mm}^3$$

$$S_{eff} = S_{external} + S_{internal} - S_{contacts} =$$

$$S_{eff} = (\pi \times D_{half} \times h_1) + (\pi \times d_{internal} \times h_1) = 38.754,64 \text{ mm}^2$$

$$M_1 = \frac{V_1}{S_{eff_1}} = \frac{131.253,8 \text{ mm}^3}{38.754,64 \text{ mm}^2} = 3,39 \text{ mm}$$

- **Zone 2: Cylinder choke**

$$V_2 = \frac{\pi}{4} (D_{half}^2 - d_{int}^2) \times h_2 = 35.735,75 \text{ mm}^3$$

$$S_{eff_2} = S_{external} + S_{internal} - S_{contacts} =$$

$$S_{eff_2} = (\pi \times D_{half} \times h_2) + (\pi \times d_{internal} \times h_2) = 14.294,25 \text{ mm}^2$$

$$M_2 = \frac{V_2}{S_{eff_2}} = \frac{35.735,75 \text{ mm}^3}{14.294,25 \text{ mm}^2} = 2,50 \text{ mm}$$

- **Zone 3: Crankcase/Crankcase**

$$V_3 = 158.552,26 \text{ mm}^3$$

$$S_{eff_3} = S_{tot3} - S_{contact} = 57.365,43 \text{ mm}^2$$

$$M_3 = \frac{V_3}{S_{eff_3}} = 2,76 \text{ mm}$$

The values obtained are reported in the following table:

Area	Description	Volume [mm ³]	Effective area [mm ²]	Module [mm]
1	Cylinder barrel	131.253,8	38.754,64	3,39
2	Cylinder choke	35.735,75	14.294,25	2,50
3	Crankcase/crankcase	158.552,26	57.365,43	2,76

From the analysis of the results it can be observed that the area with the highest solidification modulus is the cylinder barrel, with:

$$M_1 = 3,39 \text{ mm}$$

This area will therefore tend to solidify more slowly than the others and represents the main thermal node of the casting.

The crankcase/crankcase instead has a module equal to:

$$M_3 = 2,76 \text{ mm}$$

Although not the maximum value, this area must still be carefully considered because it has a large volume and is separated from the upper part of the block by the cylinder constriction, which is characterized by a lower module:

$$M_2 = 2,50 \text{ mm}$$

So Zone 1, It is configured as the main thermal node of the component, the region that will tend to solidify more slowly than the others.

The liquid metal present in this zone will therefore be the last to complete the transition from the liquid to the solid state. Consequently, the cylinder liner represents a critical zone from the point of view of the formation of shrinkage cavities.

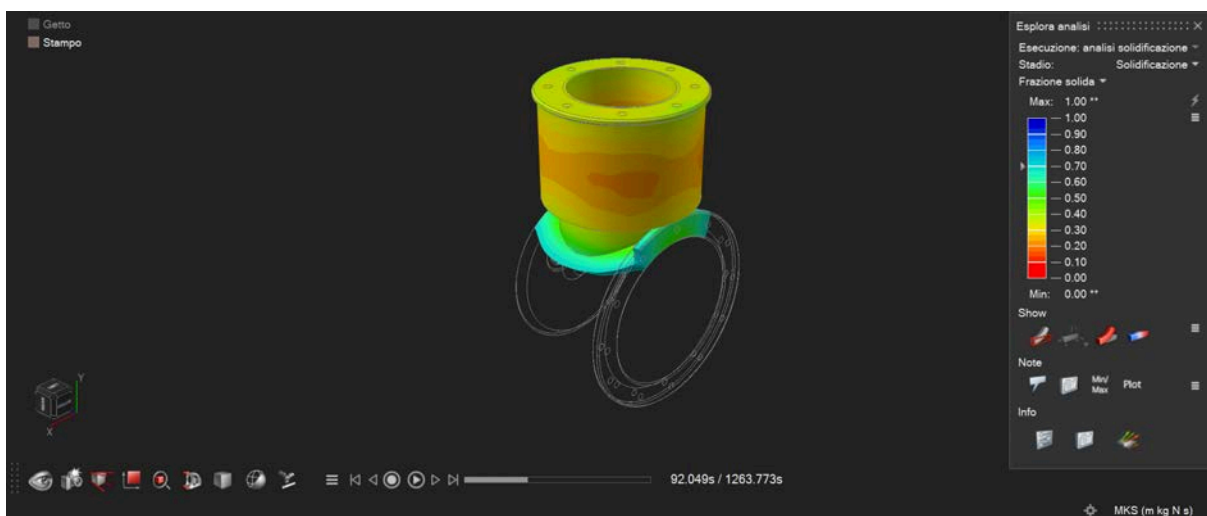
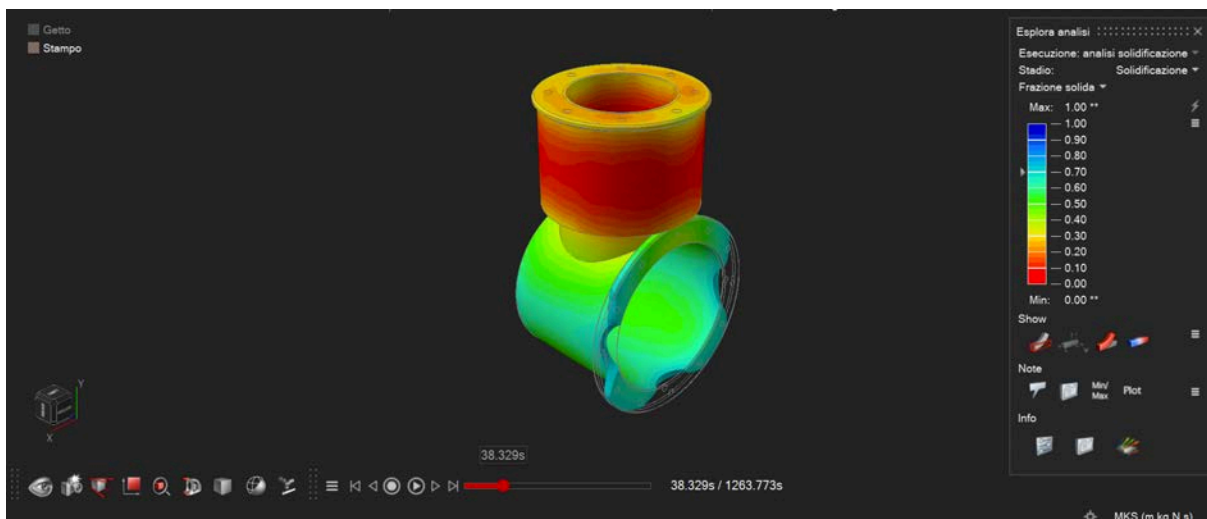
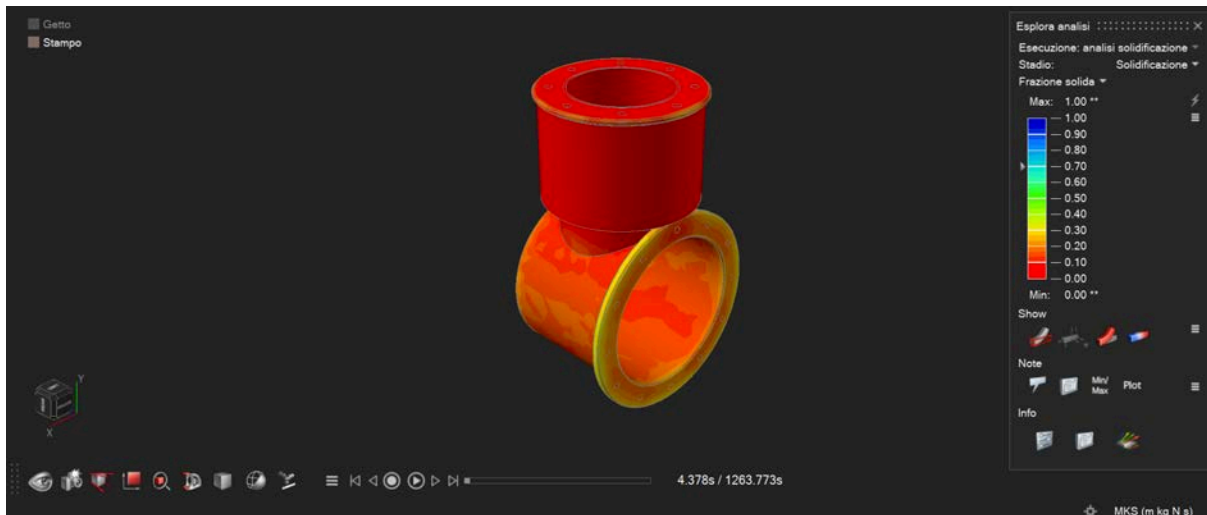
To prevent the volumetric contraction of the material during cooling from causing internal defects in the casting, a suitable feeding system must be provided. Specifically, the sprue must be positioned near the area identified as the main thermal node, so as to act as a reservoir for molten metal and compensate for shrinkage during solidification.

However, the crankcase/crankcase cannot be neglected, as it has a large volume and is separated from the upper part by the cylinder constriction, which has a lower modulus. This constriction will tend to solidify first and could interrupt the liquid connection between the upper and lower parts of the casting. For this reason, when designing the sprues, it will be necessary to consider not only the cylinder liner, but also the crankcase/crankcase area.

Manual modulus calculation therefore allows for preliminary identification of critical areas of the casting. These results must then be verified using software simulation to monitor the actual solidification progression and the location of any shrinkage porosity.

3.4.2 Solidification simulation using software

We used Altair Inspire Cast software to verify the accuracy in identifying the final solidification points.



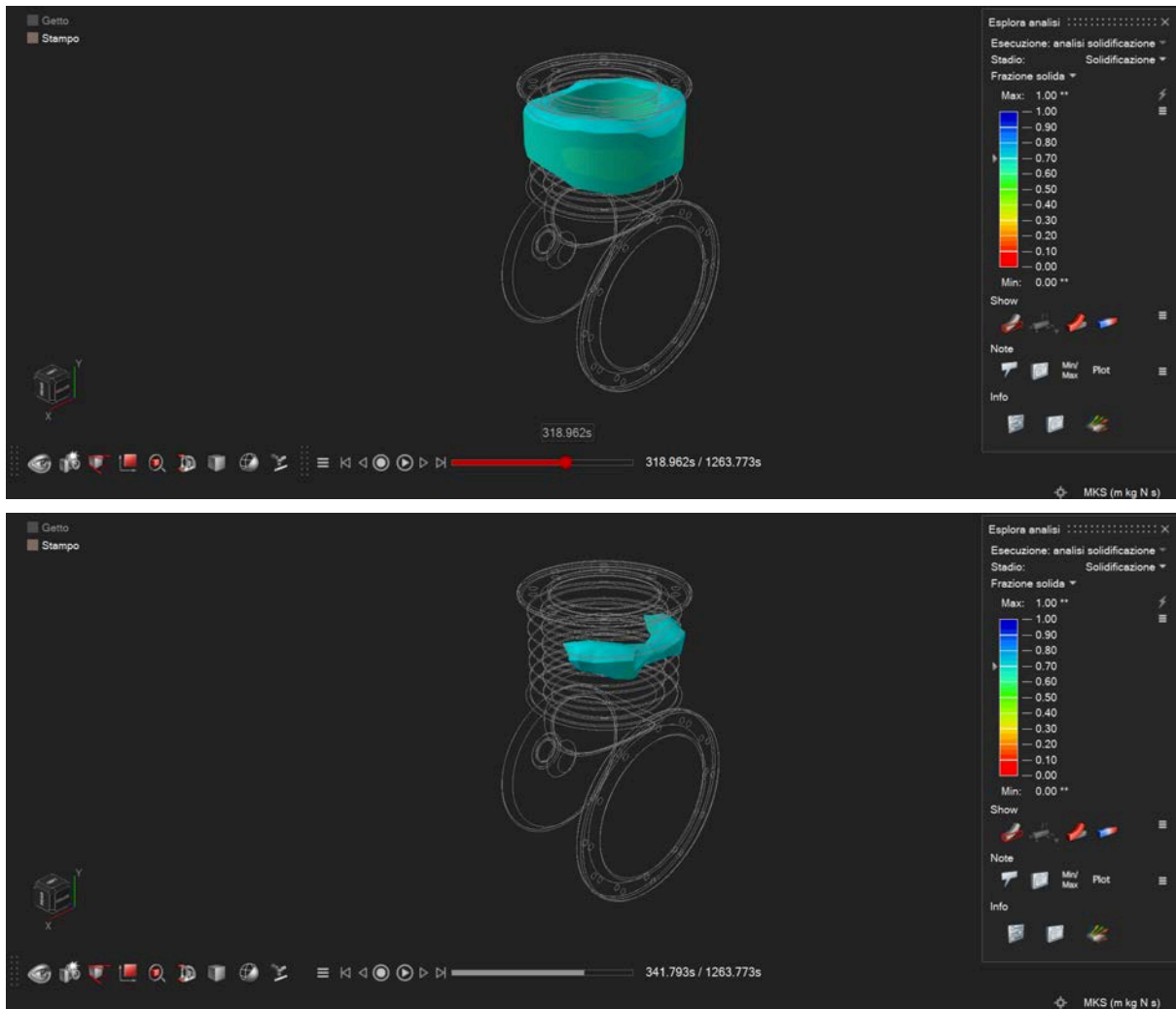
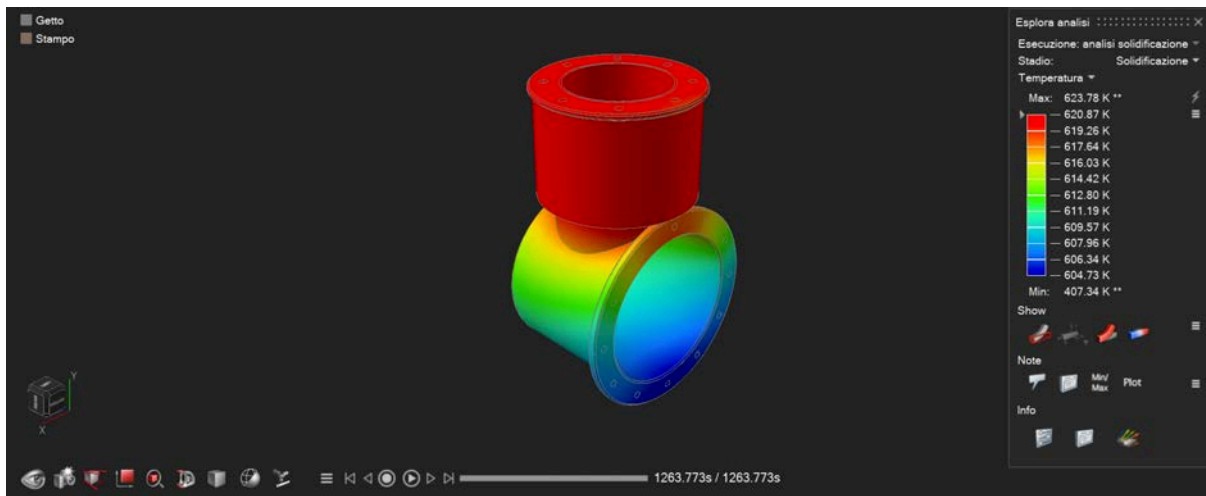


[Fig.10] Solidification process of component no.1 - engine block.

The areas that maintain low solid fraction values, or higher temperatures, for longer correspond to the areas that complete solidification last.



From the obtained images, it can be seen that the upper part of the block, corresponding to the cylinder barrel, remains liquid longer than the other areas. This result is consistent with the manual calculation performed in the previous paragraph, in which Zone 1 had the highest solidification modulus, equal to $M_1 = 3,39$ mm.

The cylinder liner is therefore confirmed as the main thermal node of the component, i.e. the area that tends to solidify last and that is most subject to the formation of shrinkage cavities.

The final temperature analysis also highlights a greater heat retention in the upper part of the casting, confirming the need for a power supply system near this area. The base/casing, although not presenting the maximum modulus, is still considered in the subsequent design of the risers, since it has a large volume and is separated from the upper area by a constriction that tends to solidify first.

The simulation thus confirms the identification of the cylinder liner as the main critical zone and supports the results obtained through the theoretical calculation of the solidification modulus. To avoid shrinkage defects, it will therefore be necessary to design a feeding system capable of maintaining the metal liquid in the critical zones for a sufficient period of time.

3.4.3 Design and sizing of the sprues

After analyzing the solidification behavior through modulus calculations and software simulation, the casting feed system must be designed. This system consists of the feeders, which compensate for the volumetric contraction of the metal during the transition from the liquid to the solid state.

During cooling, the liquid metal tends to reduce its volume. If the last areas to solidify are not fed properly, internal defects such as shrinkage cavities or porosity can form. To avoid this problem, the risers must remain liquid longer than the casting, acting as reservoirs of molten metal.

From the previous analysis it emerged that the maximum modulus is found in the **Zone 1**, corresponding to the cylinder liner. To ensure proper feeding and avoid the formation of shrinkage cavities inside the casting, it is therefore necessary to position one or more risers near this area.

For a sprue to perform its function correctly, its solidification modulus must be greater than that of the area to be fed. In particular, it is assumed that the sprue modulus must be *at least 20% higher with respect to the maximum jet modulus*:

$$M_{\text{riser}} \geq 1,2 \cdot M_{\text{max}}$$

Substituting the chosen value for the sprue, we obtain the value of the collar:

$$M_{\text{riser}} \geq 1,2 \cdot 3,39 = 4,10 \text{ mm}$$

This value therefore represents the theoretical minimum modulus that the sprue must possess to solidify after the critical zone of the component.

However, considering the geometric complexity of the engine block, the presence of thickness variations and the need to ensure greater safety in the power supply, it is decided to adopt a more conservative design value of $M_{\text{riser}} = 7 \text{ mm}$.

This choice allows to increase the solidification time of the sprue and to guarantee better compensation of volumetric shrinkage.

3.4.3.1 Geometric dimensioning of the sprue

We opt for one **open-air cylindrical sprue**, as it offers a good ratio between available volume and dispersing surface. Furthermore, this geometry is simple to produce and easily applicable to the mold parting plane.

For this standard geometric configuration, an optimal ratio between height (H_{mat}) and diameter (D_{mat}) equal to 1 is assumed:

$$H_{mat} = D_{mat}$$

The solidification modulus of a cylindrical sprue with $H = D$ is related to its geometric dimensions by the analytical relationship:

$$M_{riser} = \frac{V_{riser}}{S_{eff,riser}} = \frac{\frac{\pi}{4} D_{riser}^2 \cdot H_{riser}}{\pi D_{riser} \cdot H_{riser} + \frac{\pi}{4} D_{riser}^2}$$

Replacing $H_{riser} = D_{riser}$ and simplifying, the formula reduces to:

$$M_{riser} = \frac{D_{riser}}{5}$$

Imposing the project value $M_{riser} = 7 \text{ mm}$, we obtain the minimum diameter required through the inverse formula:

$$D_{riser} = 5 \cdot M_{riser} = 5 \cdot 7 \text{ mm} = 35 \text{ mm}$$

Calculation of the sprue attachment collar module:

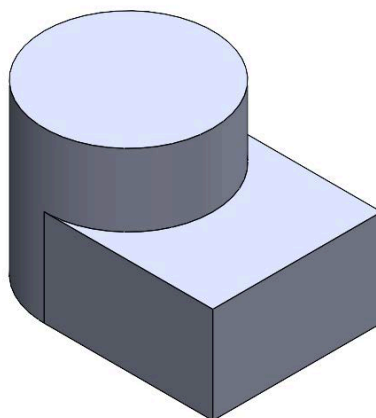
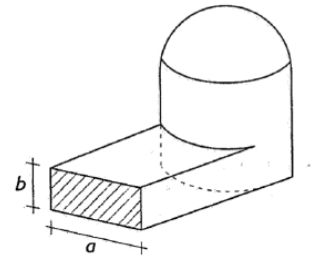
$$M_c = \frac{a \cdot b}{2(a + b)}$$

Knowing that:

- $a = 35 \text{ mm}$
- $M_c = 1.2 : 1.1 : 1$

I also know that $M_c = \frac{7 \text{ mm}}{1.1} = 6,36 \text{ mm}$ and I can get b:

$$b = 19,7 \text{ mm approximated to } b = 20 \text{ mm}$$



3.4.3.2 Positioning of the sprues

After defining the geometric dimensions of the standard riser, it is necessary to establish the position of the risers on the casting blank. The positioning must be chosen based on the areas that solidify last, identified by calculating the solidification modulus and subsequent software simulation.

The *Zone 1* therefore represents the main thermal node of the component and must be fed efficiently during the volumetric contraction of the metal. For this reason, two open sprues are positioned in the upper part of the engine block, near the cylinder liner.

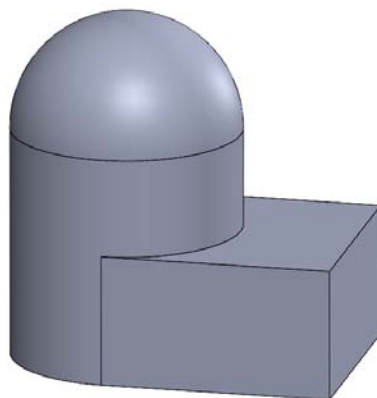
The choice to use **two upper sprues**, instead of just one, allows for better distribution of the liquid metal feed and reduces the distance between the sprue and the areas to be fed. Furthermore, the symmetrical arrangement of the two sprues allows for a more balanced feed of the upper part of the casting.

In addition to the cylinder liner, the crankcase/crankcase must also be considered. This area has a lower modulus ($M_3 = 2.76 \text{ mm}$) compared to the barrel.

However, the crankcase/crankcase has a large volume and is separated from the upper part of the component by the cylinder constriction. The latter, having a lower modulus, tends to solidify first and can therefore interrupt the liquid connection between the upper and lower areas of the casting.

For this reason the crankcase/crankcase is considered as a second thermal node to be powered independently. It is therefore expected that the third **sprue is positioned** laterally on the crankcase, in correspondence with the most massive area of the crankcase.

Unlike the two upper sprues, the side sprue is designed as *blind sprue*, that is, completely contained within the mold sand. This solution is advantageous because, being surrounded by the mold material, the sprue disperses heat more slowly than an open sprue and keeps the metal in a liquid state longer.



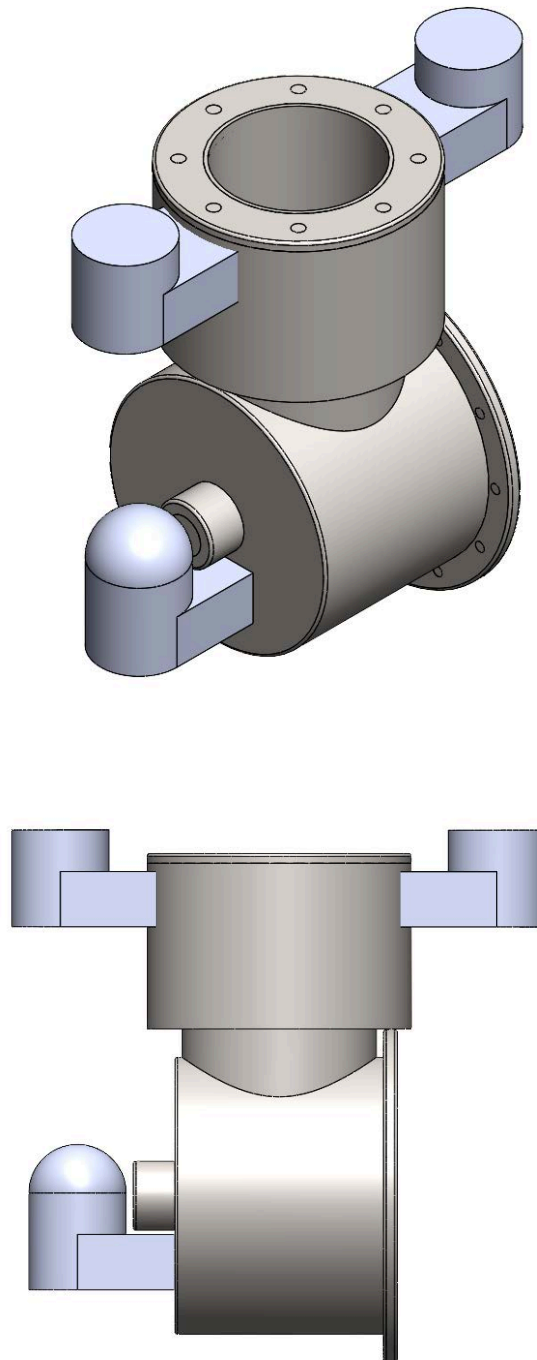


*[Fig. 11] Positioning of the risers on the casting rough.**

*In the rough model, the small-diameter holes are not through holes, but are closed with added material. Their position remains recognizable only as a geometric reference, since these holes will be machined later.

3.5 Casting system

After defining the feed system via sprues, it is necessary to design the casting system, i.e. the set of channels that allow the liquid metal to reach the mold cavity in a controlled manner.

The casting system is responsible for ensuring the mold is filled correctly, avoiding unwanted phenomena such as excessive turbulence, air inclusion, sand erosion, and premature solidification of the metal before the casting is completely filled.

In the case of an engine block, the casting system must be designed taking into account the component's complex geometry, the presence of internal cores, variations in thickness, and the position of the sprues. It is therefore essential that the metal reaches the various areas of the casting uniformly, without hindering the operation of the feed system.

The chosen system is composed of the following main elements:

- casting basin;
- descent channel;
- distributor channel;
- casting attacks;
- sprues and related feed collars.

A system positioned along the parting line will be used to optimize the flow of metal.

3.5.1 Calculation of total mass and pouring time

To correctly size the casting system, it is necessary to determine the mass of the metal to be poured and the filling time of the mold.

Total volume calculation:

$$V_{tot} = V_{riser} + V_{casting}$$

$$V_{tot} = 66.777,47 + 48.552,82 + 48.552,82 + 285.764,80 = 449.647,91 \text{ mm}^3$$

Calculate the mass to be cast:

$$G = V_t \cdot \rho$$

$$\rho = 2.7 \text{ kg/dm}^3$$

$$G = 0,4496 \text{ dm}^3 \cdot 2.7 \text{ kg/dm}^3 = 1,20 \text{ kg}$$

The mass of the metal to be cast is therefore equal to approximately **1,20 kg**.

Casting time calculation:

$$T = S \cdot \sqrt{G}$$

Where:

- T is the casting time [s]
- G is the mass of the jet [kg]
- S is an empirical coefficient dependent on the material and the type of casting

The coefficient S is assumed to be equal to 3,2, generally assumed for aluminum alloy castings.

$$S = 3,2$$

$$T = 3,2 \cdot \sqrt{1,20 \text{ kg}} = 3,5 \text{ sec}$$

Calculating volumetric flow rate Q :

$$Q = \frac{V}{T} = \frac{449.647,91}{3,5}$$

$$Q = 128.471 \text{ mm}^3/\text{s} \approx 128.500 \text{ mm}^3/\text{s}$$

Finally, for the subsequent setting of the software simulation, it may also be useful to calculate the mass flow rate K :

$$K = \frac{G}{T} = \frac{1,20}{3,5} = 0,35 \text{ kg/s}$$

3.5.2 Choke Area Sizing

The casting system must be "squeezed," generally at the base of the runner or at the casting inlet, to ensure that the runners remain filled with metal throughout the casting process. This prevents the formation of voids and the entry of air into the flow. This minimum cross-section is called the squeezed cross-section, or *choke area*.

The narrowed section is calculated using the following relationship:

$$A_c = \frac{G}{\rho \cdot T \cdot c \cdot \sqrt{2 \cdot g \cdot H}}$$

Where

g = Acceleration due to gravity

H = Loading height

The useful load height H is assumed to be 120 mm. This value is closely linked to the geometric choice of the upper bracket, which has an overall height of 150 mm.

c = Coefficient of friction/system efficiency

The coefficient of c comes assumed equal to 0,5. This value takes into account the concentrated and distributed pressure losses along the casting system ducts, due to changes in flow direction and friction with the walls of the sand mold, ensuring a prudent sizing of the squeezed section.

Calculation

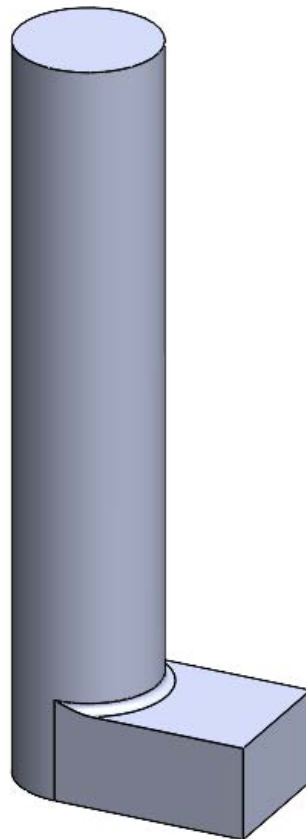
$$A_c = \frac{1,20 \text{ kg}}{2700 \cdot 3,5 \cdot 0,5 \cdot \sqrt{2 \cdot 9,81 \cdot 0,12}} = 152,55 \text{ mm}^2$$

Sprue side calculation (square glide path):

$$side = \sqrt{152,55 \text{ mm}^2} = 12,35 \text{ mm} \approx 13 \text{ mm}$$

For ease of modeling and construction, the sprue is designed with a square cross-section. Calculating the narrowed cross-section yields a theoretical side length of approximately 12.35 mm; therefore, a rounded value of 13 mm is adopted.

The runner connects the vertical descent channel to the casting and allows the liquid metal to reach the mold cavity. This element does not belong to the final component, but is removed after solidification along with the sprues and other elements of the casting system. [Fig. 11].



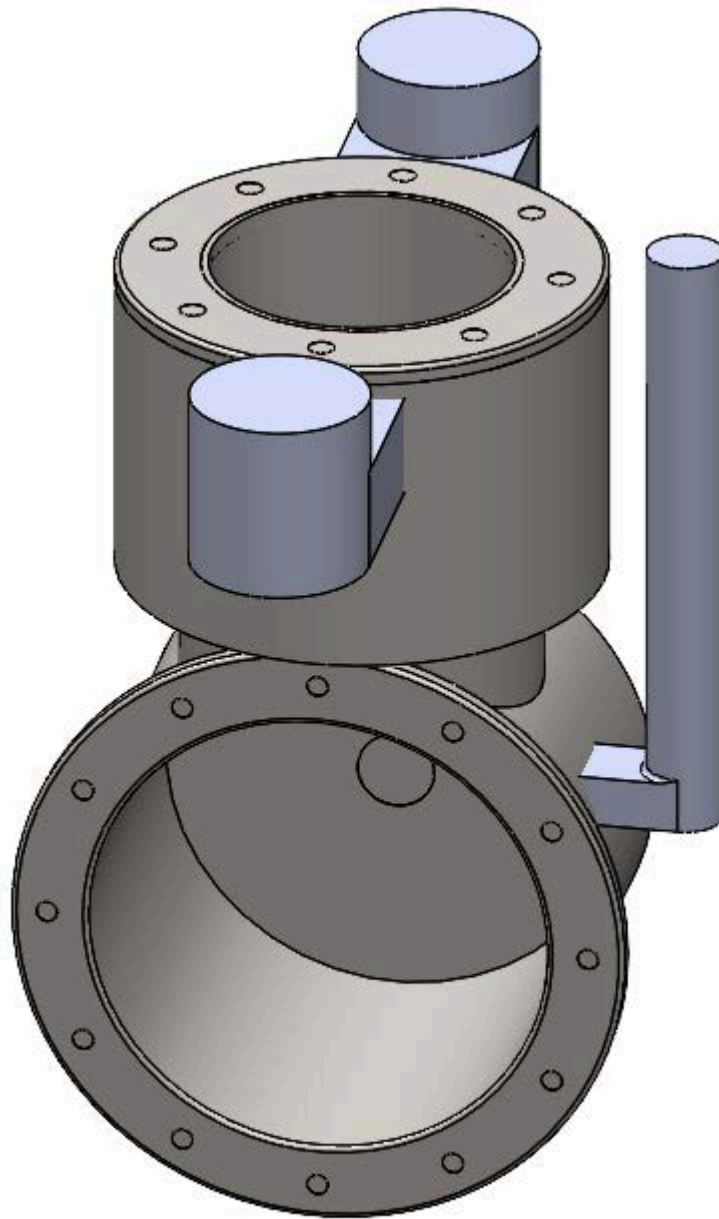


[Fig. 12] Cast blank complete with overmetals, fittings, sprues and casting system.

3.5.3 Fluid dynamics verification of the flow

To ensure that the metal does not damage the sand mold during filling, it is necessary to demonstrate that the flow regime is not excessively turbulent. To do this, the Reynolds number (Re) is calculated in the squeezed section, i.e., the point where the metal flows fastest.

Calculation of the fluid velocity (v) in the squeezed section:

$$v = c \cdot \sqrt{2 \cdot g \cdot H}$$

$$v = 0.5 \cdot \sqrt{2 \cdot 9,81\text{m/s}^2 \cdot 0,12\text{m}} = 0,77 \text{ m/s}$$

Calculate the Reynolds Number (Re):

$$Re = \frac{v \cdot Dh}{\nu}$$

Where

$$Dh = 0,013 \text{ m}$$

The kinematic viscosity of liquid aluminum at about 700°C is a tabulated data and is equal to approximately $\nu = 0,55 \cdot 10^{-6} \text{ m}^2/\text{s}$

$$Re = \frac{0,77 \text{ m/s} \cdot 0,013\text{m}}{0,55 \cdot 10^{-6} \text{ m}^2/\text{s}} = 18.130$$

The resulting value indicates a turbulent flow regime. This result is normal in casting systems, as the liquid metal flows through small-section channels at a relatively high speed.

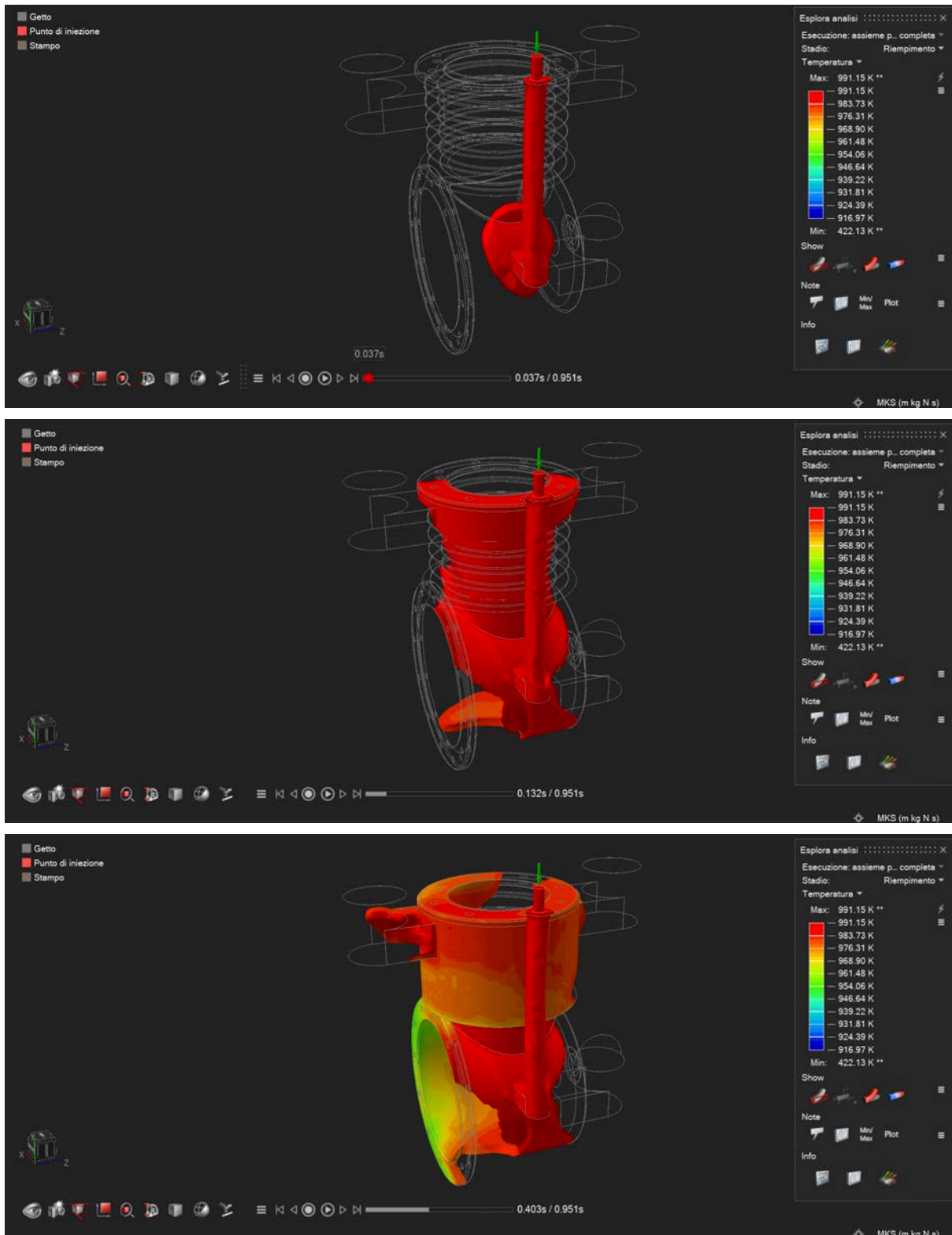
However, the resulting value does not necessarily lead to destructive conditions for the sand mold, provided the casting system is properly designed. To limit the negative effects of turbulence, the downspout, the distribution channel, and the casting connections are connected and sized to avoid sudden changes in direction and sharp edges.

Analytical considerations:

When sand casting small light alloy castings, a certain degree of turbulence is difficult to avoid. For this reason, the goal is not to achieve perfectly laminar flow, but to limit the more harmful effects of turbulence, such as sand erosion, air entrapment, and oxidation of the liquid metal.

In this application, the presence of correctly sized and positioned sprues is also essential to compensate for volumetric shrinkage during solidification. The designed casting system therefore allows for the filling of the casting, while the sprues ensure the feeding of critical areas, reducing the risk of macroscopic defects such as shrinkage cavities inside the base and cylinder liner.

3.5.4 Final casting and solidification simulation



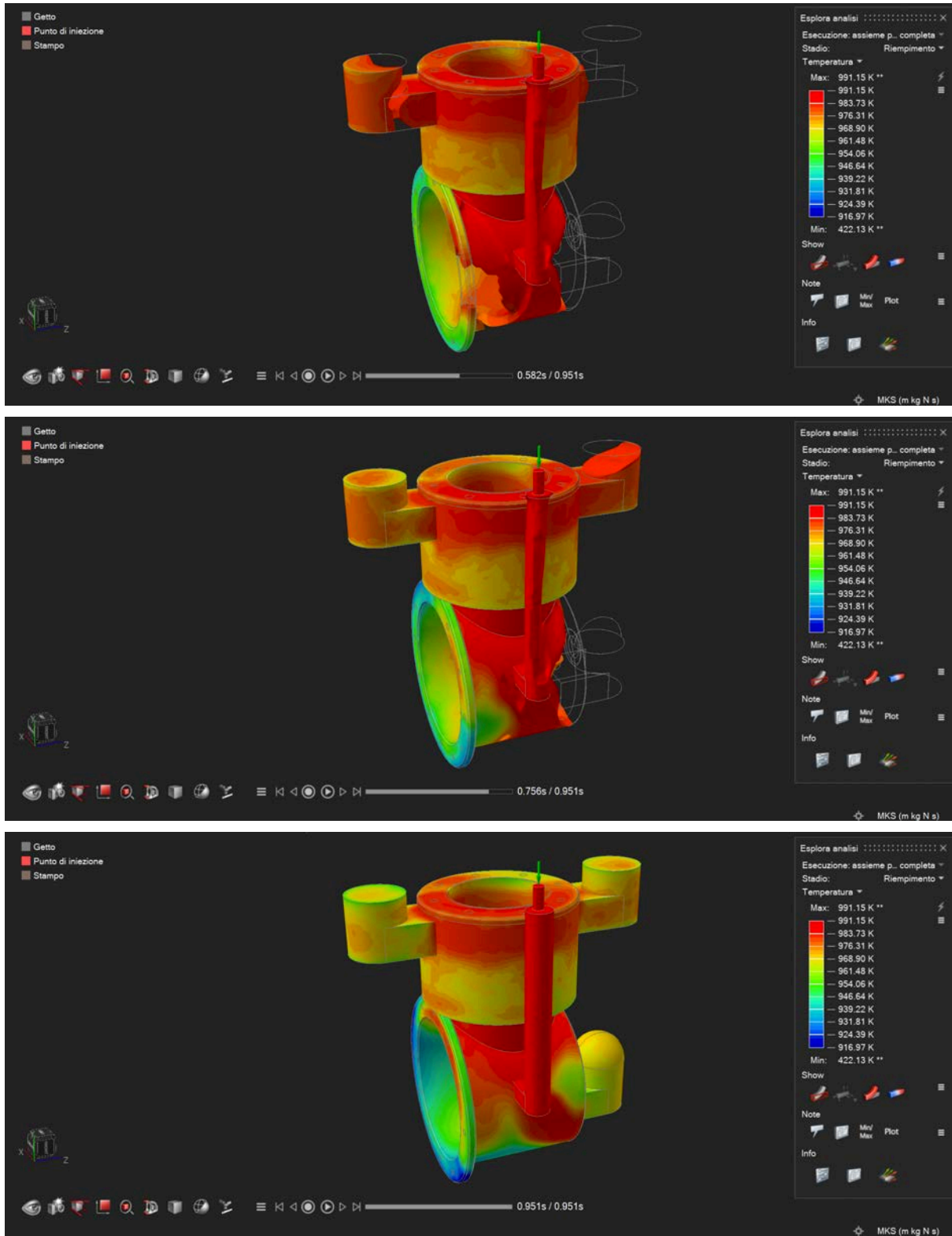


[Fig. 13] Final simulation.

3.5.5 Analysis of the times and costs of the Merger Phase

To evaluate the feasibility of the production process, an estimate was made of the main processing times and related costs associated with the production of the engine block using the shell-molding process.

The overall production time was divided into the main phases of the process:

Operation	Pace (min)
Mold preparation	12 min
Soul placement	5 min
Closing the mold	3 min
Casting	0,06 min
Cooling and de-sanding	15 min

Total time: 35.06 min

As regards the cost of the material, considering a total mass of cast metal equal to

$$G_{tot} = 1,20 \text{ kg}$$

and an average cost of the EN AC-AISi7Mg0.3 alloy equal to

$$2,50 \text{ €/kg}$$

A 5% material loss is also assumed due to the casting system, sprues and scrap.

The cost of the material is therefore:

$$C_{riser} = 1,20 \cdot 1,05 \cdot 2,50 = 3,15 \text{ €}$$

Assuming an average hourly labor cost of 35 €/h

the cost of processing is:

$$C_{work} = 35 \cdot \frac{35,06}{60} = 20,45 \text{ €}$$

The overall production cost of the casting is therefore:

$$C_{tot} = C_{work} + C_{riser} = 23,60 \text{ €}$$

The analysis shows that labor costs represent the main component of the overall cost, while material costs have a lesser impact. In the case of small or medium-sized production runs, the manufacturing process is shell-molding. However, it is still convenient thanks to the good surface quality that can be achieved, the reduction of subsequent mechanical processing and the high repeatability of the process.

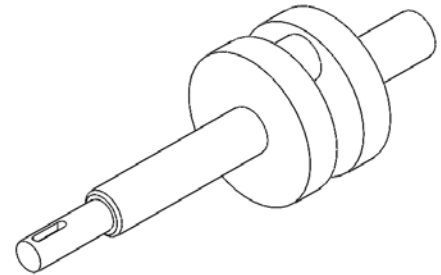
4. INTRODUCTION OF THE COMPONENT: SHAFT (N.2)

Piece made in the laboratory

4.1 Description of the piece

The crankshaft present inside the four-stroke petrol engine is a truly fundamental component.

Its main function is to transform the reciprocating linear motion of the pistons, generated by combustion, into a continuous rotary motion. This motion is then transmitted to the vehicle's various drivetrains.



Typically, the crankshaft is made of forged steel or spheroidal cast iron, materials chosen for their mechanical strength and fatigue resistance.

It is composed of several main parts [Fig....]:

1. **cranks**: connect the main bearing severly one connecting rod bearings and allow the conversion of reciprocating motion into rotary motion;
2. **main journals**: they support the crankshaft inside the crankcase, thus allowing it to rotate;
3. **connecting rod pin**: they are the connection point with the connecting rods, which transfers the movement of the piston;
4. **control end** One side of the shaft connects to the timing belt via a toothed pulley that runs to the camshaft and camshaft cups; the other side is connected to the flywheel, which helps ensure smooth movement.

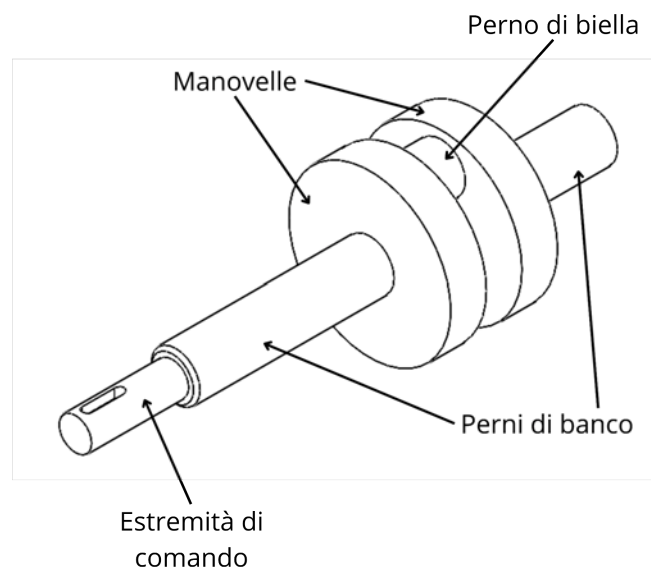


[Fig. 14] Illustration of engine block parts.

The crankshaft is essential for the correct functioning of the engine, because it transforms the energy of combustion into a movement useful for the transmission of the vehicle, ensuring that the motion of the pistons and the camshaft are synchronized, regulating the suction, compression phases, expansion and expulsion.

It also reduces vibrations thanks to the counterweights, ensuring smooth operation and reducing wear on other components and allowing connection with other mechanical parts, such as the clutch and gearbox, to transfer motion to the vehicle's wheels.

The crankshaft is therefore a crucial element for the efficient and reliable operation of a four-stroke engine, directly influencing performance, fuel consumption and engine life.

In a four-stroke engine, the crankshaft usually has lubrication holes, which help oil flow throughout the engine and keep the crankshaft well lubricated. Lubrication holes will be drilled during one of the phases of the machining cycle.

4.2 Analysis of the technical drawing and project data

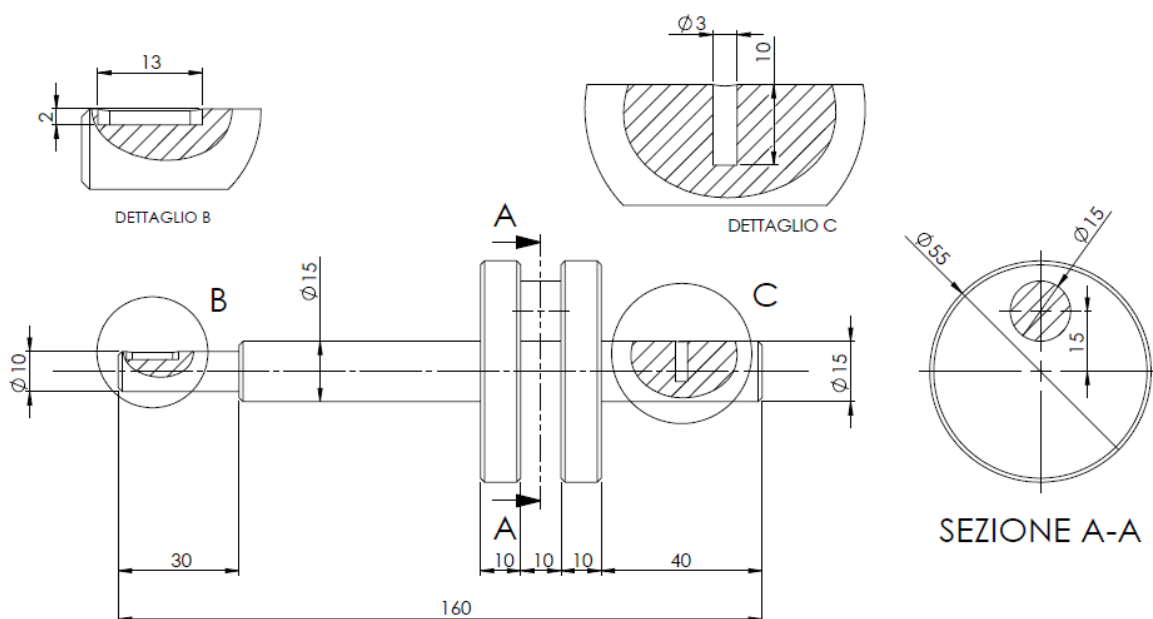
In the production of the piece in question in the laboratory we took a raw cylinder of carbon steel Q40.

A cylindrical blank made of C40 steel with a diameter of 60 mm and a length of 170 mm was used, from which we removed 10 mm of material through machining for a better finish. The diameter of the bar is 60 mm, brought with turning and milling to 55 mm.

The overall dimensions of the tree are as follows:

- total length = 160 mm
- maximum diameter = 55 mm

The other dimensions needed for the construction are shown in the following drawing.



**lubrication holes not shown for practical production purposes, but present.*

[Fig. 15] Technical drawing with dimensions - piece no. 8.

4.2.1 Quantity of pieces to be produced for a hypothetical company

The component was produced as a single piece during laboratory work carried out at the affiliated technical institute. Consequently, the production cycle was developed with unit production in mind and the use of conventional machine tools, without resorting to special equipment dedicated to mass production.

4.2.2 Production costs

Since the component was produced as a single piece, the production process was developed using exclusively standard equipment and conventional machine tools. Under these conditions, production costs are closely linked to the time required to perform the individual machining operations. The following paragraphs will therefore estimate the machine times and related costs associated with producing the component.

4.3 Choice of material

4.3.1 Component requirements

The crankshaft is one of the main components of a four-stroke engine and is subject, during operation, to high-intensity, predominantly cyclic mechanical stresses. In particular, the component is subjected to combined bending and torsional loads, as well as concentrated stresses in the main journals and connecting rod pin, which can cause fatigue and wear.

For this reason the material must possess the following characteristics:

- high mechanical resistance;
- good fatigue resistance;
- adequate toughness to avoid brittle breakage;
- good wear resistance in mating surfaces;
- good machinability;
- possibility of being subjected to heat treatments to improve its properties.

The choice of material must therefore guarantee the correct functioning of the component, while keeping production costs low.

4.3.2 Rationale for the choice of material

Based on the previously identified requirements, the material selected for the construction of the component is steel. **Q40**, belonging to the category of medium carbon content quenched and tempered steels.

The **Q40** is chosen because it perfectly balances strength, machinability, cost, and heat treatability. This makes it ideal for the large-scale production of crankshafts with standard requirements..

The **Q40** belongs to the category of "quenched and tempered steels," used for the construction of mechanical components subjected to static and dynamic loads. It is widely used in the mechanical industry for shafts, axle shafts, rods, connecting rods, connecting elements, levers, stems, and press columns..

For small batch production, such as that examined in this report, the **C40** therefore represents a technically valid and economically convenient solution.

4.3.3 Alternative materials

The crankshaft is usually made of special high-strength steels, both heat and surface treated to ensure excellent performance, resistance to fatigue and wear.

Among the most commonly used steels we can mention:

- Carbon alloy steels (like 42CrMo₄, **Q40**, C45), which offer an excellent balance between strength and workability, thanks to hardening and tempering treatments.
- Nickel-chromium-molybdenum steels (come 34CrNiMo₆, 40CrNiMo₇), which guarantee high mechanical strength and good fatigue resistance, and are usually case-hardened to increase surface hardness.

42CrMo4	Low-alloy chromium-molybdenum steel characterized by high mechanical strength, excellent hardenability and good fatigue resistance.
34CrNiMo6 - 40CrNiMo7	Nickel-chromium-molybdenum steels are used in highly stressed applications, thanks to their high toughness and the possibility of achieving high surface hardness through heat treatments.
40NiCrMo2	It offers a good balance between mechanical strength and toughness.
30NiCrMo12	Characterized by high hardening capacity and excellent fatigue resistance even under harsh conditions.
39NiCrMo3	Used for large components requiring high mechanical performance.
16NiCrMo2	Particularly suitable for small and medium-sized crankshafts thanks to its good hardenability and limited deformability during heat treatments.
36CrMn5	A cheaper solution that still guarantees a good compromise between hardness and toughness.

- High-strength ductile irons (such as GJS-700-2), used in series engines to keep production costs low, without compromising mechanical characteristics and wear resistance.

Although these materials generally offer superior performance to C40, they entail higher procurement and processing costs that are not justified for the component under study.

UnderHere is a table summarizing the most common alloys and their main characteristics:

Lega di Acciaio	Resistenza alla trazione (kg/mm ²)	Durezza Brinell (HB)	Allungamento (%)
40NiCrMo2	90-105	241	12
30NiCrMo12	Fino a 115	260	14
39NiCrMo3	Fino a 115	260	14
16NiCrMo2	90-105	241	12
36CrMn5	80-95	227	14

4.3.4 Mechanical properties of C40

C40 is a steel with a carbon content of approximately 0.37% to 0.44%, characterized by a good combination of strength, ductility and workability.

The main mechanical properties of the material are reported in the *Table 4.1*.

Property	Indicative value
Carbon content	0.37 - 0.44 %
Yield strength R _{and}	320 - 380 MPa
Tensile strength R _m	550 - 700 MPa
Elongation at break	16 - 20 %
Hardness	170 - 220 HB
Elastic modulus	210 GPa
Density	7850 kg/m ³

These properties allow the material to effectively withstand the operating stresses typical of a crankshaft.

In particular:

- the **yield strength limits** permanent deformations;
- the **tensile strength guarantees** the ability to withstand high mechanical loads;
- the **elongation at break ensures** sufficient ductility, reducing the risk of sudden breakages;
- the **hardness contributes** to the wear resistance of contact surfaces;
- The **elastic modulus ensures** high rigidity of the component.

Following the tempering treatment, these characteristics can be further improved, increasing the mechanical strength and fatigue life of the crankshaft.

COMPOSIZIONE CHIMICA (RIF. UNI EN 10083-2 / UNI EN ISO 683-1)											
	C	Mn	Si	P	S*	Cu	B**	Cr	Ni	Mo	Al***
Min	0.38	0.50	0.15		0.020		0.0050				0.015
Max	0.43	0.80	0.25	0.025	0.035	0.30	0.0100	0.20	0.25	0.08	0.040

PROPRIETÀ MECCANICHE		
Rm (N/mm ²)	A5 (%)	Z (%)
670 - 750	≥ 18	≥ 40

The chemical composition of C40 features a carbon content between 0.38% and 0.43%, a value that provides a good compromise between mechanical strength and workability. The presence of manganese improves the material's hardenability, while the limited content of alloying elements keeps production costs low.

From a mechanical point of view, the material has a tensile strength between 670 and 750 MPa, a minimum elongation of 18% and a minimum area reduction of 40%, characteristics that make it suitable for the production of components subject to dynamic and cyclic loads such as the crankshaft.

4.3.5 Conclusions

In light of the analysis carried out, the C40 represents the most suitable choice for the construction of the crankshaft under study.

Although there are materials with superior mechanical performance, such as nickel-chromium-molybdenum steels, their use would be less economically viable for small batch production obtained through chip removal machining.

C40 offers an excellent balance between mechanical strength, workability, commercial availability and material cost, as well as the possibility of being subjected to heat treatments that further improve its performance.

The choice is therefore consistent with both the functional requirements of the component and the identified production process, allowing for the production of a reliable, precise and economically competitive crankshaft.

4.4 Choice of processing technique

Once the most suitable material for the component has been identified, the most suitable manufacturing process must be defined. Given the geometry of the crankshaft and the good machinability of steel, Q40, the chosen solution is the **chip removal machining**, which allows to obtain the component with high dimensional precision and low costs, especially in the case of limited production runs.

The crankshaft is in fact primarily composed of a succession of coaxial cylindrical surfaces with different diameters, to which is added the connecting rod pin, characterized by an eccentric axis with respect to the main axis of the component. This geometric configuration is particularly suitable for turning operations, which can be performed both using traditional lathes and computer numerically controlled (CNC) machine tools.

Any axial and radial holes can be easily created using standard drilling operations, without the need for special machining or equipment. Furthermore, the workpiece's characteristic dimensions fall within the ranges normally handled by standard machine tools and do not have particularly complex geometries that would require the use of dedicated manufacturing technologies.

In the case in question, characterized by the creation of a single prototype for educational purposes, chip removal machining represents the most appropriate solution, as it guarantees a good compromise between geometric precision, surface quality, production flexibility and production costs.

For the practical production of the component, mainly turning and milling operations were used, carried out using the machine tools available at the workshop of the affiliated Technical Institute.

4.4.1 Comparison of possible production techniques

Once chip removal machining was identified as the most suitable manufacturing process, an analysis of the main available techniques was conducted to identify those most compatible with the crankshaft geometry. Specifically, turning, milling, drilling, and grinding operations were considered, evaluating their advantages, limitations, and applicability to the component under study.

The choice of machining processes was made taking into account the geometric characteristics of the piece, the required tolerances, the availability of machine tools and the limited number of components to be produced.

Processing	Advantages	Disadvantages	Application in the piece
Turning	High precision on cylindrical surfaces, good productivity, excellent surface quality.	Requires equipment specific for creating eccentric or non-coaxial surfaces. ¹	Main machining of the crankshaft.
Milling	It allows you to create flat surfaces and complex geometric details.	Longer times than turning.	Creation of surfaces that cannot be obtained with a lathe.
Drilling	Simple and economical process for making holes.	Applicable to axial or radial geometries only.	Lubrication holes.
Correction	High dimensional accuracy and very low roughness.	High costs and times.	Not used in this project.

¹But no particularly significant disadvantages for the component in question.

The analysis shows that turning is the predominant process for producing crankshafts, as most of the surfaces it comprises are coaxial cylindrical elements. Milling and drilling, however, play a complementary role, being necessary for the creation of specific geometries that cannot be achieved with turning. Grinding was not considered necessary, as the level of precision required by the prototype can be achieved by conventional machining available at the institute's workshop..

The only significant criticality is represented by the machining of the connecting rod pin, whose axis is eccentric with respect to the main axis of the crankshaft. This characteristic required an appropriate repositioning of the workpiece during turning operations, as will be described in the following paragraphs.

4.4.2 Machine tools used

To produce the crankshaft, the machine tools available at the affiliated technical institute's workshop were used. The machines were chosen based on the geometric characteristics of the component and the machining operations required for its production.

The main operations were carried out using a parallel lathe, while the complementary processes were carried out using a milling machine and a column drill.

Padovani Labor 180S-800 parallel lathe

The main machine tool used to make the component is the *Padovani Labor 180S-800 parallel lathe*, present in the workshop of the affiliated Technical Institute [Fig.14]. This machine is particularly suitable for machining shafts and cylindrical components, allowing the surfaces of revolution envisaged in the technical drawing to be obtained with high precision.

The lathe was used to carry out the following operations: *facing, rough turning, finishing turning, production of shoulders, chamfers and eccentric connecting rod pin*. Furthermore, during the preliminary stages of machining, centering holes were drilled at the ends of the shaft using a dowel drill mounted on the tailstock. These holes allowed for the correct positioning and support of the piece during subsequent turning operations, ensuring an adequate level of geometric precision and concentricity.

The choice of this machine was determined by the predominantly cylindrical nature of the component, which makes turning the most efficient process both from a production point of view and in terms of achievable geometric precision.

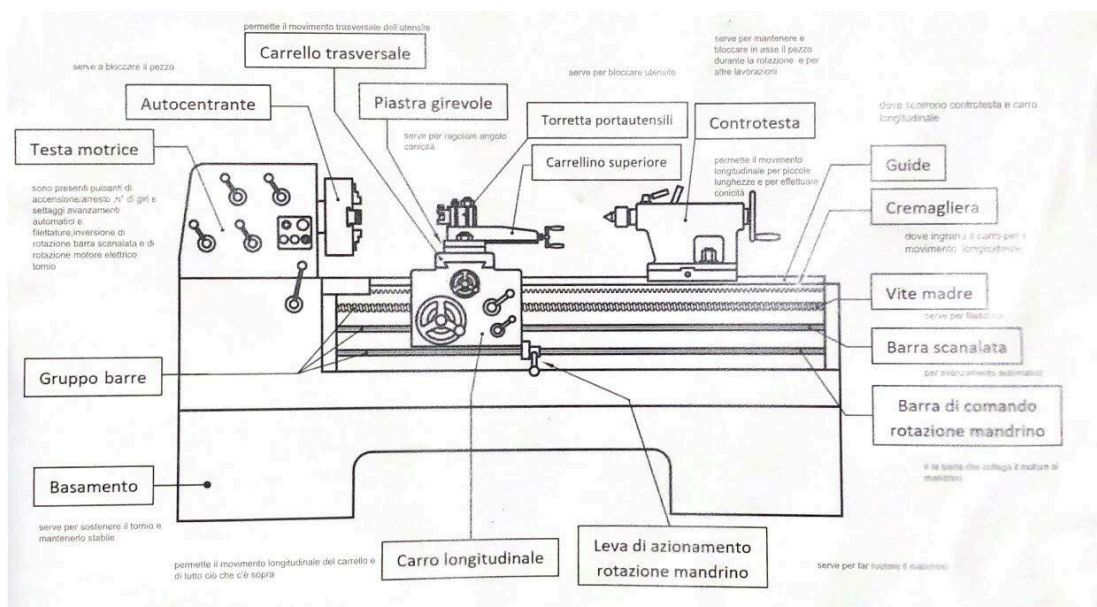


[Fig.16] Illustrative drawing of the Padovani Labor 180S-800 parallel lathe.



[Fig.17] Padovani Labor 180S parallel lathe.

Main features of the lathe

Characteristic	Value
Model	Padovani Labor 180S
Engine power	4.5 kW
Height of tips on the bench	180 mm
Distance between tips	1000 mm
Max. turning diameter under head	360 mm
Spindle hole	56 mm
Spindle motor power	5.5 Hp
Spindle speed	46 - 1750
Refrigeration system	Present
Closed and open lunettes	Present
Double-guide self-centering chuck	Present
Dimensions and weight	1750 x 1100 x 1240H mm - 1250 kg

Technical characteristics of parallel lathe.

Gualdoni FU77 milling machine

The milling machine was used exclusively to create the keyway. This process cannot be achieved by turning, as it requires removing material along a cylinder generator and creating a straight groove.

The use of the milling machine made it possible to obtain the geometry envisaged in the technical drawing with adequate dimensional precision.



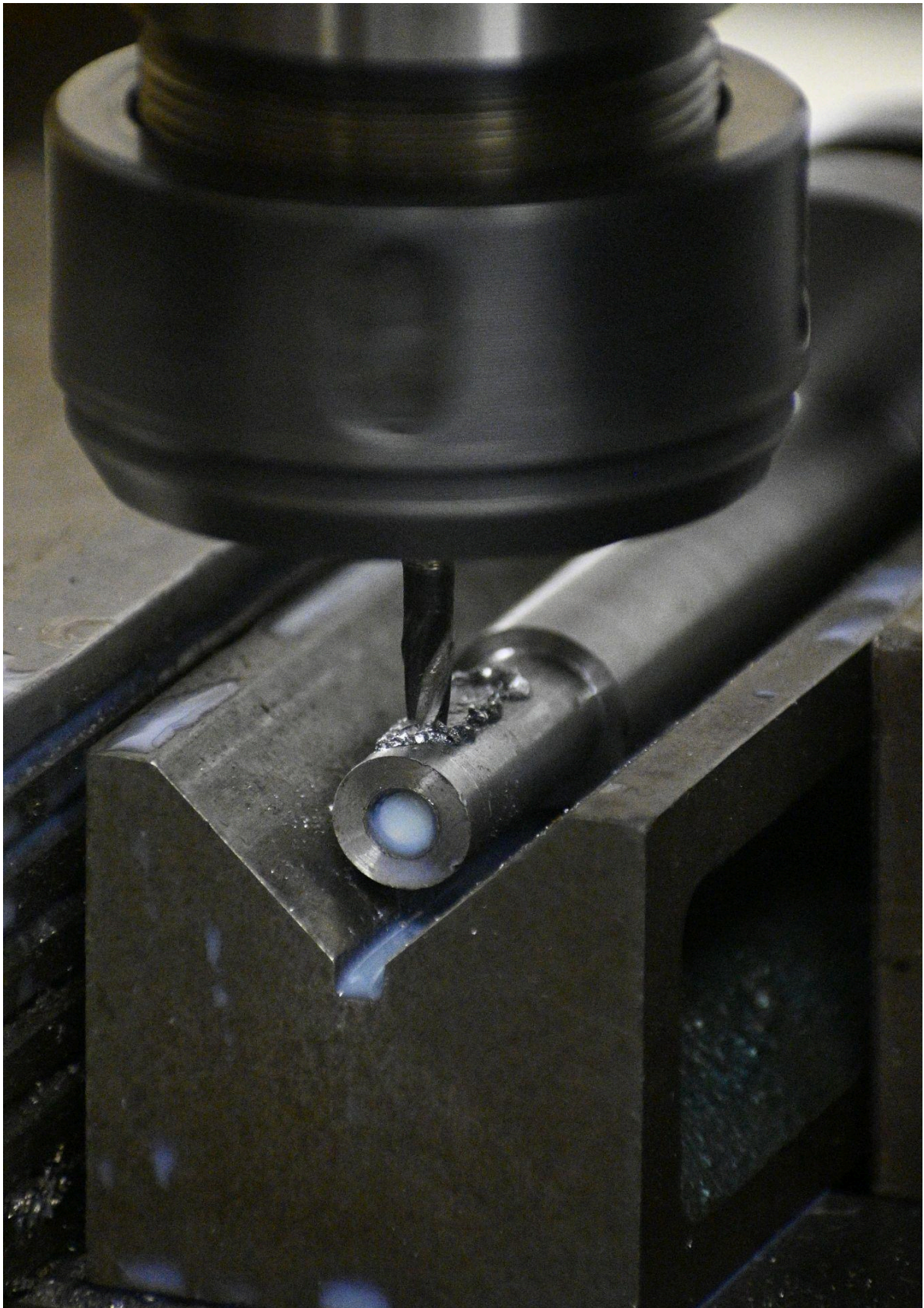


[Fig. 18] Making the tongue seat with the vertical milling machine.

Bimak 32ME column drill

An industrial drill press was used to create the hole intended to accommodate a possible coupling pin.

The use of this machine allowed the drilling operation to be performed simply and precisely, ensuring the correct positioning of the hole with respect to the component geometry.



Considerations on unfinished work

The original technical drawing also included several small-diameter lubrication holes on the crankshaft shoulders. These machining operations were not performed during the practical prototype construction, as the workshop did not have drills of adequate diameter. Using unsuitable tools would have resulted in a high risk of drill breakage or irreversible damage to the machined part. Therefore, to preserve the integrity of the component, it was decided to omit these holes from the practical implementation.

The combined use of a lathe, milling machine, and drill press allowed us to produce all the geometries required by the project using only conventional machine tools, without the need for CNC machining centers or special equipment. This solution is particularly suited to the production of prototypes and small batches, while ensuring dimensional accuracy, production flexibility, and cost containment.

4.4.3 Location of the machines

The practical realization of the piece was carried out at the workshop of the ITI “Enrico Mattei”, equipped with the machine tools described in the previous paragraph and arranged as shown in the figure. [Fig. 16].

When calculating processing times¹, the location of the machines allows us to ignore the times required to move the piece between the various phases of the production process.

¹PerFor further details on the calculation of processing times, please refer to the total paragraph.

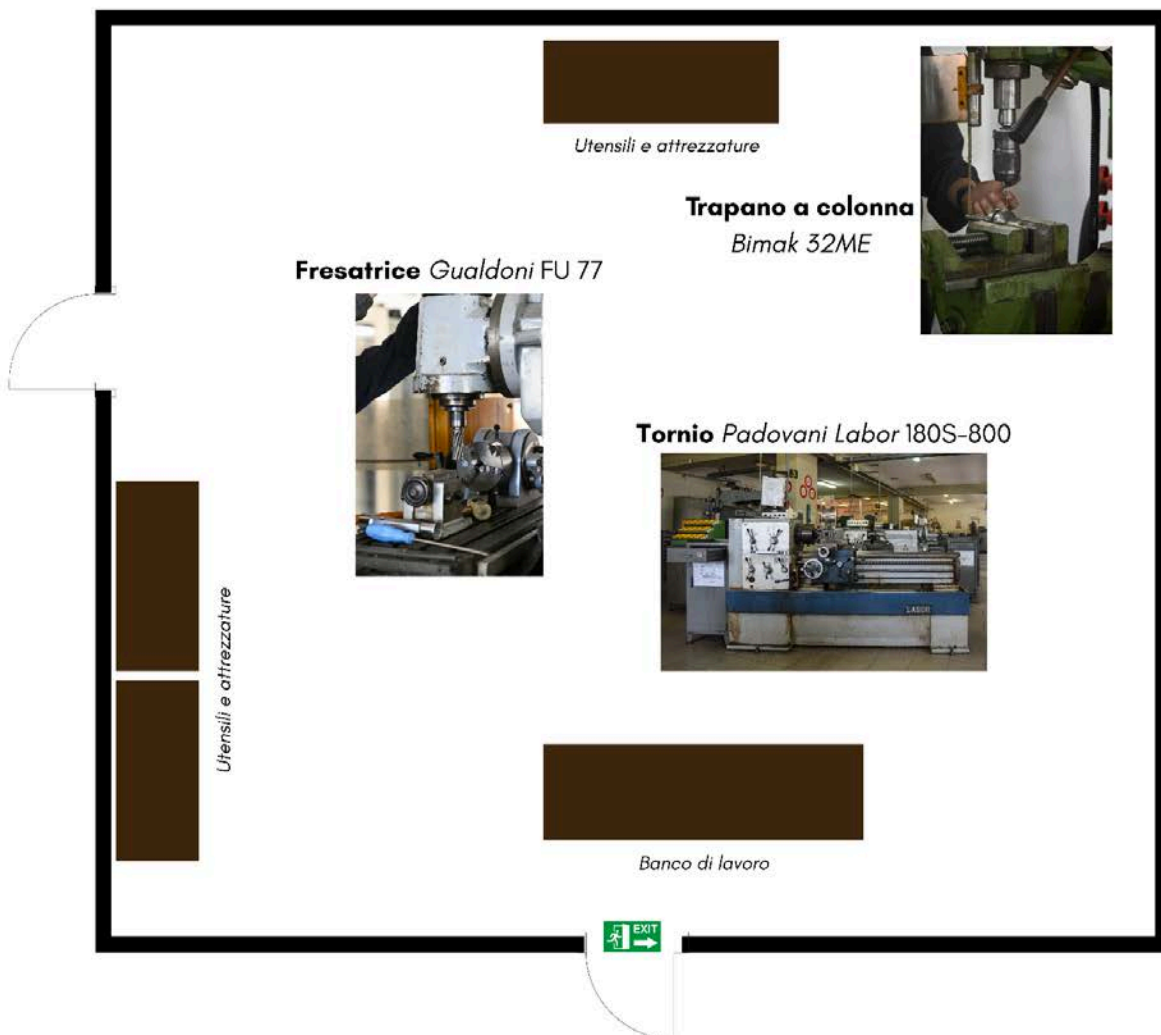


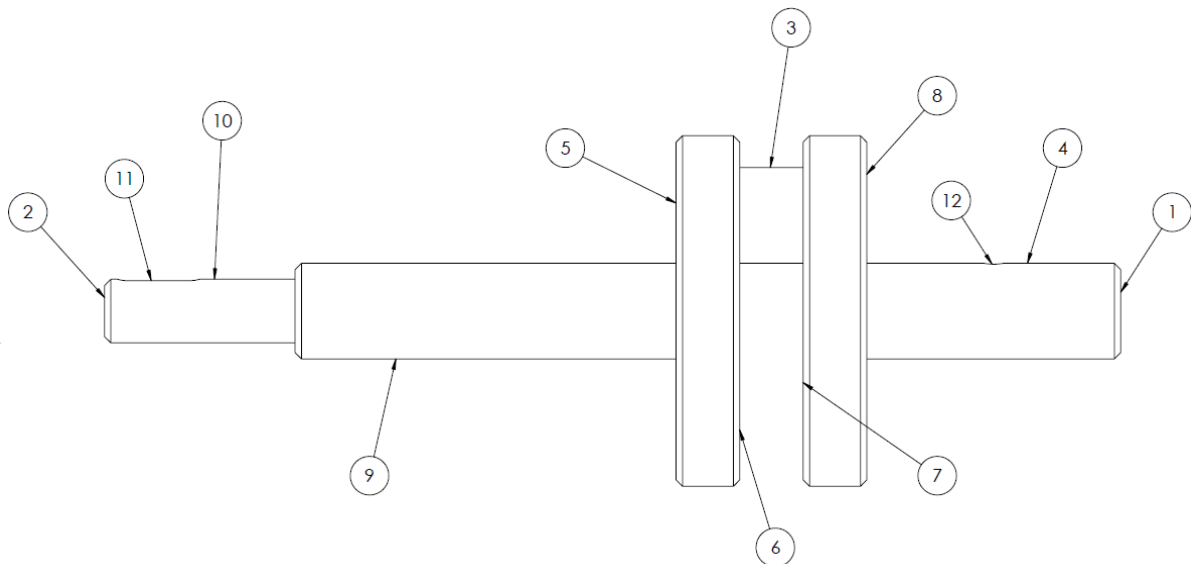
[Fig. 19] Plan of the workshop.

4.4.4 Surface analysis and technological constraints

Before defining the manufacturing cycle, it is necessary to analyze the various surfaces that make up the component, identifying the most suitable machining process for each of them and the related technological constraints.

The crankshaft under consideration consists primarily of coaxial cylindrical surfaces that can be obtained through turning operations. In addition, there are some special geometries, such as the eccentric connecting rod pin, the keyway, and the hole for the coupling pin, which require specific machining and appropriate planning of the production sequence.

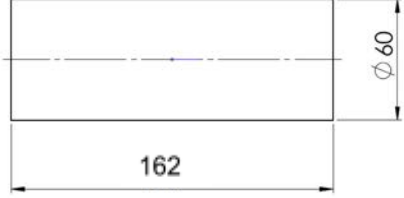
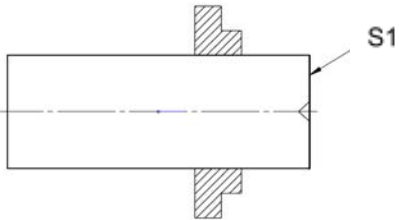
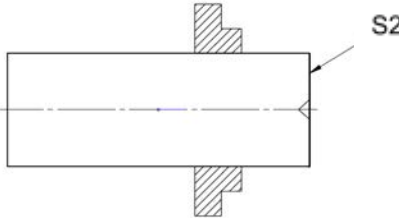
To facilitate the analysis of the component, the main surfaces have been numbered as shown in the following drawing.

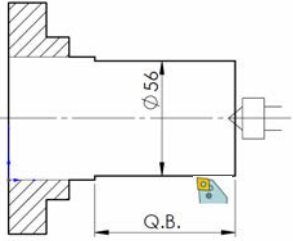
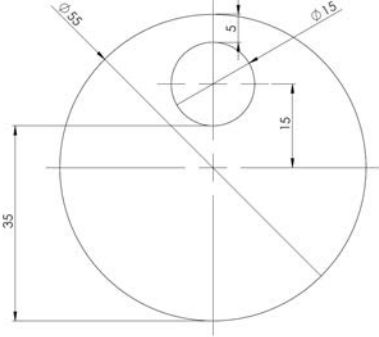
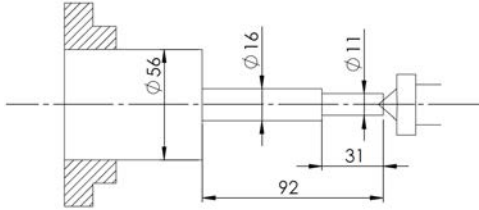


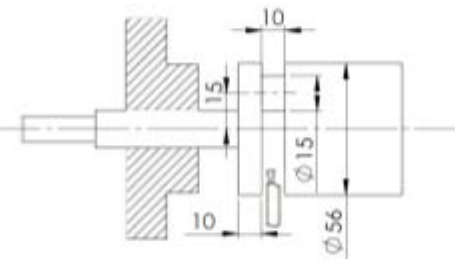
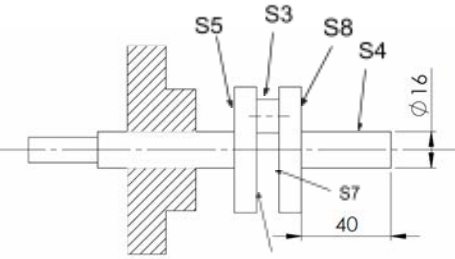
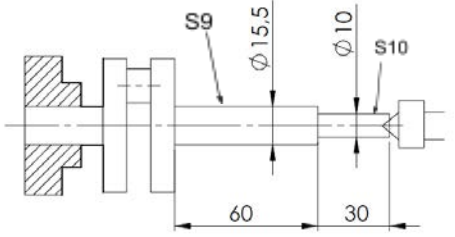
N. SURFACES	PROCESS / MACRO-PROCESSING
1, 2, 3, 4, 5, 6, 7, 8, 9, 11	Turning (Coaxial and Eccentric)
10	Milling
12	Drilling

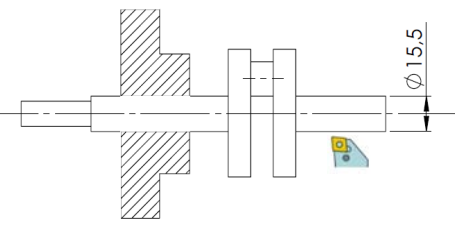
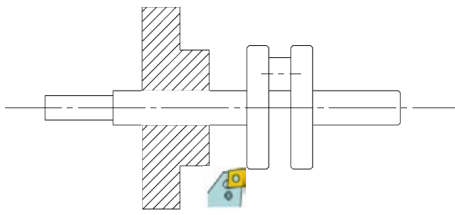
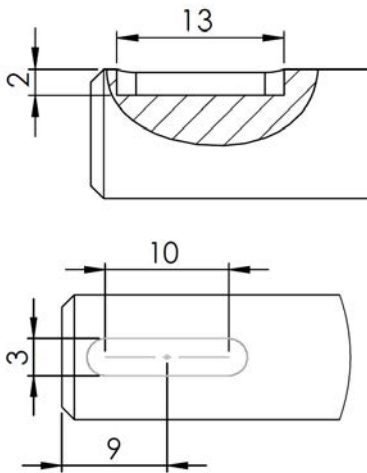
N. AREA	TYPE	PROCESSING - MAIN PROCESS	N. PHASE OF THE WORKING CYCLE
1, 2	Flat end surfaces (orthogonal to the axis).	Turning (heading) and drilling center holes.	Stages 20, 30
4, 9, 11	Coaxial external cylindrical surfaces (main journals and end sections).	External cylindrical turning (roughing and finishing).	Stages 40, 50, 60, 70, 80
3, 6, 7	Eccentric cylindrical surface and its internal faces/grooves (crank pin).	Eccentric turning (15mm offset mounting for grooving, roughing and finishing).	Stages 60, 80
5, 8	External flat shoulders (side faces of the cranks).	Shoulder turning / Facing (thickness finish).	Phase 60
10	Tongue seat.	Milling (tab seat execution with end mill).	Phase 110
12	Blind geometric hole.	Drilling (radial hole drilling using a column drill).	Phase 120

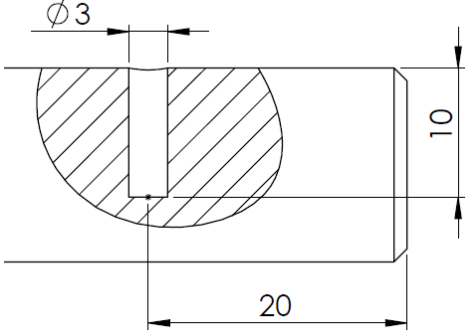
4.4.5 Processing cycle

N. PHASE	DESIGN/OPERATION	MACHINE DEPARTMENT	TOOLS TOOLS CALIBERS	TIME
10	 <p>10.1 Cutting the piece to</p> <ul style="list-style-type: none"> - L = 162 mm - Ø 60 	welding workshop	twentieth caliber jigsaw without a millimeter	$t_{tot10} = 1 \text{ min}$
20	 <p>20.1 certification S1 Q.B.</p> <p>20.2 centering hole creation</p> <p>Roughness: $R_a = 6.3 \mu\text{m}$</p>	O.M.U	Tornio certifying tool aim to hit the mark	$t_{tot20} = 38 \text{ sec}$
30	 <p>30.1 certification S2 up to</p> <ul style="list-style-type: none"> - L = 162 mm (finished) <p>30.2 centering hole creation</p> <p>Roughness: $R_a = 6.3 \mu\text{m}$</p>	O.M.U	Tornio certifying tool aim to hit the mark twentieth caliber	$t_{tot30} = 38 \text{ sec}$

<p>40</p>	 <p>40.1roughing cylinder up to - $\varnothing 56$ - $L = Q.B.$</p> <p>40.2tracing the position of the connecting rod pin with eccentricity $e = 15$ mm</p> 	<p>O.M.U</p>	<p>Tornio</p> <p>back point</p> <p>twentieth caliber</p> <p>roughing tool with widia plate</p>	<p>$t_{tot40} = 5.5 \text{ min}$</p>
<p>50</p>	 <p>50.1roughing cylinder a $\varnothing 16$ and $L = 92$ mm</p> <p>50.2roughing cylinder a $\varnothing 11$ and $L = 31$ mm</p> <p>50.3 elimination of the 1 mm excess metal</p>	<p>O.M.U</p>	<p>Tornio</p> <p>roughing tool with widia plate</p> <p>twentieth caliber</p> <p>back point</p>	<p>$t_{tot50} = 8 \text{ min}$</p>

<p>60</p>	 <p>60.1throat execution $\varnothing 15$ and L = 10 mm of a sudden leap. Eccentric mounting of the piece with a 15 mm offset from the main axis.</p>  <p>60.2roughing cylinder a $\varnothing 16$ and L = 40 mm</p> <p>Roughness S3: $R_a = 3.2 \mu\text{m}$ Roughness S4: $R_a = 6.3 \mu\text{m}$ Roughness S5: $R_a = 6.3 \mu\text{m}$ Roughness S6: $R_a = 6.3 \mu\text{m}$ Roughness S7: $R_a = 6.3 \mu\text{m}$ Roughness S8: $R_a = 6.3 \mu\text{m}$</p>	<p>O.M.U Grinding machine</p>	<p>Tornio twentieth caliber rugosimeter</p>	<p>$t_{tot60} = 10 \text{ min}$</p>
<p>70</p>	 <p>70.1execution finishing $\varnothing 15$ and L = 60mm</p> <p>Roughness S9: $R_a = 3.2 \mu\text{m}$</p> <p>70.2 execution of finished measure finishing $\varnothing 10$ and L = 30mm</p> <p>Roughness S10: $R_a = 3.2 \mu\text{m}$</p>	<p>O.M.U</p>	<p>Tornio</p>	<p>$t_{up\ to\ 70} = 30 \text{ sec}$</p>

80	 <p>80.1finishing execution $\varnothing 15.5$ and L = 40 mm</p> <p>Roughness S4: $R_a = 3.2 \mu\text{m}$</p> <p>80.2 Finish turning to eliminate residual excess metal.</p>	O.M.U	Tornio	$t_{tot80} = 28 \text{ sec}$
90	<p>90.1 Removal of residual stock left during roughing operations.</p> <p>90.2 1 mm chamfer execution</p>	O.M.U	Tornio	$t_{tot90} = 1 \text{ minute } 10 \text{ se}$
100	 <p>100.1 1 mm chamfer execution provided by the drawing on the edges of the piece</p>	O.M.U	Tornio	$t_{tot100} = 1 \text{ minute } 15 \text{ se}$
110	 <p>110.1 tongue seat execution on the S10 surface by means of a milling machine.</p>	O.M.U	milling machine	$t_{tot110} = 12 \text{ sec}$

<p>120</p>	 <p>120.1 Making the radial blind hole $\text{Ø}3 \times 10$ mm on the S4 main journal using column <i>drill</i>.</p> <p>Roughness: $R_a = 12.5 \mu\text{m}$</p>	<p>O.M.U</p>	<p>Pillar drill</p>	<p>$t_{tot120} = 17 \text{ sec}$</p>
<p>130*</p>	<p>130.1 Creation of axial lubrication holes by means of <i>drill press</i>.</p>	<p>O.M.U</p>	<p>Tornio</p>	<p>$t_{tot130} = 2 \text{ min}$</p>

*Step 130 was included in the manufacturing cycle because it was included on the part's construction drawing. However, the radial lubrication holes were not drilled during the workshop due to the lack of specific equipment required for correct positioning of the part and to avoid the risk of compromising geometric conformity. Therefore, this operation was considered exclusively at the design and documentation level.

4.4.6 Tools and equipment used

Various cutting tools and clamping fixtures were used to produce the crankshaft, selected based on the processes required by the production cycle and the machine tools available at the workshop of the affiliated Technical Institute.

The tools used allowed us to perform the turning, milling and drilling operations necessary to obtain the final geometry of the component.

4.4.6.1 Turning tools (parallel lathe)

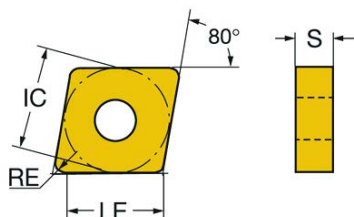
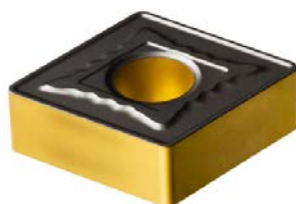
The operations of acing (S1, S14), turning of roughing (S2, S3, S4, S5, S6) and realization of the bevels (S8, S9, S10) were performed using a tool equipped with **insert CNMG 12 04 16-MR 4405** mounted on the **star DCLNR 2020K 12**.

The chosen insert has a particularly versatile geometry, which makes it suitable for general turning operations on carbon steels and low-alloy steels. Its robustness allows it to withstand the stresses typical of roughing operations, while the cutting edge geometry allows for good surface quality even in facing operations and chamfering. The insert is also made of hard metal (Widia), characteristic which increases wear resistance and thermal stability during chip removal operations, thus ensuring greater reliability and tool life.

For the realization of the centering holes a 60° center drill, compliant with DIN 333-A, was used at the ends of the shaft (S1, S2). This tool allows for obtaining conical seats suitable for supporting the workpiece between the lathe centers, ensuring correct positioning and greater precision during subsequent turning operations.

The operations of finish cylindrical surfaces (S2, S3, S4, S5 and S6) were machined using a tool equipped with **insert CCMT 09 T3 08-WF 1525** mounted on the **star SCLCR 2020K09**.

The insert features a positive geometry particularly suited to finishing operations on carbon steels, achieving good surface quality and reducing cutting forces. The small nose radius also allows for the precise production of small shoulders and cylindrical surfaces.

CNMG 12 04 16-MR 4405 T-Max® P, turning insert

Valori iniziali (KAPR 95 deg)

P2.1.Z.AN, Durezza: 175 HB




a_p 4 mm (1.5 - 8)
 f_n 0.6 mm/r (0.35 - 0.9)
 h_{ex} 0.6 mm/r (0.35 - 0.9)
 v_c 295 m/min (350 - 255)

K2.2.C.UT, Durezza: 245 HB

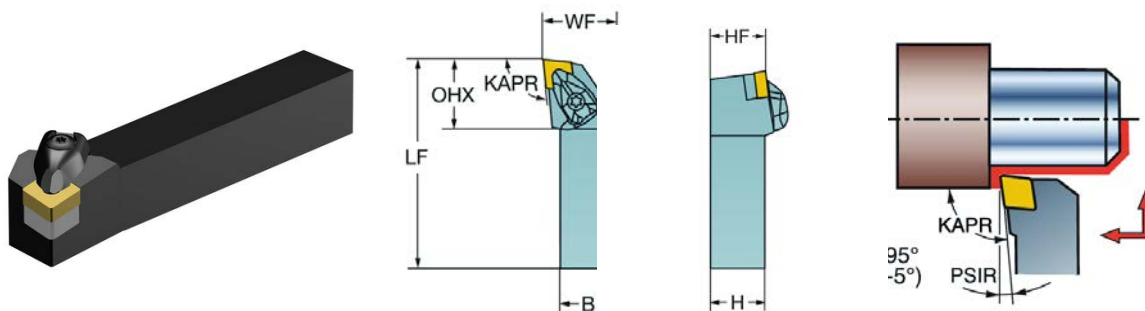


a_p 4 mm (2 - 8)
 f_n 0.5 mm/r (0.4 - 0.77)
 h_{ex} 0.5 mm/r (0.4 - 0.76)
 v_c 235 m/min (255 - 205)

Name	CNMG 12 04 16-MR 4405
Classification Level 1 (TMC 1 ISO)	
Type of operation(CTPT)	Roughing, facing, chamfering
Insert Mounting Type Code (Metric) (IFS)	Cylindrical fixing hole
Fixing hole diameter (D1)	5,156 mm
Size and shape of the insert	CN 1204
Number of Cutting Edges (CEDC)	4
Diameter of the inscribed circle (IC)	12,7 mm
Insert Shape Code (SC)	Rhombic 80
Effective cutting edge length (LE)	11,2959 mm
Tip radius (RE)	1,5875 mm
Version (HAND)	Neutral
Quality (GRADE)	4405
Substrate	HC
Coating (COATING)	CVD TiCN+Al ₂ O ₃ +TiN
Insert thickness (S)	4,7625 mm
Main clearance angle (AN)	0°
Insert seat (SSC M)	12
Price	17.90 €

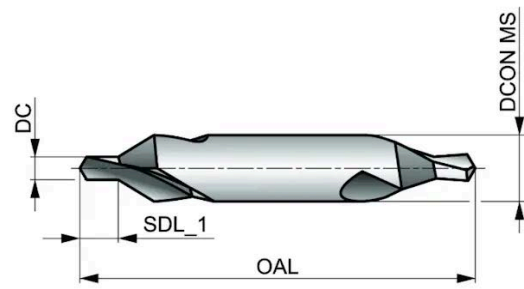
The insert is mounted on the following stem:

DCLNR 2020K 12 T-Max® P, shank tool for turning



Name	DCLNR 2020K 12
Tool cutting edge angle (KAPR 1)	95°
Tool lead angle(PSIR)	-5°
Mounting Type Code (MTP)	Clamp on top of insert and into hole.
Part 2 Interface identifiers for cutting items(CUTINT MASTER)	CNMG 120408
Machine Side Adapter Interface (ADINTMS)	Rectangular shank -metric: 20 x 20
Maximum working angle of the inclined plane (RMPX)	0°
Body Angle Workpiece Side (BAWS)	0°
Body Angle Machine Side (BAMS)	0°
Maximum Overhang (OHX)	32 mm
Version (HAND)	Right
Stem width (B)	20 mm
Stem height (H)	20 mm
Functional Length (LF)	125 mm
Functional Width (WF)	25 mm
Functional height (HF)	20 mm
Insert seat (SSC M)	12
Tilt angle(LAMS)	-6°
Price	113 €

Center drill - 60° A237 4.0X10.0



Name	A237 4.0X10.0
Material	HSS
Measure	4,00 x 10,0
Length	55 mm
Diameter	4,00 mm
Price	18.95 €

4.4.6.2 Milling tools (milling machine)

The tongue seat was made by milling using a **CoroMill® Plura solid carbide end mill for stable multi-operation milling**, with a diameter of 3 mm. The tool is particularly suitable for machining carbon steels and guarantees high rigidity, good surface quality, and effective chip evacuation. The cutter's diameter also allows for rounded slot ends, as required by the component geometry.

The tool diameter determines a terminal radius of the slot equal to 5.5 mm, consistent with the final geometry of the keyway.

The machining was carried out on a vertical milling machine by progressively removing the material until the required depth was reached.

Sandvik Coromant CoroMill® Plura solid cylindrical end mill (Widia)



Name	Cylindrical end mill
Material	Widia
Producer	Sandvik Coromant
Series	CoroMill® More
Diameter	3 mm
Number of cutting edges	4
Advance per tooth	0.04 mm/tooth
Price	85 €

4.4.6.3 Drilling tools (drill press)

The operations of drilling planned for the component were performed using appropriately sized twist drills based on the diameter required by the technical drawing.

In particular, the hole intended to house the coupling pin (or the fixing screw) was made using a **DIN 338 twist drill bit Ø3 mm in high-speed cobalt steel (HSS-Co)**. This tool guarantees good wear resistance and high reliability when machining C40 steel.

DIN 338 twist drill bit Ø3 mm



Name	DIN 338 twist drill bit
Material	HSS-Co
Diameter	3 mm
Tip angle	118°
Application	Plug hole
Price	4 €

The original crankshaft design also included lubrication holes, necessary to ensure the passage of oil to the surfaces most subject to friction during engine operation. These holes, characterized by particularly small diameters, would have required the use of precision micro-twist drills, preferably made of solid carbide or high-speed steel (HSS), with diameters between 1 and 2 mm. This type of tool is generally used for deep, high-precision drilling operations, but at the same time, it is more fragile and sensitive to cutting conditions.

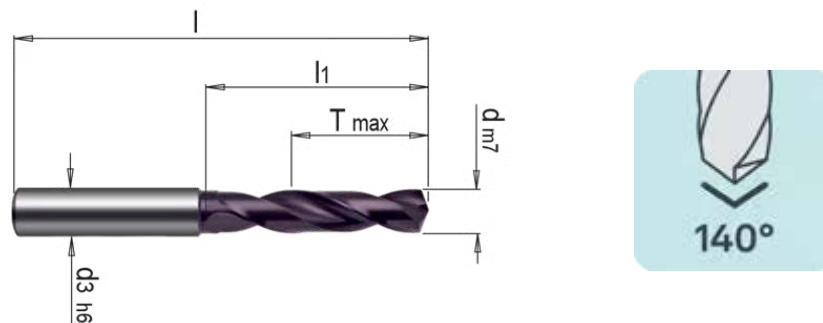
During the technological design phase, a more operationally stable alternative solution was also identified, which involves drilling holes on the shoulders of the workpiece (diameter Ø55 mm), in order to guarantee greater rigidity of the workpiece-tool system during machining and better centering precision.

However, due to the unavailability of suitable micro-drilling equipment at the workshop and the high risk of tool breakage, such holes were not drilled into the physical part produced.

They were therefore considered exclusively at the design level, while remaining an integral part of the analysis of the manufacturing cycle and the technological choices adopted, as they represent a functional solution to the correct functioning of the shaft lubrication system.

Therefore, if the machining had been carried out, a micro solid carbide (VHM) twist drill with a diameter between 1 and 2 mm, suitable for drilling medium-alloy steels such as C40, would have been used to create the lubrication holes. This choice is justified by the greater rigidity of the tool compared to HSS drills, necessary to ensure precision and reduce the risk of breakage during machining.

Micro punta WZB 12222 - VHM 3xD



Name	WZB 12222 - Punta VHM 3xD
Material	Solid carbide (VHM)
Diameter	Ø1–2 mm (microforatura)
Tip angle	140°
Application	Lubrication holes
Price	35 €

4.5 Choice of cutting parameters

4.5.1 Preliminary considerations

Once the component material, the machine tools and the tools used have been defined, it is necessary to determine the cutting parameters to be adopted during the machining operations. removal of wood shavings.

The correct choice of these parameters directly influences the productivity of the process, the achievable surface quality, the dimensional accuracy of the component, the tool life and the power required from the machine tool.

In the case in question, the parameters were determined by considering:

- the material of the piece (normalized C40 steel);
- the type of machining to be performed (roughing, finishing, cheekiness, drilling and milling);
- the material of the tools used (sintered hard metal – Widia);
- the technical characteristics of the machines available at the Technical Institute's workshop;
- the operating conditions actually adopted during the practical realization of the component.

The parameters were selected following a progressive procedure. First, the recommended cutting speed was identified based on the workpiece material and tool. Subsequently, the theoretical spindle speed was calculated and compared with the speeds actually available on the machine tool, thus obtaining the actual cutting speed for the machining operation.

Once the cutting speed and RPM were defined, the feed rate and depth of cut were selected based on the type of machining required. Roughing operations were performed with higher feed rates and depths of cut, prioritizing material removal, while finishing operations used lower feed rates to ensure greater dimensional accuracy and a higher surface quality.

Finally, for each machining operation, the required power was checked by comparing it with the power actually available at the machine tool spindle, equal to approximately 3.15 kW, a value obtained considering the actual efficiency of the mechanical transmission.

4.5.2 Formulas and notations used

Spindle speed:
$$n = \frac{Vt \cdot 1000}{\pi \cdot D} [rpm]$$

Where:

- n = number of turns[rpm]
 - Vt = cutting speed[m/min]
 - D = diameter of the piece[mm]
-

Cutting speed:
$$Vt = \frac{n \cdot D \cdot \pi}{1000} [m/min]$$

Where:

- Vt = cutting speed[m/min]
 - D = diameter of the piece[mm]
 - n = number of turns[rpm]
-

Feed speed:
$$Va = n \cdot a [mm/rev]$$

Where:

- And = feed rate[mm/min]
 - a = feed per revolution[mm/rev]
-

Depth of pass:
$$p = \frac{D-d}{2} [mm]$$

Where:

- D = initial diameter
 - d = final diameter
-

Active processing time:
$$t_a = \frac{L+e}{Va}$$

Where:

- L = worked length
- e = tool overtravel
- Va = feed rate

4.5.3 Reference values for cutting speed and feed

Materiale da lavorare	Sgrossatura			Finitura			Sgrossatura e finitura				Troncatura				Filettatura				Foratura
	R	RR	W	R	RR	W	R	W	R	W	R	R	R	R	R	R	R	RR	
R = acciaio rapido RR = acciaio superrapido W = placchetta di metallo duro (widia)																			
Acciaio extra dolce	60	90	100	80	120	150	40	70	70	100	45	95	50	15	15	20	7	35	
Acciai duri	35	50	95	45	70	120	25	40	50	95	50	70	30	9	8	18	6	31	
Acciai extra duri	30	40	65	40	50	80	20	30	40	65	18	55	25	8	6	10	5	23	
Acciai bonificati	20	25	60	30	35	70	15	18	35	60	15	50	20	7	5	8	4	20	
Ghisa dolce	40	60	90	50	70	100	30	40	65	90	25	80	30	14	7	10	6	22	
Ghisa dura	20	40	60	30	55	70	15	20	40	60	18	55	18	8	6	8	4	20	
Rame - Bronzo	45	65	165	60	90	260	35	45	80	160	30	100	40	14	11	18	9	50	
Ottone	100	200	220	200	300	350	75	100	100	220	55	200	80	20	15	20	10	85	
Alluminio	200	300	400	300	500	600	150	200	300	400	150	300	150	30	24	30	15	175	

Recommended cutting speeds for lathe operations.

	tornire esterno		tornire interno		formare	troncare
	sgrossatura	finitura	sgrossatura	finitura		
Acciaio dolce	0,1-0,4	0,05-0,2	0,05-0,3	0,05-0,2	0,02-0,05	0,05-0,1
Acciaio duro	0,1-0,4	0,05-0,25	0,05-0,3	0,05-0,2	0,02-0,05	0,05-0,1
Acciaio extraduro	0,1-0,4	0,05-0,2	0,05-0,3	0,05-0,2	0,02-0,05	0,05
Acciaio trattato	0,1-0,4	0,05-0,2	0,05-0,3	0,05-0,2	0,02-0,05	0,05
Ghisa dolce	0,1-0,8	0,05-0,2	0,05-0,6	0,05-0,2	0,02-0,05	0,05-0,1
Ghisa dura	0,1-0,6	0,05-0,25	0,05-0,5	0,05-0,2	0,02-0,05	0,02-0,05
Rame-Bronzo	0,1-0,6	0,05-0,25	0,05-0,5	0,05-0,025	0,02-0,05	0,05-0,1
Ottone	0,1-0,8	0,05-0,25	0,05-0,6	0,05-0,2	0,02-0,1	0,05-0,2
Alluminio	0,1-0,8	0,05-0,25	0,05-0,4	0,05-0,2	0,05-0,2	0,05-0,3

Recommended feed rates for lathe operations.

The values reported in the previous tables represent indicative ranges obtained from technical literature and tool catalogues.

To choose the parameters actually used, reference was made to the characteristics of the C40 steel (extra hard steels) and of the hard metal tools used during the machining process.

4.5.4 Power available at the spindle

The lathe used at the *Technical Institute workshop* has a nominal engine power of 4,5 kW.

Considering a *mechanical efficiency of the transmission* equal to approximately 70%, the power actually available to the spindle is:

$$P_m = P_n \cdot \eta$$

$$P_m = 4,5 \cdot 0,70 = 3,15 \text{ kW}$$

This value was assumed as the maximum limit available during processing.

If the required power is greater than the available power, it will be necessary to reduce the cutting depth or the tool feed rate.

4.5.5 Parameters adopted for the processes

Based on the indicative values reported in the previous paragraphs, the characteristics of C40 steel and the limitations imposed by the machine tools available in the workshop, the cutting parameters actually adopted during the production of the component were defined.

To determine them, the procedure normally adopted in turning operations on traditional machine tools was followed.

First, the theoretical cutting speed was identified n_t . Referring to the technology tables for machining C40 steel using carbide tools (Widia). The values chosen depend on the type of machining to be performed (roughing, finishing, facing, drilling, or milling).

Once the theoretical cutting speed was defined, the **theoretical number of revolutions** of the spindle using the following relationship:

$$n_t = \frac{1000 \cdot V_t}{\pi \cdot D}$$

Where:

- diameter of the machined surface: D [mm]
- theoretical cutting speed: V_t [m/min]
- theoretical spindle speed: n_t [rpm]

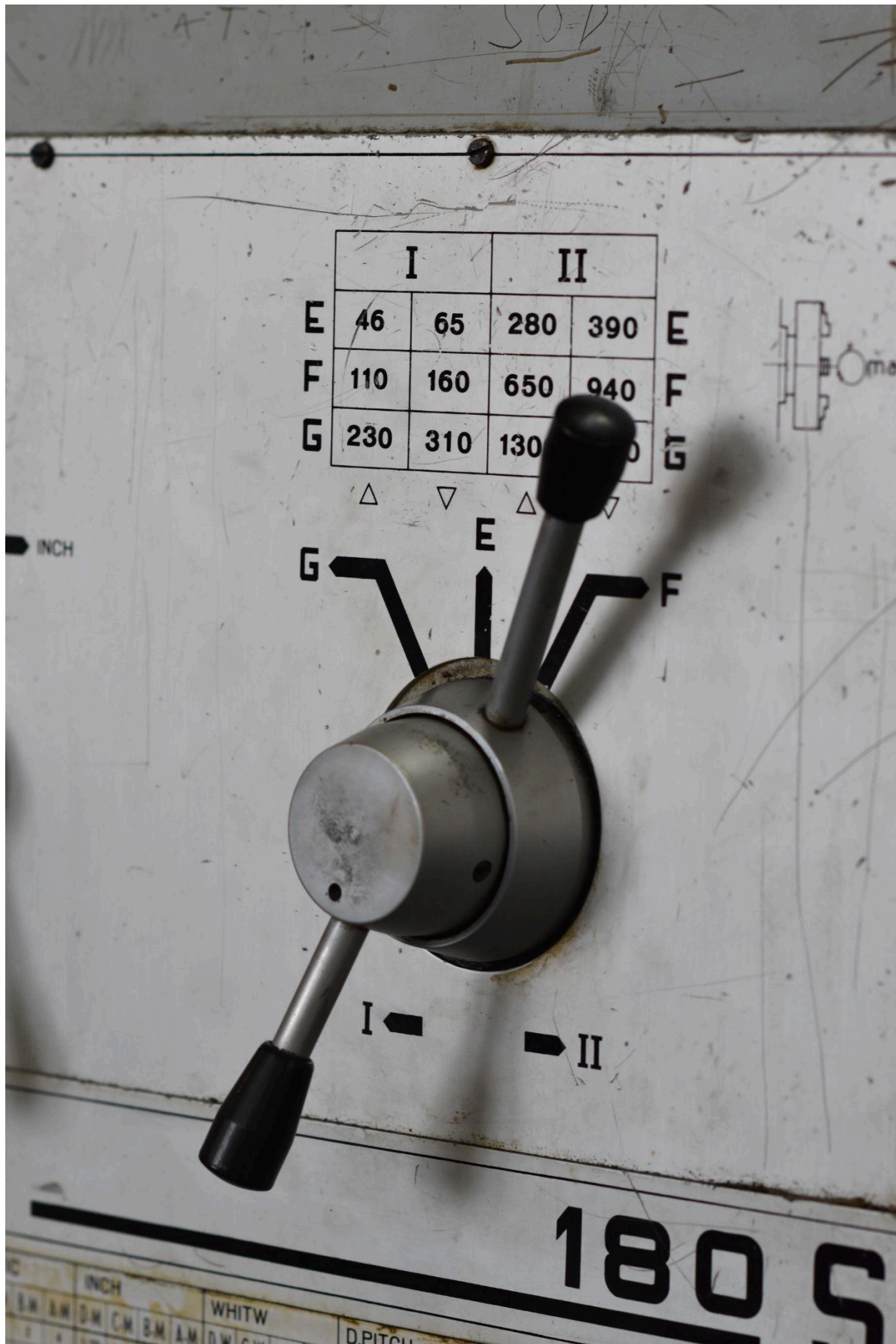


[Fig.21] Table of spindle speeds that can be set on the Labor parallel lathe in the workshop.

Since the parallel lathe used has a discrete number of selectable speeds, it is not always possible to set the calculated theoretical value exactly. For this reason, the **actual number of revolutions** n_c available on the machine closest to the theoretical value obtained [Fig. 17].

Starting from the number of revolutions actually set, it was then recalculated the effective cutting speed using the relationship:

$$V_c = \frac{\pi \cdot D \cdot n_c}{1000}$$

Where:

- diameter of the machined surface: D [mm]
- effective cutting speed: V_c [m/min]
- effective spindle speed: n_c [rpm]

Subsequently, the feed rate and depth of cut were defined based on the type of machining to be performed. Higher feed rates and depths of cut were used for roughing operations to maximize productivity and material removal. For finishing operations, however, lower values were used to ensure better surface quality and greater dimensional accuracy.

The parameters thus identified were finally verified by calculating the required cutting power, comparing it with the power actually available at the machine tool spindle.

Processing	Theoretical speed [m/min]	Average diameter [mm]	theoretical [rpm]	n adopted [rpm]	a [mm/giro]	p [mm]
Facing	65	60	345	390	0,15	1
Roughing	65	60	345	390	0,30	2
Finish	80	16	1592	1750	0,10	0,25
Bevels	80	16	1592	1750	0,10	0,50
Drilling	25	3	2653	1650*	0,05	/
Milling	90	/	2204	2000	0.04 [mm/tooth]	2

*For some machining operations performed on small diameters, the theoretical rpm was higher than the maximum speed available on the machines. In these cases, the maximum available rpm was adopted, accepting an actual cutting speed lower than the theoretically optimal one.

Before proceeding with the calculation of the machining parameters, it is also necessary to know the spindle speed values that can be selected on the **Gualdoni FU77 milling machine**.

The theoretical number of revolutions, calculated as a function of the cutting speed and the diameter of the tool, is in fact compared with the speeds available on the machine, choosing the closest value among those that can actually be set.

The following table shows the reference values used for selecting the spindle speed.

nc available spindle speed (rpm) <i>Gualdoni FU77 milling machine</i>	
55	90
140	220
355	560
900	1400
2240	3550

Similarly to what happens with the milling machine, also in the column drill **Bimak 32ME** the spindle speed is determined from the theoretical value calculated using the machining formulas and then adjusted to the values actually available on the machine.

The following table shows the spindle speed values considered as a reference for performing drilling operations.

nc available spindle speed (rpm) <i>Bimak 32ME column drill</i>	
200	280
400	560
800	1120
1600	2000
2240	2500

The values reported in the following tables represent the parameters used for the main operations performed on the piece.

4.5.5.1 Facing

Parameter	Value
Material	Q40
Tool	CNMG 12 04 16-MR 4405
Initial diameter	60 mm
n theoretical laps	345 rpm
n turns adopted	390 rpm
Theoretical cutting speed/ n_t	65 m/min
Effective cutting speed/ n_c	74 m/min
Progressa	0,15 mm/giro
Depth of pass p	1 mm

$$V_c = \frac{\pi \cdot D \cdot n_c}{1000} = \frac{\pi \cdot 60 \cdot 390}{1000} = 73.48 \text{ m/min}$$

4.5.5.2 Roughing turning

Parameter	Value
Material	Q40
Tool	CNMG 12 04 16-MR 4405
Average worked diameter	60 mm
n theoretical laps	345 rpm
n turns adopted	390 rpm
Theoretical cutting speed/ n_t	65 m/min
Effective cutting speed/ n_c	74 m/min
Progressa	0,30 mm/giro
Depth of pass p	2 mm

$$V_c = \frac{\pi \cdot D \cdot n_c}{1000} = \frac{\pi \cdot 60 \cdot 390}{1000} = 73.48 \text{ m/min}$$

4.5.5.3 Finish turning

Parameter	Value
Material	Q40
Tool	CCMT 09T308-WF 1525
Average diameter	16 mm
n theoretical laps	1592 rpm
n turns adopted	1750 rpm
Theoretical cutting speed/ n_t	80 m/min
Effective cutting speed/ n_c	88 m/min
Progressa	0,10 mm/giro
Depth of pass p	0,25 mm

$$V_c = \frac{\pi \cdot D \cdot n_c}{1000} = \frac{\pi \cdot 16 \cdot 1750}{1000} = 88 \text{ m/min}$$

4.5.5.4 Making chamfers

Parameter	Value
Tool	CNMG 12 04 16-MR 4405
Average diameter	16 mm
Theoretical cutting speed/ n_t	80 m/min
Effective cutting speed/ n_c	88 m/min
Progressa	0,10 mm/giro
Depth of pass p	0,50 mm
Chamfer angle	45°

$$V_c = \frac{\pi \cdot D \cdot n_c}{1000} = \frac{\pi \cdot 16 \cdot 1750}{1000} = 88 \text{ m/min}$$

4.5.5.5 Milling the tongue seat

Parameter	Value
Tool	CoroMill® Multiple Ø3 mm
Tool diameter	3 mm
Theoretical cutting speed/ n_t	90 m/min
Effective cutting speed/ n_c	33.44 m/min
n theoretical laps	9554 rpm
n turns adopted	3550 rpm
Number of cutting edges	4
Advance per tooth	0.04 mm/tooth
Depth of pass p	2 mm
Seat length	13 mm
Seat width	3 mm
Seat depth	2 mm

$$V_c = \frac{\pi \cdot D \cdot n_c}{1000} = \frac{\pi \cdot 3 \cdot 3550}{1000} = 33.44 \text{ m/min}$$

4.5.5.6 Drilling hole Ø3 mm

Parameter	Value
Tool	HSS-Co twist drill bit Ø3 mm
Theoretical cutting speed/ n_t	25 m/min
Effective cutting speed/ n_c	23.55 m/min
Hole diameter	3 mm
n theoretical laps	2654 rpm
n turns adopted	2500 rpm
Progress	0,05 mm/giro
Hole depth	10 mm
Tip diameter	3 mm

$$V_c = \frac{\pi \cdot D \cdot n_c}{1000} = \frac{\pi \cdot 3 \cdot 2500}{1000} = 23.55 \text{ m/min}$$

4.5.5.7 Lubrication holes

Parameter	Value
Tool	Microtip in hard metal $\varnothing 1 \div 2$ mm
Diameter	1,5 mm
Theoretical cutting speed v_t	20 m/min
n theoretical laps	rpm
Progress	0,03 mm/giro

Although not physically drilled into the component, lubrication holes were considered in the design phase. Drilling them would have required the use of precision micro-drills and particularly conservative machining parameters to avoid tool breakage.

The number of holes was chosen based on the need to ensure a uniform distribution of the lubricating film on the sliding surfaces of the bushings.

4.5.6 Checking the cutting power

Once the cutting parameters have been defined, it is necessary to verify that the power required for the machining operation is compatible with that actually available at the machine tool spindle.

The check is performed on the most demanding machining operation in the production cycle, represented by roughing turning, as it is characterised by the highest feed rates and depth of cut.

For roughing the following were adopted:

- pass depth $a = 2$ mm
- progress $f = 0,30$ rpm
- effective cutting speed $v_c = 122.5$ m/min

Chip cross-section calculation

$$A = a \cdot f$$
$$A = 2 \cdot 0,30 = 0,60 \text{ mm}^2$$

Cutting force calculation

For C40 steel, a specific *cutting pressure*:

$$k_s = 1800 \text{ N/mm}^2$$

Therefore

$$F_c = k_s \cdot A$$

$$F_c = 1800 \cdot 0,60 = 1080 \text{ N}$$

Cutting power calculation

The power required for the processing is:

$$P_c = \frac{F_c \cdot V_c}{60000}$$

Where:

- F_c is expressed in N;
- V_c is expressed in m/min.

$$P_c = \frac{1080 \cdot 122,5}{60000} = 2,21 \text{ kW}$$

Final check

So long as:

$$P_c = 2,21 \text{ kW} < P_c = 3,15 \text{ kW}$$

The machining is compatible with the power available at the lathe spindle.

The cutting parameters adopted can therefore be considered correctly sized for the machine tool used.

4.6 Calculation of processing times

Once the cutting parameters for the various processes have been defined, the time required to produce the component can be determined. Calculating processing times allows us to evaluate the productivity of the process and forms the basis for subsequent production cost estimates.

This study will only consider active machining times, i.e., the time during which the tool is actually engaged in material removal. Ancillary times related to workpiece positioning, tool changes, and movement between machine tools are considered negligible, as this is a single prototype being created in a school setting.

4.6.1 Application to work cycles

The times required to execute a work cycle are divided into active times (T_a), that is, the processing times effective during which the removal of material occurs, and passive times (T_p), which include all the phases that do not involve direct mechanical processing but are still necessary for completing the piece, such as tool assembly and disassembly, piece positioning, and machine setup operations. Their determination is often done using empirical tables, which allow for an indicative time estimate.

The active times derive directly from the cutting parameters adopted and the extension of the surfaces to be machined.

To determine the active times, in the case of turning and drilling operations, the following relationship is used:

$$t_a = \frac{L + e}{Va}$$

While for milling operations the formula is used:

$$t_a = \frac{L' + e}{Va}$$

Where:

- L it is the length of the processing;
- L' represents the travel in mm of the cutter axis required to complete the machining;
- e it is the extra race;
- a it is the advancement per revolution;
- N it is the rotation speed of the spindle;
- Va It is the speed of advancement.

Phase 10

10.1 Cutting the clip

Initial data:

- $L_i = 170\text{mm}$,
- $L_f = 162\text{ mm}$,
- $L_t = 8\text{ mm}$,
- $\varnothing 60$

$V_a = 0.012\text{ m/min}$ (linear speed of the blade)

$$t_{tot\ 10.1} = \frac{L_t}{V_a} = \frac{0,008}{0,012} = 0,67\text{ min} \rightarrow 40\text{ seconds}$$

We factor in the downtime required to position the piece, adjust the blade, and start cutting, which will be about 10 seconds. The cutting alone will take about 50 seconds, a value obtained from the calculation. Adding the preparation time, we arrive at a total time of about 1 minute.

$$t_{tot10} = 1\text{ min}$$

Phase 20

20.1 Certification surface 1

Initial data:

- material to be removed = 2 mm (standard certification light),
- Initial diameter $\varnothing 60$,
- $V_t = 65\text{ m/min}$

Taking the calculated values and inserted in the *Table 4.5.5.1 Facing turning*, we have:

$$n_t = 345\text{ rpm}$$

$$n_c = 390\text{ rpm}$$

$$a = 0,15\text{ mm/giro}$$

$$t_{tot\ 20.1} = \frac{2}{390 \cdot 0,15} = 0,034\text{ min} \rightarrow 2\text{ seconds}$$

20.2 Making a center hole

Standard data:

- centering hole depth = 3 mm
- drill feed (extra hard steels) = 0.030 m/min

$$t_{tot\ 20.2} = \frac{0,003}{0,030} = 0,10\text{ min} \rightarrow 6\text{ seconds}$$

We take into account the downtime required to position the piece on the lathe and start its rotation, which will be approximately 30 seconds. The cutting alone will take 2 seconds or a little more, a value obtained from the calculations. By subsequently adding the preparation, we arrive at a total time of

$$t_{tot\ 20} = 32 + 6 = 38\text{ sec}$$

Phase 30

30.1 Certification surface S2

Initial data:

- material to be removed = 2 mm (*standard certification light*),
- Ø60,
- $V_t = 65$ m/min

Taking the calculated values and inserted in the *Table 4.5.5.2 Facing turning*, we have:

$$n_t = 345 \text{ rpm}$$

$$n_c = 390 \text{ rpm}$$

$$a = 0,30 \text{ mm/giro}$$

$$t_{tot\ 30.1} = \frac{2}{390 \cdot 0,15} = 0,034 \text{ min} \rightarrow 2 \text{ seconds}$$

30.2 Making a center hole

Standard data:

- centering hole depth = 3 mm
- drill feed (extra hard steels) = 0.030 m/min

$$t_{tot\ 30.2} = \frac{0,003}{0,030} = 0,10 \text{ min} \rightarrow 6 \text{ seconds}$$

We take into account the downtime required to position the turned piece on the lathe and start its rotation, which will be approximately 30 seconds. The cutting alone will take 2 seconds or a little more, a value obtained from the calculations. By subsequently adding the preparation, we arrive at a total time of

$$t_{tot\ 30} = 32 + 6 = 38 \text{ sec}$$

Phase 40

40.1 Roughing cylinder

Initial data:

- Initial D = Ø60
- Final D = Ø56mm,
- L = Q.B. (about 120 mm),
- $V_t = 65$ m/min

$$n_t = \frac{1000 \cdot 65}{\pi \cdot 56} = 370 \text{ giri/min}$$

$$n_c = 390 \text{ rpm}$$

$$a = 0,30 \text{ mm/giro}$$

$$t = \frac{120 + 2}{390 \cdot 0,3} = 1 \text{ min (for each pass)}$$

We have established that at each pass we have to remove 4 mm of diameter, that is $60\text{mm} \rightarrow 56\text{mm}$, so the number of passes is 1.

$$t_{40.1} = 1 \cdot 1 = 1 \text{ min}$$

If we also consider downtime such as piece positioning, tailstock adjustment, etc., we add about 2 minutes. Therefore, the total time will be:

$$t_{tot\ 40.1} = 1\text{min} + 2\text{min} = 3 \text{ min}$$

40.2 Tracing by misalignment

Initial data:

- L = 120 mm
- *simple tracing*= standard low time

The following are taken into account:

- piece grip and fixing
- piece alignment
- tracking operation
- check and confirmation

all for an estimated time of 2.5 minutes.

$$t_{tracking\ 40.2} = 2,5 \text{ min}$$

$$t_{tot\ 40} = 3 + 2,5 \approx 5,5 \text{ min}$$

Phase 50

50.1 Roughing cylinder

Initial data:

- Final diameter S9 = $\varnothing 16$,
- L = 92 mm,
- $Vt_t = 65 \text{ m/min}$
- Initial D = $\varnothing 55 \text{ mm}$

$$n_t = \frac{1000 \cdot 65}{\pi \cdot 55} = 376 \text{ giri/min}$$

$$n_c = 390 \text{ rpm (actual)}$$

$$Vt = \frac{\pi \cdot 55 \cdot 390}{1000} = 67 \text{ m/min}$$

$$a = 0,30 \text{ mm/giro}$$

$$t = \frac{92 + 2}{390 \cdot 0,30} = \frac{94}{117} = 0,8 \text{ min} = 48 \text{ sec}$$

We have established that at each pass we have to remove 4 mm of diameter, that is $55\text{mm} \rightarrow 51\text{mm} \rightarrow 47\text{mm} \dots \rightarrow 16\text{mm}$, so the number of passes is 10.

$$t_{tot\ 50.1} = 0,8 \cdot 10 \approx 8 \text{ min}$$

50.2 Roughing cylinder

Initial data:

- Final diameter S10 = \varnothing 11,
- L = 31 mm,
- $In_t = 65$ m/min
- Initial D = \varnothing 16 mm

$$n_t = \frac{1000 \cdot 65}{\pi \cdot 16} = 1294 \text{ giri/min}$$

$$n_c = 1300 \text{ giri/min}$$

$$a = 0,10 \text{ mm/giro}$$

$$t = \frac{31+2}{1294 \cdot 0,1} = \frac{33}{129,4} = 0.25 \text{ min} = 15 \text{ sec}$$

We have established that at each pass we have to remove 4 mm of diameter, that is $16\text{mm} \rightarrow 12\text{mm}$, so the number of passes is approximated to 1.

$$t_{tot\ 50.2} = 15 \cdot 1 \approx 15 \text{ sec}$$

50.3 Elimination of excess metal (finishing)

n.b. For each job it takes 5 seconds to go back and reposition the tool.

$$n_t = \frac{1000 \cdot 80}{\pi \cdot 16} = 1592 \text{ giri/min}$$

$$n_c = 1750 \text{ giri/min}$$

$$a = 0,10 \text{ mm/giro}$$

$$V_a = 1592 \cdot 0.10 = 160 \text{ mm/min}$$

As this is a finishing step, 1mm of material can generally be removed in a single pass.

$$T_c = \frac{L_{tot}}{V_a}$$

Section 1 (\varnothing 11):

- Diametro: \varnothing 11
- Working length: 31 mm
- repositioning time: 5 sec

$$T_{c1} = \frac{31}{160} = 0.19 \text{ min} = 11 \text{ sec}$$

Section 2 (\varnothing 16 mm):

- Diameter: \varnothing 16 mm
- Working length: 61 mm
- repositioning time: 5 sec

$$T_{c2} = \frac{61}{160} = 0.38 \text{ min} = 23 \text{ sec}$$

$$t_{up\ to\ 50} = 8\text{min} + 15\text{sec} + 11\text{sec} + 5\text{sec} + 23\text{sec} + 5\text{sec} = 9 \text{ min}$$

Phase 60

60.1 throat execution at Ø15 and L = 10mm overhang.

Initial data:

- Cylinder diameter Ø56,
- L = 10 mm,
- Throat final diameter Ø15,
- $a = 0,30 \text{ mm/giro}$
- $V_t = 65 \text{ m/min}$

$$n_t = \frac{1000 \cdot 65}{\pi \cdot 56} = 369 \text{ giri/min}$$

$$n_c = 390 \text{ rpm (actual)}$$

$$V_c = \frac{\pi \cdot 56 \cdot 390}{1000} = 69 \text{ m/min}$$

$$V_a = n \cdot a = 390 \cdot 0.30 = 117 \text{ mm/min}$$

Considering an extra trip of 2 mm, we have:

$$L_t = 10 + 2 = 12 \text{ mm}$$

The time for each single pass is: $T_p = \frac{L_t}{V_a}$

$$T_p = \frac{12}{117} = 0.34 \text{ min} = 6 \text{ sec}$$

Now let's move on to calculating the number of passes to be made:

- material to remove: $56 - 15 = 41 \text{ mm}$ on the diameter;
- radial depth: $a_p = 2 \text{ mm}$;

$$n_{\text{past}} = \frac{41}{4} = 10,25 \approx 11 \text{ past}$$

This way we can calculate the total time:

$$t_{\text{tot}} = 6 \cdot 11 \approx 1 \text{ min } 10 \text{ sec}$$

We must take into account the eccentric assembly time of the piece with a 15 mm offset from the main axis. Add about 5 minutes. Therefore, the total time will be:

$$t_{\text{tot } 60.1} = 1 \text{ min } 10 \text{ sec} + 5 \text{ min} \approx 6 \text{ minutes } 10 \text{ seconds}$$

60.2 Roughing cylindrical grinding S4

Initial data:

- Final diameter Ø16
- Initial diameter Ø56,
- L = 40 mm
- $V_t = 65$ m/min
- $a = 0,30$ mm/giro

$$n_t = \frac{1000 \cdot 65}{\pi \cdot 56} = 369 \text{ giri/min}$$

$$n_c = 390 \text{ giri/min}$$

$$V_c = \frac{\pi \cdot 56 \cdot 390}{1000} = 68.6 \text{ m/min}$$

$$t = \frac{40}{390 \cdot 0,3} = \frac{40}{117} = 20 \text{ sec}$$

We have established that at each pass we have to remove 4 mm of diameter, that is 55mm → 51mm → 47mm... → 16mm, so the number of passes is 10.

$$t_{tot\ 60.2} = 20\text{sec} \cdot 10 = 3,5 \text{ min}$$

Since the workpiece is mounted eccentrically and the machining involves significant imbalances, a reduced feed rate of 0.10 mm/rev was chosen to limit vibrations and stresses.

$$t_{tot\ 60} = 3,5 + 6\text{min } 10\text{sec} = 10 \text{ min}$$

Phase 70

70.1 S9 finishing execution

Initial data:

- Final diameter Ø15
- L = 60 mm
- $In_t = 80$ m/min
- $a = 0,1$ mm/giro

$$n_t = \frac{1000 \cdot 80}{\pi \cdot 15} = 1698 \text{ giri/min}$$

$$n_c = 1750 \text{ giri/min}$$

$$V_c = \frac{\pi \cdot 15 \cdot 1750}{1000} = 82.42 \text{ m/min}$$

$$t_{tot\ 70.1} = \frac{60}{1750 \cdot 0,1} = \frac{60}{175} = 0.34 \text{ min} = 20 \text{ sec}$$

70.2 S10 finishing execution

Initial data:

- Final diameter Ø10
- L = 30 mm
- $V_t = 80$ m/min
- $a = 0,1$ mm/giro

$$n_t = \frac{1000 \cdot 80}{\pi \cdot 10} = 2547 \text{ giri/min}$$

$$n_c = 1750 \text{ giri/min}$$

$$V_c = \frac{\pi \cdot 10 \cdot 1750}{1000} = 55 \text{ m/min}$$

$$t_{tot\ 70.2} = \frac{30}{1750 \cdot 0,1} = \frac{30}{175} = 0.17 \text{ min} = 10 \text{ sec}$$

$$t_{up\ to\ 70} = 20 + 10 = 30 \text{ sec}$$

Phase 80**80.1S4 finishing execution**

Initial data:

- Final diameter Ø 15.5
- L = 40 mm
- $In_t = 80$ m/min
- $a = 0,1$ mm/giro

$$n_t = \frac{1000 \cdot 80}{\pi \cdot 15,5} = 1643 \text{ giri/min}$$

$$n_c = 1750 \text{ giri/min}$$

$$V_c = \frac{\pi \cdot 15,5 \cdot 1750}{1000} = 85 \text{ m/min}$$

$$t_{tot\ 80.1} = \frac{40}{1750 \cdot 0,1} = \frac{40}{175} = 0.23 \text{ min} = 14 \text{ sec}$$

80.2 Finishing execution - elimination of excess metal S4

Initial data:

- Final diameter Ø 15
- L = 40 mm
- $V_t = 80$ m/min
- $a = 0,1$ mm/giro

$$V_c = \frac{\pi \cdot 15 \cdot 1750}{1000} = 82.42 \text{ m/min}$$

$$t_{tot\ 80.2} = \frac{40}{1750 \cdot 0,1} = \frac{40}{175} = 0.23 \text{ min} = 14 \text{ sec}$$

$$n_t = \frac{1000 \cdot 80}{\pi \cdot 15} = 1698 \text{ giri/min}$$

$$n_c = 1750 \text{ giri/min}$$

$$t_{tot\ 80} = 14 + 14 = 28 \text{ sec}$$

Phase 90

90.1 Finishing execution -S9 and S10 overmetal removal

$$D_{half} = \frac{10+15}{2} = 12,5 \text{ mm}$$

90.1.1 S9 excess metal removal

Initial data:

- Final diameter $\varnothing 15$
- $L = 60 \text{ mm}$
- $V_t = 80 \text{ m/min}$
- $a = 0,1 \text{ mm/giro}$

$$n_t = \frac{1000 \cdot 80}{\pi \cdot 15} = 1698 \text{ giri/min}$$

$$n_c = 1750 \text{ giri/min}$$

$$V_c = \frac{\pi \cdot 15 \cdot 1750}{1000} = 82,42 \text{ m/min}$$

$$t = \frac{60}{1750 \cdot 0,1} = \frac{60}{175} = 0,34 \text{ min} = 20 \text{ sec}$$

90.1.2 S10 excess metal removal

Initial data:

- Final diameter $\varnothing 10$
- $L = 30 \text{ mm}$
- $V_t = 80 \text{ m/min}$
- $a = 0,1 \text{ mm/giro}$

$$n_t = \frac{1000 \cdot 80}{\pi \cdot 10} = 2547 \text{ giri/min}$$

$$n_c = 1750 \text{ giri/min}$$

$$V_c = \frac{\pi \cdot 10 \cdot 1750}{1000} = 55 \text{ m/min}$$

$$t = \frac{30}{1750 \cdot 0,1} = \frac{30}{175} = 0,17 \text{ min} = 10 \text{ sec}$$

$$t_{tot\ 90.1} = 20 + 10 = 30 \text{ sec}$$

90.21 mm chamfering on S9 and S10

For a $1 \times 45^\circ$ chamfer on a lathe, 3–5 seconds are normally considered, using the tool working from right to left.

The following are considered:

- total number of bevels: 2;
- Average chamfer time: 5 sec.

In total, the estimated time would be: $t = 2 \cdot 5 = 10 \text{ sec}$

By adding additional time to position and check the piece, we add a passive time of about 30 seconds.

$$t_{tot\ 90.2} = 10 + 30 = 40 \text{ sec}$$

$$t_{tot\ 90} = 40 + 30 = 1 \text{ minute } 10 \text{ seconds}$$

Phase 100

100.1 Execution of 1 mm remaining chamfers

For a $1 \times 45^\circ$ chamfer on a lathe, 3–5 seconds are normally considered, using the tool working from right to left.

The following are considered:

- total number of bevels: 5;
- Average chamfer time: 5 sec.

In total, the estimated time would be: $t = 5 \cdot 5 = 25 \text{ sec}$

By adding additional time to position and check the piece, we add a passive time of about 30 seconds.

$$t_{tot\ 100.2} = 25 + 30 = 55 \text{ sec}$$

$$t_{tot\ 100} = 55 + 30 = 1 \text{ minute } 15 \text{ seconds}$$

Phase 110

110.1 Tongue seat execution on S10

Initial data:

- CoroMill Plura tool diameter $\varnothing 3$
- advancement per tooth $f_{With} = 0.04 \text{ mm/tooth}$
- No. of tool teeth $z = 4$
- $L = 13 \text{ mm}$
- $V_t = 90 \text{ m/min}$

$$n_t = \frac{1000 \cdot 90}{\pi \cdot 3} = 9554 \text{ giri/min}$$

$$n_c = 3550 \text{ giri/min}$$

$$V_c = \frac{\pi \cdot 3 \cdot 3550}{1000} = 33.44 \text{ m/min}$$

The calculated actual speed is less than half the theoretical one. Due to the milling machine's maximum rotation speed ($n = 3550 \text{ mm/rev}$), which is lower than the calculated theoretical value (9554 mm/rev), it was necessary to adopt a reduced cutting speed.

As a result, the actual feed rate is lower than the theoretical one, resulting in an increase in machining time. However, this choice is forced by the machine constraints and ensures that the cutting conditions set for the tool are maintained, avoiding uncontrolled changes in the load per tooth.

But keeping the advance per tooth unchanged ($f_z = 0.04 \text{ mm/tooth}$), the linear advance is proportionally reduced according to the relation $V_a = f_z \cdot z \cdot n_c$.

Let's consider an extra trip of 3 mm of tool entry and exit to be added to the total length of the seat and we go to calculate the time.

$$t_{active\ 110} = \frac{L_{tot}}{V_a} = \frac{13+3}{0,04 \cdot 4 \cdot 3550} = \frac{16}{568} = 0,028 \text{ min} \approx 2 \text{ sec}$$

To this value it is necessary to add the downtime related to non-productive machine movements, such as rapid approach, entry and exit from the tool and small connection movements between the trajectories, which we estimate to be around 10 seconds in total.

$$t_{tot\ 110} = 2 \text{ sec} + 10 \text{ sec} = 12 \text{ sec}$$

Phase 120

120.1 Drilling of the $\varnothing 3 \times 10$ mm blind radial hole on the S4 main journal

Initial data:

- Tool diameter: $\varnothing 3$
- hole depth: 10 mm
- $V_t = 25 \text{ m/min}$
- $a = 0,05 \text{ mm/giro}$

$$n_t = \frac{1000 \cdot 25}{\pi \cdot 3} = 2654 \text{ giri/min}$$

$$n_c = 2500 \text{ giri/min}$$

$$V_c = \frac{\pi \cdot 3 \cdot 2500}{1000} = 23.55 \text{ m/min}$$

The feed rate per revolution was assumed to be 0.05 mm/rev, resulting in a linear feed rate of:

$$V_a = 0,05 \cdot 2500 = 125 \text{ mm/min}$$

Considering the hole depth of 10 mm and the correction due to the drill bit of 1.2 mm, the cutting time is equal to:

$$t_{active\ 120} = \frac{11,2}{125} = 0.09 \text{ min} = 5 \text{ sec}$$

By adding the additional times of positioning, approach and retraction of the tool of 12 seconds, the overall cycle time for a single hole can be estimated in the order of:

$$t_{tot\ 120} = 5 \text{ sec} + 12 \text{ sec} = 17 \text{ sec}$$

Phase 130

130.1 Drilling 6 axial lubrication holes using a pillar drill

Initial data:

- Tool tip diameter $\varnothing 1.5$ mm
- Hole type: through
- $V_t = 15$ m/min
- $a = 0,03$ mm/giro
- No. of holes: 6

$$n_t = \frac{1000 \cdot 15}{\pi \cdot 1,5} = 3185 \text{ giri/min}$$

Since this value exceeds the maximum available speed of the drill press (2500 rpm), the maximum settable speed has been adopted:

$$n_c = 2500 \text{ giri/min}$$

$$V_c = \frac{\pi \cdot 1,5 \cdot 2500}{1000} = 12 \text{ m/min}$$

As a result of the machine constraint, the actual cutting speed is approximately 12 m/min. The feed rate per revolution of 0.03 mm/rev results in a linear feed rate of:

$$V_a = 0,03 \cdot 2500 = 75 \text{ mm/min}$$

Considering a drilling length of approximately 12 mm, the cutting time is

$$t_{active\ 130.1} = \frac{12}{75} = 0.16 \text{ min} = 10 \text{ sec}$$

Adding the additional positioning and movement times, the overall cycle time for a single hole of approximately 10 seconds, we obtain a total time of:

$$t_{all\ 130\ in\ forum} = 10 \text{ sec} + 10 \text{ sec} = 20 \text{ sec for each hole}$$

The total time for the 6 holes is therefore approximately $t_{tot\ 130} = 6 \cdot 20 = 2 \text{ min}$

4.6.2 Conclusions

On the basis of the cutting parameters adopted and the times calculated for each phase of the processing cycle, an overall production time of 1898 seconds was determined, corresponding to approximately **31.6 minutes** (\approx **32 minutes**) for the production of a single crankshaft. The resulting time includes both the active machining times and the downtime required for positioning the piece, tool changes, machine adjustments, and dimensional checks.

Since the component was made as **single piece**, intended for educational activities or as a possible spare part, the production time is consistent with processing carried out using traditional machine tools, without the use of dedicated equipment or automated processes.

4.7 Calculation of processing costs

The crankshaft production cost was determined by considering the main cost items involved in the production process: materials, machine tool usage, labor, and tool wear. Since this involves the production of a single component, the values reported represent a technical estimate aimed at assessing the economics of the process.

4.7.1 Cost of materials

The material used to make the component is C40 steel, used in the form of a solid cylindrical bar with a diameter of 60 mm and a length of 170 mm.

The material cost was estimated based on the average market price of C40 steel, approximately €1.20/kg. This value was assumed in the absence of an official supply price.

The weight of the blank was calculated from the volume of the cylinder and the density of the steel (7,850 kg/m³), obtaining a mass value of approximately 3.75 kg.

As a result, the estimated material cost per single piece is approximately:

€4.50 per piece

4.7.2 Cost of machines

The cost of using machine tools was estimated by considering the actual time spent on the lathe, the universal milling machine and the drill press during the machining cycle.

For the economic estimate, an average hourly cost was assumed, including energy consumption, machine wear and tear, and operating costs.

Machine	Usage time (approximate)	Hourly cost of using the tool*	Cost
<i>Tornio</i>	30 min	8 €/h	4 €
<i>Milling machine</i>	1 min	10 €/h	0,20 €
<i>Drill</i>	3 min	6 €/h	0,30 €
4,50 €			

*Since the tools used are designed to perform a high number of operations before being replaced, the individual component was not attributed its purchase cost, but rather the **cost of use**, or the cost portion corresponding to wear caused during machining. We adopt this process because the tools continue to be used until the end of their useful life and are not replaced after a single piece has been produced.

4.7.3 Labor costs

The labor cost was calculated considering the presence of two operators involved in the production process.

The hourly cost of an operator was assumed to be:

€20/h per operator

The cost of labor is then determined by multiplying the total processing time by the number of operators and the hourly cost.

In this case, labor costs are a significant component of the overall cost, as both resources are required to simultaneously manage the manufacturing and support phases.

Total time: 31.6 minutes = 0.527 h

Cost of labor per person: $0,527 h \cdot 20 \text{ €/h} = 10,54 \text{ €}$

Total labor cost: $10,54 \text{ €} \cdot 2 = 21,08 \text{ €}$

4.7.4 Tool Cost

The cost of the tools was evaluated considering the tools used during the turning, milling and drilling operations included in the crankshaft machining cycle.

The selected tools are:

Tool	Cost (€)
Insert CNMG 12 04 16-MR 4405	17.90
DCLNR 2020K12 Shank Tool	113
Center drill A237 4.0×10	18.95
CoroMill® Plura end mill	85
DIN 338 twist drill bit Ø3 mm	4
Micro-punta VHM Ø1–2 mm	35

Since the production process in question involves a single piece, it is incorrect to attribute the entire cost of the tools to the component. In fact, most tools have a long service life and can be used for numerous subsequent processes.

For this reason, their purchase cost was not entirely attributed to the single component, as this approach would lead to an unrealistic overestimation of the economic impact.

The cost of the tools was therefore estimated according to a consumption criterion, considering the actual wear generated by the machining operations and the average useful

life of the tools themselves. Specifically, each tool contributes to the cost of the part only for the portion corresponding to its consumption during the production of the individual component, while the remaining residual value is attributed to subsequent machining operations.

In this way, the unit cost is obtained as the ratio between the total consumption of tools in the batch and the overall production, according to the relationship:

$$\text{Tool cost per piece: } \frac{\text{total cost of tools consumed}}{\text{number of pieces produced}} = 3,00 \text{ €}$$

In the absence of a real production batch, consumption was directly related to the production of a single piece, assuming a theoretical distribution of tool life. The total tool cost is therefore interpreted as the sum of the usage portions actually consumed to produce the component.

Based on this methodology, the unit tool cost was estimated to be:

3,00 €

4.7.5 Total production cost

The total production cost of the component was determined as the sum of the main cost items previously analyzed: material costs, machine tool usage, labor, and tool consumption. This approach allows for a comprehensive estimate of the economic impact of the production process, consistent with the assumptions adopted for the machining of a single piece.

Adding the contributions of the individual items we obtain:

- **Material cost:** 4,50 €
- **Machine cost:** 4,50 €
- **Labor cost:** 21,08 €
- **Tool Cost:** 3,00 €

The total production cost is therefore equal to:

Total cost: €33.08 per piece

4.7.6 Conclusions and clarifications

Energy costs were not explicitly reported as a separate item because they were already implicitly included in the hourly cost of machine tools, which was defined as the total value including energy consumption, equipment wear, and operating costs. This methodological choice avoids duplication of cost items and ensures a more consistent representation of the overall industrial cost.

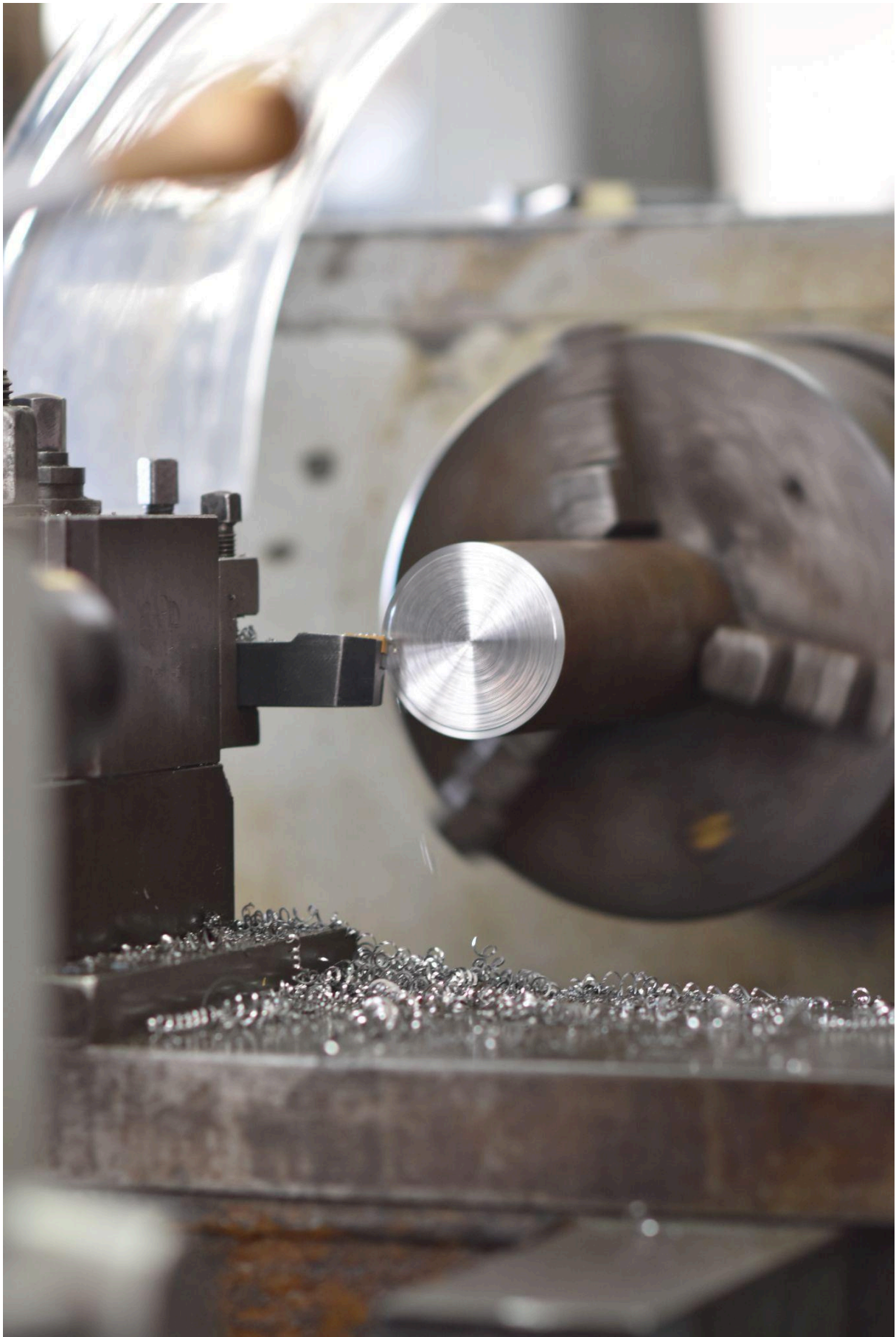


[Fig. 22] Operation of certification S1.

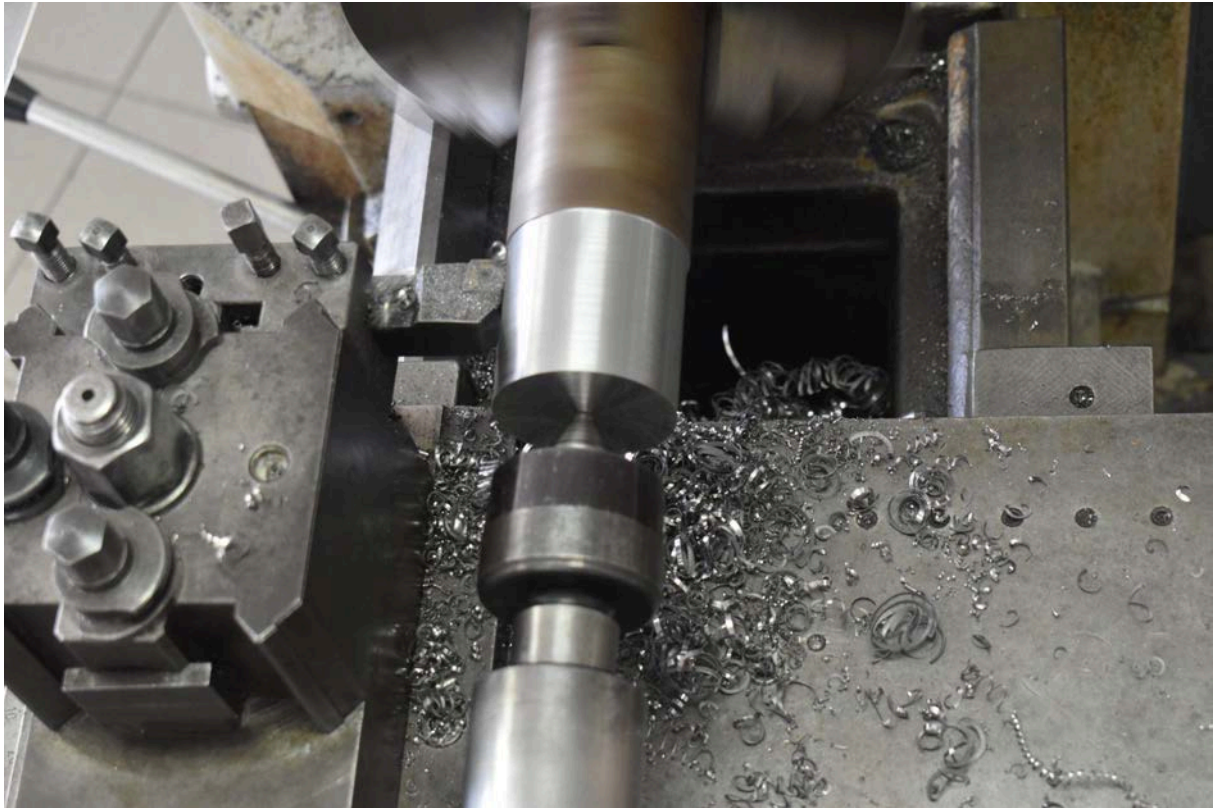


[Fig. 23] Finishing phase on the parallel lathe to optimize the surface roughness and dimensional precision of the piece.



[Fig.24] Processing and monitoring phases of the mechanical piece on the parallel lathe.



[Fig. 25] Technical Institute student during turning operations for the production of the component in the workshop.

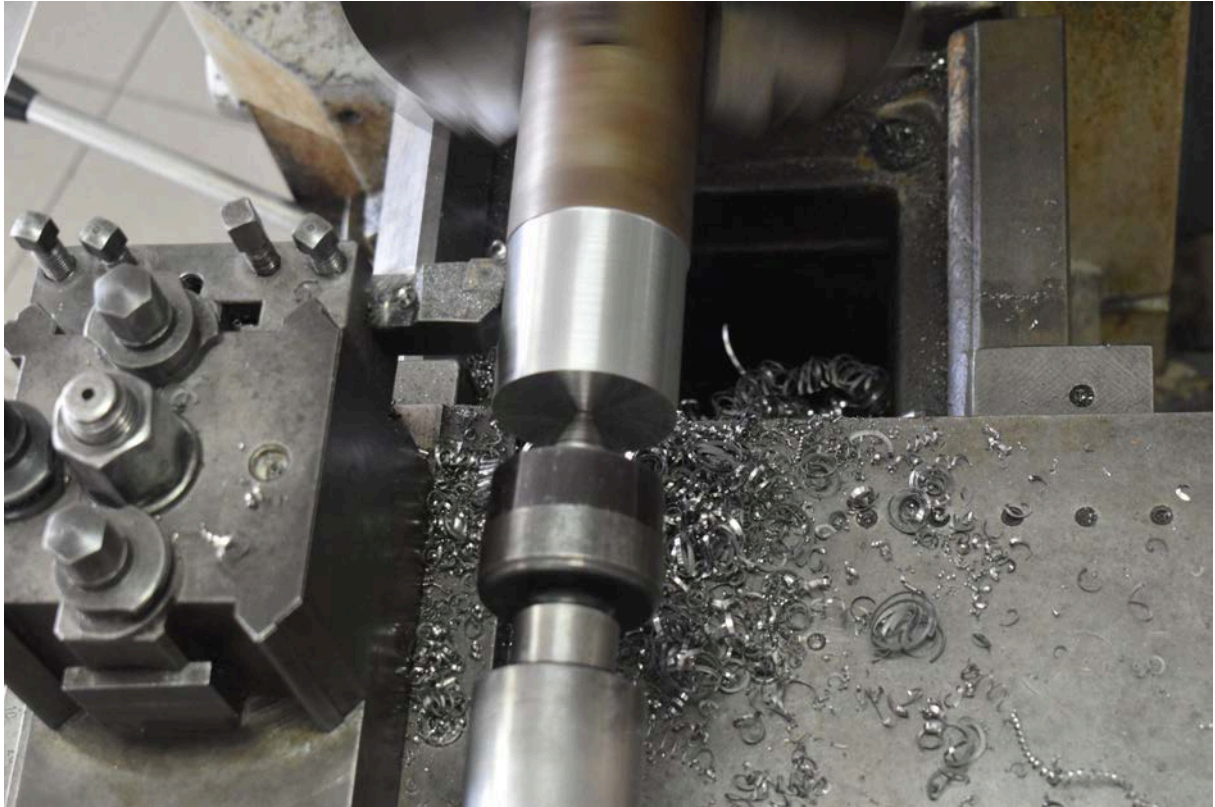
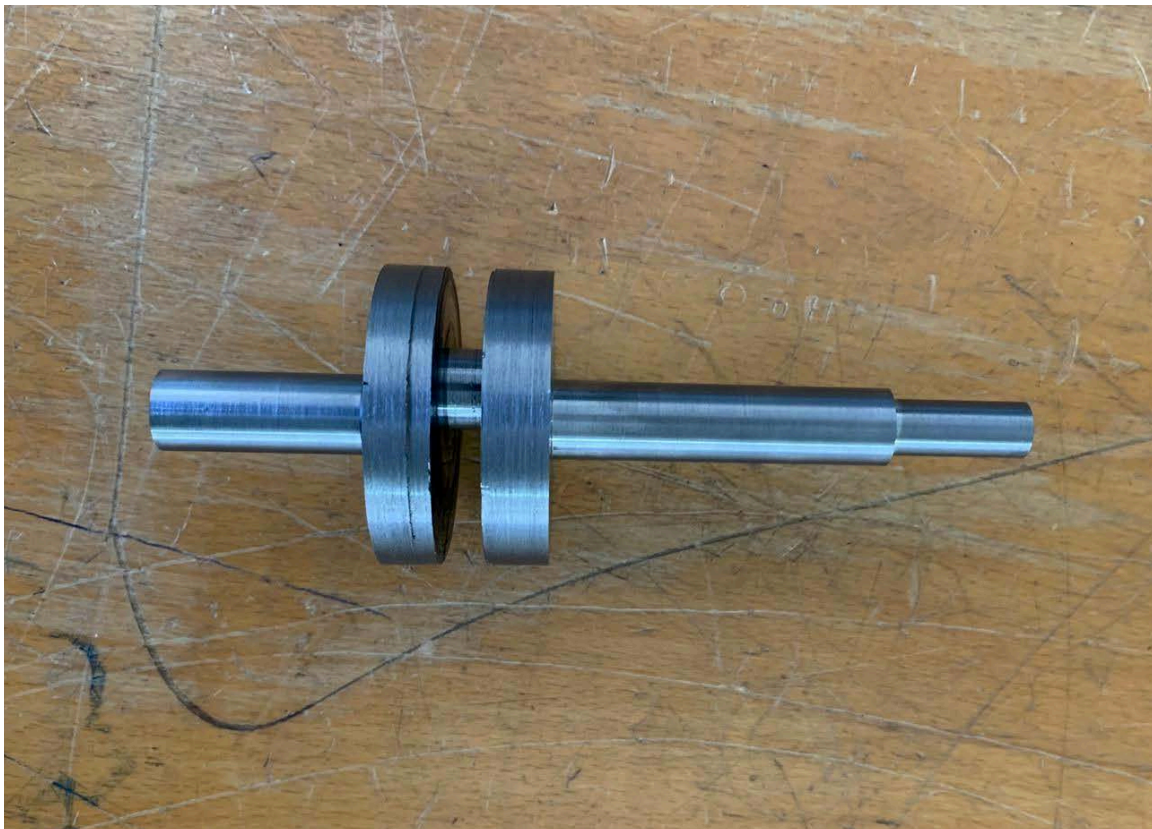


[Fig.26] Surface finishing operation on a parallel lathe with chip removal.



Finished piece without keyway and holes.

5. INTRODUCTION OF THE COMPONENT: PISTON (N.8)

Piece made in the laboratory

5.1 Description of the piece

The piston is one of the fundamental components of an internal combustion engine. It slides with reciprocating motion inside the cylinder and is responsible for converting the energy generated by the combustion of the air-fuel mixture into mechanical energy, which is then transmitted to the crankshaft via the connecting rod.

During engine operation, the piston is subjected to high mechanical and thermal stress. For this reason, it must be lightweight, mechanically strong, and have good heat dissipation capabilities to ensure reliability and longevity.

This paper will analyze two different piston manufacturing methods. The first involves the production of a prototype through 3D printing, using the equipment available in the school lab and primarily aimed at verifying the component's geometry and assembly. The second concerns a possible real-world industrial production, developed considering the materials and technologies typically used in the production of pistons for internal combustion engines.



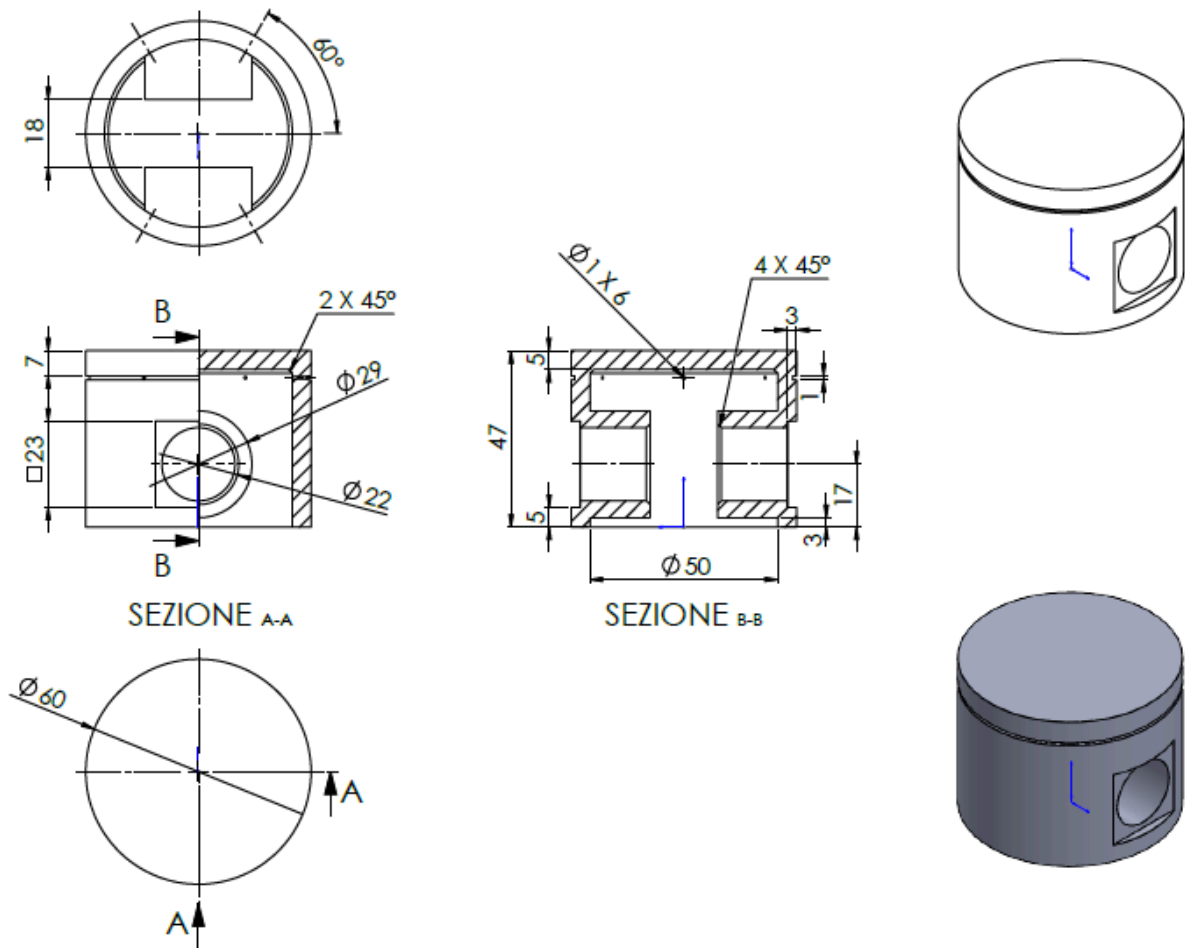


[Fig.27] Technical drawing with dimensions - piece no. 8.

5.2 Produced in collaboration with ITI

5.2.1 Choice of material:

PLA (polylactic acid) was chosen to create the prototype, a thermoplastic material widely used in FDM 3D printing applications due to its ease of processing, good dimensional accuracy, and reduced risk of deformations during printing.

PLA is made from renewable resources such as corn starch and sugarcane and has a relatively low extrusion temperature, generally between 180°C and 220°C. These characteristics make it particularly suitable for prototypes and demonstration models.

The choice of PLA was dictated by the availability of the material in the school lab and the need to obtain an accurate geometric model of the component. However, this material would not be suitable for real-world use as a piston in an internal combustion engine, as it lacks the mechanical and thermal characteristics necessary to withstand the high temperatures and stresses of operation..



5.2.2 Choice of production technique

FDM (Fused Deposition Modeling) technology, one of the most widespread additive manufacturing techniques, was chosen to create the prototype.

The process involves depositing molten thermoplastic material layer by layer until the component is completely created. The filament is fed to the extruder, heated to melting temperature, and then deposited onto the print bed following the trajectories generated by the slicing software.

FDM technology was chosen because it allows for rapid, dimensionally accurate prototypes, at low costs and reduced production times. Furthermore, it allows for the creation of complex geometries without the need for dedicated equipment.

5.2.3 Machine selection

To create our piece, we used a “Renkforce Pro 7 Dual” printer located at the Industrial Technical Institute of Rosignano Solvay.

We didn't choose this machine, as the institute only has this model. In the end, it proved to be quite capable and allowed us to complete the job without any problems.

The Renkforce Pro 7 Dual is a 3D printer with two independent extruders, allowing you to use two different filaments in the same print. This is very convenient for creating two-color objects or using different materials, such as the main filament and a water-soluble support for more complex structures. It supports nozzles from 0.2 to 0.8 mm and can work with a wide range of materials, including PLA, TPU, and even technical filaments like carbon fiber.

The printer is completely enclosed, with doors in the front and a lid on top, which helps maintain a safer and more temperature-stable printing environment, and the print surface measures 360 x 250 x 200mm, enough to create medium-sized objects or even something a little larger.

An interesting aspect of the “Pro 7 Dual” is its cooling system, which includes seven fans: two for the extruders, one at the back to regulate the internal temperature, one for the controller, and others that help keep everything balanced. It can reach up to 260°C on the extruders and up to 120°C on the heated bed, so it can work with even the most difficult materials.

For file transfer, you can use an SD card or connect via USB, and it is compatible with both Windows and macOS.

While printing, the noise is around 60 dB, which is quite quiet, comparable to a normal conversation. The interface is simple and intuitive, making it easy to use.

Even though it wasn't our direct choice, the “Renkforce Pro 7 Dual” proved to be reliable and versatile and helped us successfully print our components.

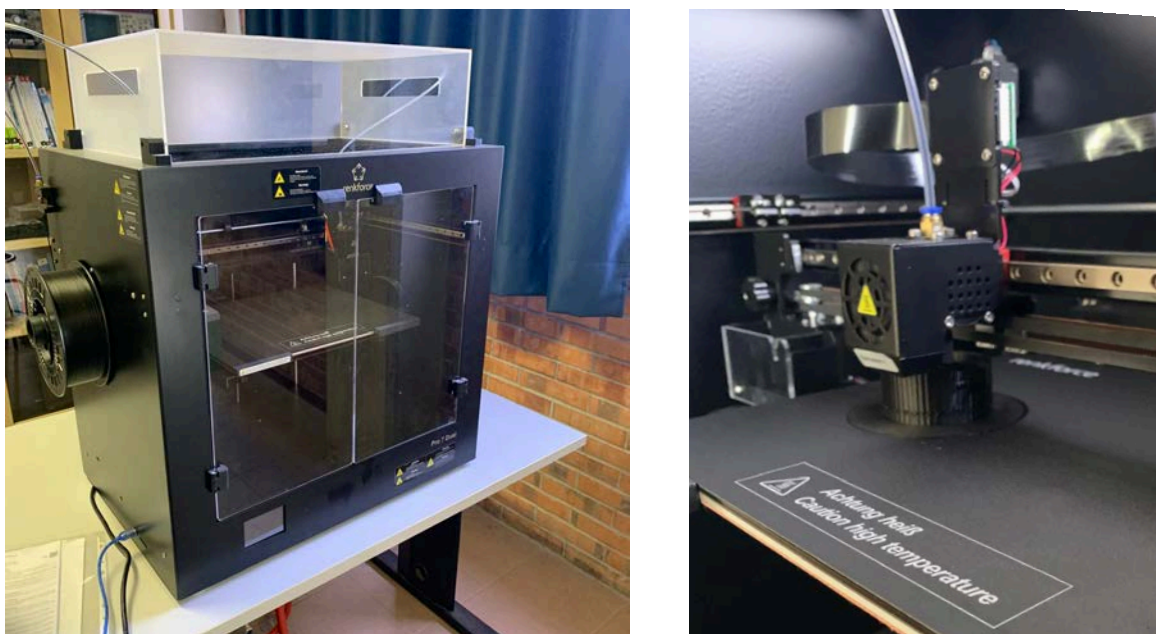


(Fig. 28)



<https://www.conrad.it/it/p/renkforce-pro-7-dual-stampante-3d-2584537.html>

5.2.4 Printing parameters

The parameters shown in the following table were used to create the piston.

Parameter	Value
Material	PLA
Nozzle diameter	0,4 mm
Layer height	0,20 mm
Infill	20%
Extruder temperature	210°C
Floor temperature	60°C
Supports	Not necessary
Orientation	Vertical piston axis

The vertical orientation was chosen to obtain better geometric quality of the external cylindrical surfaces and reduce the number of supports required.

5.2.5 Production times and costs

Estimating the total cost of producing a 3D printed part involves adding together multiple factors such as printing time, material consumption, the cost of electricity used, and the depreciation of the machine, along with labor costs.

Initial data

- **Printing time:** 5 hours and 30 minutes = 5.5 hours
- **Printer:** Renkforce Pro 7 Dual
- **Part type:** piston

- **Material:** PLA
- **PLA spool cost:** 25 €/kg
- **Coil weight:** 1 kg
- **PLA Density:** 1,24 g/cm³
- **Diameter of thread:** 1,75 mm
- **Coil length (approx.):** 330 meters per 1 kg

First, after collecting all the initial functional data from the print settings, we calculate the volume and subsequently the weight of the printed piece to estimate the cost of the material.

The relevant dimensions of the piston are:

- external diameter Ø50 mm
- total height 47 mm

The walls and internal structure vary, but as a reasonable estimate we can approximate the piston volume as a partially filled cylinder, with 20% infill, meaning only 20% of the inside of the part's volume is filled with material, while the remaining 80% is empty, but closed off by the outer walls.

Full cylinder volume:

$$V = \pi \cdot r^2 \cdot h = \pi \cdot (2,5)^2 \cdot 4,7 \approx 92,2 \text{ cm}^3$$

Considering infill and emptying:

The thin walls and holes reduce the actual volume, so we estimate an infill of 20%:

$$\text{actual material volume} = 92,2 \cdot 0,20 = 18,44 \text{ cm}^3$$

Consequently, the real volume taking that percentage into consideration turns out to be **18,44 cm³**.

Estimated weight with PLA density (1.24 g/cm³):

$$P = 18,44 \cdot 1,24 = 22,86 \text{ g}$$

Material cost:

$$PLA\ Cost = \frac{22,86 \cdot 25}{1000} = 0,57\ \text{€}$$

Electricity cost:

The Renkforce Pro 7 Dual printer consumes an average of about 120 watts while printing. Let's convert watts to kilowatts to calculate energy costs.

$$\frac{120\ \text{watt}}{1000} = 0,12\ \text{kW}$$

Now we can move on to calculating the energy consumed.

$$\text{energy consumed} = 0,12 \cdot 5,5 = 0,66\ \text{kWh}$$

Considering that the price of electricity is €0.30/kWh, we calculate:

$$\text{energy cost} = 0,66 \cdot 0,30 = 0,198\ \text{€} \approx 20\ \text{cents}$$

Finally, let's consider the cost of labor, which we assume was €15/h, for a total of 30 minutes between file preparation, print start, checking and removal of the piece. It will therefore be 7,50 €.

Let's now add up all the data we obtained from the calculations:

- **0,57 €** for 22.86 g of PLA (at a cost of €25/kg)
- **0,20 €** of electricity (consumption 120 W for 5.5 hours, at €0.30/kWh)
- **7,50 €** of manpower

$$0,57 + 0,20 + 7,50 = 8,27\ \text{€}$$

Therefore, the total cost for producing the piston via 3D printing is **8,27 €**.

Since we have previously assumed that only one piece will be produced, the final cost remains unchanged.

5.3 Real industrial production of the piston

5.3.1 Choice of material

For the industrial production of the piston using additive technologies, it is necessary to use a material capable of withstanding the high temperatures and significant mechanical stresses present during engine operation.

After comparing several metallic materials compatible with additive manufacturing processes, an aluminum alloy AlSi10Mg was selected.

This alloy is one of the most widely used materials in metal 3D printing processes thanks to its combination of lightness, good mechanical strength, and excellent thermal conductivity. It also has good printability and allows for the production of components characterized by high dimensional precision and low porosity.

The main properties of the AlSi10Mg alloy are shown in the following table.

<i>Property</i>	<i>Value</i>
Density	2,67 g/cm ³
Tensile strength	400 MPa
Elastic modulus	70 GPa
Thermal conductivity	150 W/m·K
Operating temperature	250-300 °C

The choice of this material allows us to obtain a light and resistant piston, fundamental characteristics for reducing the masses in motion and improve engine performance.

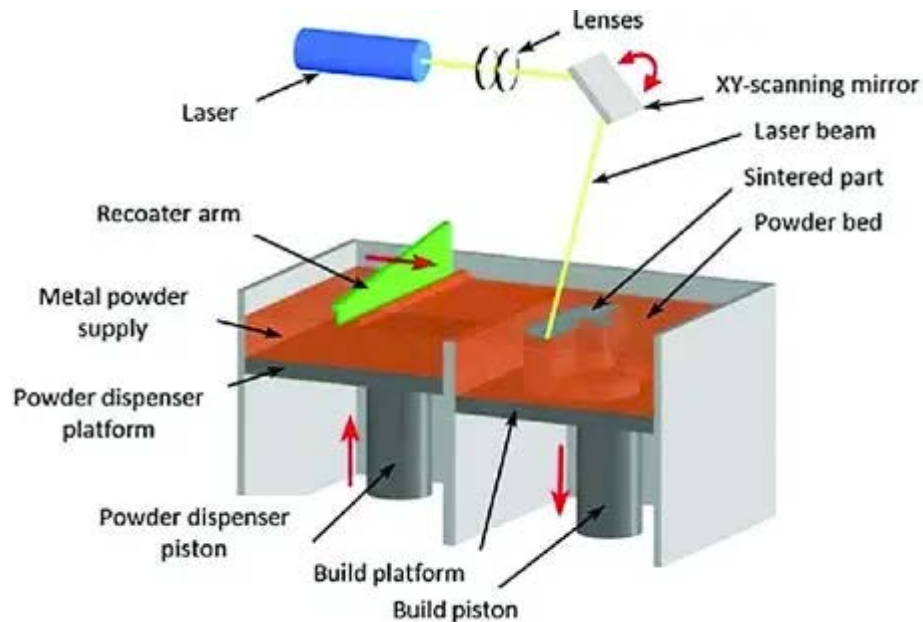
5.3.2 Choice of production technique

For industrial production the technology was selected **DMLS** (*Direct Metal Laser Sintering*), belonging to the family of powder bed additive manufacturing processes.

DMLS technology uses a high-power laser to selectively fuse successive layers of metal powder according to information from the 3D CAD model.

The process begins with a thin layer of metal powder being applied to the work surface. The laser then melts only the areas corresponding to the component's geometry. Once the layer is complete, the build surface is lowered and a new layer of powder is applied. The process is repeated until the part is complete.

This technology allows for the creation of complex geometries that are difficult to obtain using traditional processes and allows for a significant reduction in material waste.



5.3.3 Machine selection

For the production of the piston, an EOS M 290 industrial metal printer was chosen, one of the most popular machines for DMLS applications.



<i>Characteristic</i>	<i>Value</i>
Model	EOS M 290
Technology	DMLS
Material	AlSi10Mg
Construction volume	250 × 250 × 325 mm
Layer thickness	20 - 60 μm
Laser power	400 W
Working atmosphere	Argon

The machine guarantees high dimensional accuracy and adequate mechanical properties for components subject to high loads.

5.3.4 Production cycle

The production of the piston using DMLS technology involves the following phases:

- CAD modeling of the component.
- Preparing the STL file.
- Media generation.
- Model slicing.
- Loading of AlSi10Mg powder.
- Printer DMLS.
- Removing the piece from the build plane.
- Removal of supports.
- Stress-relieving heat treatment.
- Mechanical finishing of functional surfaces.
- Final dimensional check.

5.3.5 Production times and costs

Compared to the FDM printing used for the prototype, DMLS technology has longer production times and significantly higher costs, due both to the material used and the cost of the machine.

For the piston in question we can estimate:

- Printing time: 8h
- Material: €12
- Energy: €3
- Post-processing: 10 €
- Labor: €15

Estimated total cost:

$$C_{tot} = \text{€}40/\text{piece}$$

Despite its higher cost compared to FDM printing, DMLS technology allows for the production of a metal component that can actually be used in mechanical applications and features properties much closer to those required for a piston for an internal combustion engine.

6. INTRODUCTION OF THE COMPONENT: CONNECTING ROD (N.3)

6.1 Description of the piece

The connecting rod is one of the most stressed structural and kinematic components of the entire internal combustion engine. Its main function is to convert the reciprocating rectilinear motion of the piston (to which it is connected via the piston pin in the connecting rod big end, the smaller eye) into the continuous rotary motion of the crankshaft (to which it is connected via the crankshaft in the connecting rod small end, the larger eye).

From a geometric and functional point of view, the component is divided into three distinct portions:

- **Stem (or body):**the central connecting section, characterised by a typically "I" (or "H") profile specifically designed to maximise the moment of inertia and resist the heavy peak loads (elastic instability) and bending induced by the gas pressures in the combustion chamber.
- **Connecting rod end (small eye):**the upper portion that houses the coupling bushing with the piston pin.
- **Connecting rod foot (big eye):**the lower portion, in which an attachment is provided for the connection of the connecting rod.



During operation, the connecting rod is subjected to severe tensile (due to inertia forces at high rotational speeds) and compression (due to combustion) cycles, requiring exceptional mechanical properties, the absence of internal structural defects, and perfect mass balance. The planned annual production batch, in line with the other components of the assembly, is set at 1,000 units.

6.2 Choice of material

To meet the stringent functional requirements described above, which require high tensile strength, excellent fatigue strength, resilience, and at the same time low weight to reduce alternating inertia forces, it is necessary to discard foundry materials (such as cast iron or cast aluminum alloys) in favor of high-quality quenched and tempered steel or stamping steel.

The choice fell on **39NiCrMo3 steel**. The main advantages that led to this choice include:

- Extremely high mechanical and fatigue resistance: ideal for withstanding the millions of load cycles undergone by the connecting rod shaft.
- Excellent hardenability: guarantees homogeneity of mechanical properties even at the heart of the section changes between the barrel and the two eyes.
- Excellent aptitude for hot plastic deformation: allows the perfect filling of the mold impressions without triggering cracks or surface tears.

The main advantages that led to this choice include the extremely high mechanical resistance and the excellent aptitude for hot plastic deformation.

Main mechanical and physical properties of quenched and tempered steel (quenched and tempered state):

- **Yield strength (R_{and}):** $\geq 650 \div 750 \text{ MPa}$
- **Tensile strength (R_m):** $900 \div 1100 \text{ MPa}$
- **Elongation at break (A_5):** $\geq 12\%$
- **Resilience (KV):** $\geq 35 \text{ J}$
- **Density:** 7.85 kg/dm^3

In support of the data listed, in **Figure 29** and **Figure 30**. The technological diagrams and experimental plastic flow curves obtained from the material's technical data sheets are reported, which confirm the structural properties and the drastic reduction of the deformation stress to rise of the temperature above the 1000°C .



39NiCrMo3

ACCIAI DA BONIFICA

Norma di riferimento: EN 10083-3:2006

W.n*	1,6510	AFNOR	40NCD3
AISI	9840	BS	-
UNI	39NiCrMo3	JIS	-
DIN	36CrNiMo4	Altro	UNE F1282

COMPOSIZIONE CHIMICA

C	Si	Mn	P	S	Cr	Mo	Ni
0,35-0,43 ± 0,02	0,40 ± 0,03	0,50-0,80 ± 0,04	0,025 max + 0,005	0,035 max + 0,005	0,60-1,00 ± 0,05	0,15-0,25 ± 0,03	0,70-1,00 ± 0,05

Composizione chimica media in %

Può essere fornito con aggiunta di Piombo (Pb) da 0,15 a 0,35% per lavorabilità migliorata.

TEMPERATURA IN C°

Deformazione a caldo	Normalizzazione +N	Tempra +Q	Tempra +Q	Rinvenimento +T	Distensione +SR
1.100-900 °C	860 °C in aria	850 °C in olio o polimero	840 °C in acqua	550-650 °C in aria	50 °C sotto la temperatura di rinv.

Ricottura di lavorabilità +A	Ricottura isotermica +I	Ricottura completa	Tempra provetta Jominy	Preriscaldamento per saldatura	Distensione dopo saldatura
700 °C in aria (max 240 HB)	820 °C raff. in forno fino a 650 °C poi in aria (195-240 HB)	820 °C in aria (max 235HB)	850 °C in acqua	300 °C (~ 285 HB allo stato naturale)	550 °C raffredd. in forno

PROPRIETÀ MECCANICHE

LAMINATI A CALDO — Prova di trazione in longitudinale a 20 °C Caratteristiche meccaniche allo stato bonificato EN 10083-3:2006							
Diametro/spess. (in mm)		R	Rp 0,2	A%	Z%	Kv	HB
Oltre	Fino a	N/mm ²	N/mm ² min	min	min	J min	
-	16/8	980-1.180	785	11	40	-	295-354
16/8	40/20	930-1.130	735	11	40	35	278-339
40/20	100/60	880-1.080	685	12	45	40	263-327
100/60	160/100	830-980	635	12	50	40	249-295
160/100	250/160	740-880	540	13	50	40	224-263

TABELLA DI RINVENIMENTO Valori a temperatura ambiente su tondo ø 10mm dopo tempra in olio a 850 °C													
R N/mm ²	2.160	2.070	1.950	1.820	1.700	1.580	1.500	1.430	1.340	1.220	1.100	950	800
Rp 0,2 N/mm ²	1.440	1.520	1.540	1.520	1.490	1.440	1.370	1.290	1.220	1.110	980	830	670
HB	577	560	525	496	468	442	426	409	390	362	336	286	240
HRC	56	55	53	51	49	47	45,5	44	42	39	36	30	22,5
A %	8,0	9,8	10,4	10,6	10,7	10,8	11,0	11,5	12,5	13,8	16,0	19,0	22,0
Z %	30	42	48	52	53	53	54	55	56	57	60	63	68
Kv J	28	31	32	28	28	27	27	28	36	46	86	114	128
°C	100	150	200	250	300	350	400	450	500	550	600	650	700

[Fig. 29] Technical data sheet and mechanical properties of the selected quenched and tempered alloy steel for stamping.

LAMINATO RICOTTO E TRAFILATO A FREDDO +A+C - Prova di trazione in longitudinale a 20 °C - EN 10277-5:2008						LAMINATO RICOTTO PELATO RULLATO EN 10027-5:2008 - Prova di trazione long. a 20 °C			
Diametro (in mm)		R	Rp 0,2	A%	HB	R	Rp 0,2	A%	HB
Oltre	Fino a	N/mm ² min	N/mm ² min	min	max	N/mm ² min	N/mm ² min	min	
5**	10	-	-	-	295	-	-	-	-
10	16	-	-	-	290	-	-	-	-
16	40	-	-	-	285	-	-	-	240
40	63	-	-	-	280	-	-	-	240
63	100	-	-	-	280	-	-	-	240

LAMINATO BONIFICATO E TRAFILATO +QT+C - Prova di trazione in longitudinale a 20 °C - EN 10277-5:2008						TRAFILATO BONIFICATO +C +QT EN 10027-5:2008 - Prova di trazione long. a 20 °C			
Diametro (in mm)		R	Rp 0,2	A%	HB	R	Rp 0,2	A%	HB
Oltre	Fino a	N/mm ²	N/mm ² min	min	per info.	N/mm ²	N/mm ² min	min	per info.
5	10	980-1.180	735	8	295-354	-	-	-	-
10	16	930-1.130	700	8	278-339	-	-	-	-
16	40	930-1.130	700	9	278-339	930-1.130	735	11	278-339
40	63	880-1.080	625	10	263-327	880-1.080	735	12	263-327
63	100	880-1.080	600	10	263-327	880-1.080	735	12	267-327

* Valori validi anche per + Trafilato e Bonificato (+C+QT)

FORGIATO BONIFICATO — Prova di trazione e resilienza a 20 °C UNI 7874:1979 come riferimento								
Diametro (in mm)		R	Rp 0,2	A% L	A% T	Kv L	Kv T	HB
Oltre	Fino a	N/mm ²	N/mm ² min	min	min	J min	min	
-	100	880-1.080	685	12	-	40	-	263-327
100	250	685-835	540	13	12	30	25	209-250
250	500	655-805	490	15	14	30	25	201-241
500	1.000	635-785	440	16	15	25	-	195-234
1.000	-	590-740	390	15	14	25	-	176-224

L = longitudinale | T = tangenziale

VALORI DI TEMPRABILITÀ															
Jominy in HRC EN 10083-3:2006 (grandezza grano G5 minimo secondo UNI 3245) distanza dall'estremità temprata in mm															
	1,5	3	5	7	9	11	13	15	20	25	30	35	40	45	50
Min	52	51	50	49	48	46	44	43	39	36	34	33	32	31	30
Max	60	60	59	58	58	57	57	56	55	52	51	49	48	46	45

Temperatura	Modulo elastico		Espansione termica
	GPa		
°C	E long	G tang	(m/m*K)*10 ⁻⁶ °C
20	210	80	
100	-	-	11,2

[Fig. 30] Plastic flow curves and temperature sensitivity of forging steel.

6.3 Choice of processing technique

Depending on the connecting rod geometry, the requirement for maximum mechanical performance, and the production batch size (1,000 pieces/year), the selected plastic deformation processing technology is closed-die hot forging (or impression hot forging). The connecting rod requires massive deformation. The engineering and metallurgical reasons behind the choice of hot forging are as follows:

1. **Continuous grain of the material:** Hot forging plastically deforms the crystalline grains, orienting them according to the geometric profile of the connecting rod. The metal "fibers" thus faithfully follow the transition curves between the shaft and the eyes, dramatically increasing the component's fatigue strength and resilience.
2. **Elimination of internal defects:** The high hydrostatic pressure exerted by the presses closes the microporosities and seals any blowholes originally present in the semi-finished product.
3. **Economic optimization on the lot:** For a production run of 1,000 pieces, the initial investment for the design and production of the mold blocks (including the roughing and finishing impressions) is amortizable, while guaranteeing high geometric reproducibility and a drastic reduction in oversizes compared to a connecting rod machined entirely from solid.

The process will start from a cylindrical block (piece of bar) which will be heated above the recrystallization temperature of the steel (approximately $1100 \div 1150^{\circ}\text{C}$) to reduce the yield strength and increase ductility, to then be deformed through a sequence of mechanical press blows inside the relevant moulds, culminating with the operation of shearing the perimeter metal burrs (the scrap).

6.3.1 Machine selection

The production process selected for the manufacturing of the connecting rod is the closed-die hot forging of 39NiCrMo3 steel. Since the component is subject to high plastic deformations and requires the complete filling of the mold cavity, a **hydraulic forging press**.

Compared to hammer forging, the hydraulic press allows for more controlled material deformation, improved dimensional accuracy, and greater process repeatability. Another important difference is that the hydraulic press delivers a constant force throughout the entire stroke. These features are particularly advantageous for production runs of approximately 1,000 pieces, ensuring high component quality and reduced scrap.

Below we report the dimensioned technical drawing of the component.

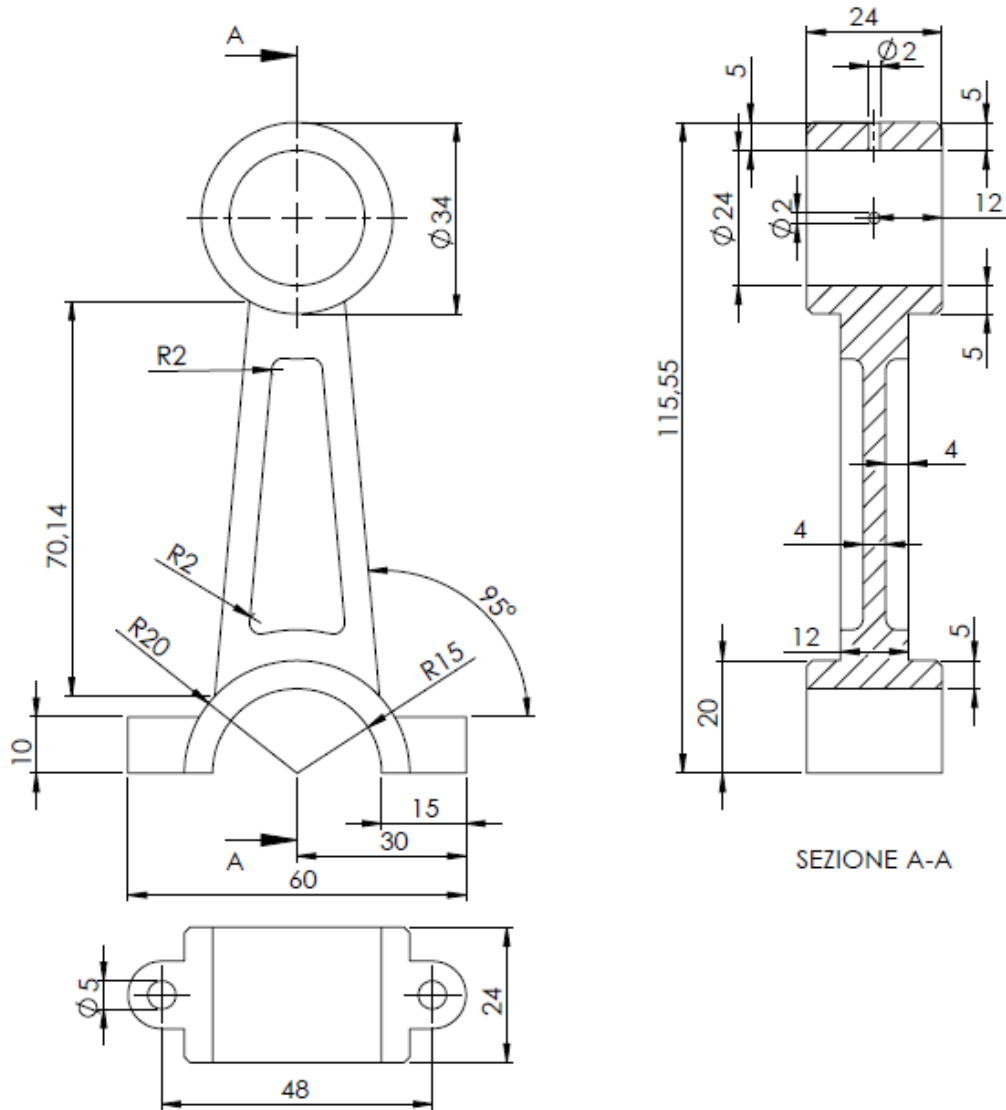


[Fig.31] Technical drawing with dimensions - piece no.3.

Considering the dimensions of the connecting rod and the mechanical characteristics of the steel used, a press with a nominal capacity of 400 t was selected, capable of providing the force necessary for the correct deformation of the material during the stamping process.

Characteristic	Value
Rated strength	400 t
Cylinder stroke	250 mm
Maximum opening	800 mm
Engine power	30 kW
Maximum operating pressure	25 MPa

The available force is adequate to ensure complete filling of the die and the correct formation of the connecting rod geometry. Furthermore, the cylinder stroke and the machine opening allow for the insertion of the stamping tools and the easy extraction of the forged piece. Finally, choosing a hydraulic press allows for better control of the material flow within the die, favoring the production of components with high mechanical characteristics and good dimensional accuracy.



[Fig. 32] Example of a 400-ton hydraulic press for hot forging and stamping operations of steel components.

6.4 Production cycle

The production of connecting rods by closed-die hot forging involves a series of operations aimed at obtaining a component with the desired geometry and adequate mechanical properties. The starting material is 39NiCrMo3 steel bars, which are first cut into pieces with the volume necessary to completely fill the die cavity. The blanks are then heated to the forging temperature, approximately between 1100°C and 1200°C, to reduce the material's resistance to deformation and promote flow within the die.

Once the desired temperature is reached, the blank is placed in the lower die of the press, which features a mold with the negative shape of the piece to be obtained, and is then subjected to the stamping operation. The action of the upper die, also featuring a mold of the final shape to be obtained, causes the material to deform plastically until it completely fills the cavity, thus assuming the shape of the connecting rod.

Once the forging process is complete, the burr, or excess material that has escaped along the die separation plane during the forging process, is trimmed. This operation allows for a geometry closer to the final component.

Subsequently, the piece is subjected to appropriate heat treatments, necessary to improve the mechanical properties of the steel and reduce any residual stresses generated during plastic deformation.

Finally, finishing mechanical processes are performed, such as boring holes, any drilling operations, and grinding of functional surfaces, in order to comply with the dimensional and geometric tolerances required by the project.

The production cycle diagram is shown below:

- *39NiCrMo3 steel bar → Cutting of the blank → Heating of the material (1100–1200 °C) → Hot forming in closed die → Trimming of the burr → Heat treatment → Finishing machining → Dimensional control → Finished connecting rod*

6.5 Calculation of the stamping force

- maximum length ≈ 116 mm;
- maximum width of the large head ≈ 48 mm.

The projected area can then be approximated as:

$$A_p = 116 \text{ mm} \cdot 48 \text{ mm} = 5568 \text{ mm}^2$$

For hot forging of alloy steels, the specific forging pressure generally assumes values between 600 and 1000 MPa. For 39NiCrMo3 steel at the forging temperature, an average value can be assumed:

$$p = 800 \text{ MPa} = 800 \text{ N/mm}^2$$

The pressing force is therefore:

$$F = p \cdot A_p$$

$$F = 4450 \text{ kN}$$

Converting to tons:

$$F = 454 \text{ t}$$

Since the value obtained represents a theoretical estimate, it is appropriate to consider a safety coefficient related to friction, temperature variations and the inevitable approximations of the model.

Therefore, the force required for the machining can be considered to be between:

$$450 - 500 \text{ t}$$

This result confirms the need to use a forging press with a capacity of at least 500 t, capable of ensuring complete filling of the die and correct deformation of the material.

6.6 Matrix design

To produce the connecting rod by hot forging, it is necessary to design a pair of dies capable of giving the material the desired geometry during plastic deformation.

Since the component has a relatively complex geometry but is symmetrical with respect to its median plane, a configuration consisting of a lower die and an upper die, both made of hot-work steel with high resistance to wear and thermal shock, was chosen.

The dividing line of the matrices was identified in the median plane of the connecting rod, so as to:

- facilitate the extraction of the piece;
- ensure correct filling of the cavity;
- reduce the construction complexity of the matrices;
- limit the formation of undercuts.

During stamping, the material tends to flow out along the parting plane, forming a thin forging burr. The presence of the burr is beneficial because it creates greater resistance to the outward flow of material, promoting complete filling of the most critical areas of the cavity.

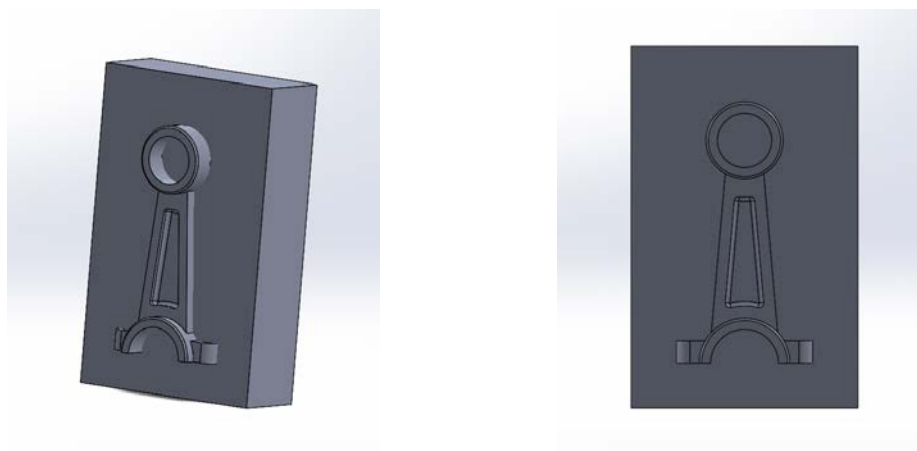
To facilitate the extraction of the piece from the dies, appropriate tools are also introduced **draft angles**, generally between 3° and 7° for hot-stamped components. In the case in question, a draft angle equal to 5° , a value that allows for easy extraction without significantly altering the geometry of the component.

Appropriate adjustments have been made in correspondence with the sudden changes in section. **connections** for the purpose of:

- improve material flow during deformation;
- reduce tension concentrations;
- increase the life of the matrices;
- limit the risk of filling defects.

The cavity of the dies was designed taking into account the subsequent mechanical processes required to create the holes and functional surfaces of the connecting rod. These processes will allow us to achieve the required dimensional tolerances and surface characteristics envisaged by the project.

The following images show a simplified diagram of the molding system used.



lower die → connecting rod → upper die



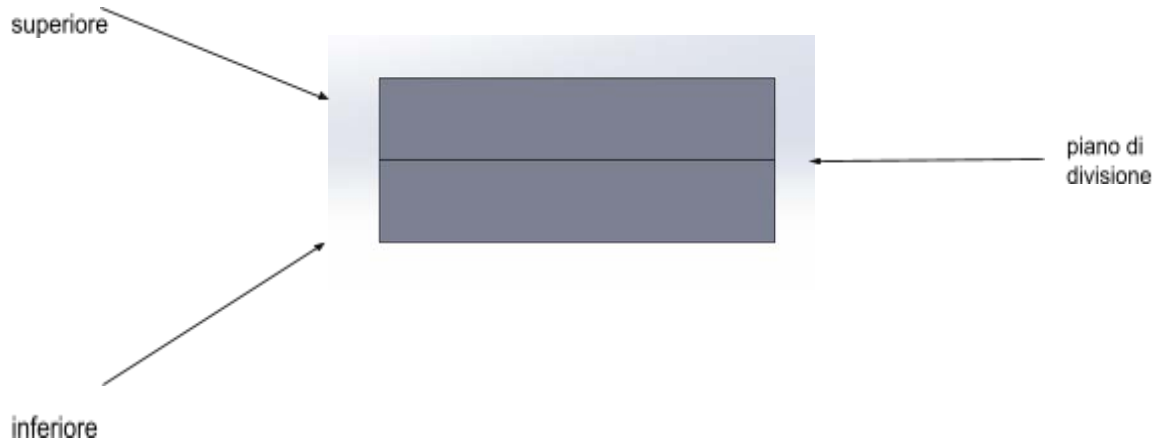


Figure 6.4 – Schematic representation of the semi-dies used for the hot stamping of the connecting rod and the relative division plane.

In reality, the matrices should be used in greater quantities because, to achieve the final shape, small modifications must be made each time until the matrix that yields the desired result is reached. The diagram used above shows the steps in a simplified manner.

6.7 Production times and costs

6.7.1 Production times

For the production of the connecting rod by hot forging in a closed die, the main phases of the production cycle are considered: cutting of the blank, heating, forging, trimming of the burr, heat treatment, final mechanical processing and dimensional control.

Phase	Estimated time per piece
Cutting the rough	1 min
Heating the raw material	10 min
Hot stamping	0,5 min
Trimming the burr	1 min
Heat treatment	15 min
Final mechanical processing	6 min
Dimensional control	1 min

The total estimated time for the production of a connecting rod is therefore:

$$T_{tot} = 1 + 10 + 0,5 + 1 + 15 + 6 + 1 = 34,5 \text{ min}$$

For a batch of 1000 pieces:

$$T_{batch} = 34,5 \text{ min} \cdot 1000 = 34,500 \text{ min} = 575 \text{ h}$$

This value represents an overall estimate of the production cycle. In actual production, some operations, such as heating and heat treatment, can be performed on multiple parts simultaneously, reducing the actual time per individual component.

6.7.2 Production costs

The cost estimate takes into account the cost of the material, the cost of the labor, the cost of using the machine and the cost of the dies.

The chosen material is 39NiCrMo3 steel. Considering an estimated mass of the blank equal to **0,25 kg** for each connecting rod and an indicative material cost equal to **3 €/kg**, we get:

$$C_{material} = 0,25 \cdot 3 = 0,75 \text{ €/piece}$$

For 1000 pieces:

$$C_{materials, everything} = 0,75 \cdot 1000 = 750 \text{ €}$$

We also consider an hourly labor cost equal to **25 €/h**

$$C_{labor} = 575 \cdot 25 = 14.375 \text{ €}$$

The cost of using the press and equipment is estimated to be **35 €/h**:

$$C_{machine} = 575 \cdot 35 = 20.125 \text{ €}$$

The cost of hot stamping dies is estimated to be **8000 €** Since the production batch is 1000 pieces, the cost of the die per single component is:

$$C_{matrix/piece} = \frac{8000}{1000} = 8 \text{ €/piece}$$

The total cost of the lot is therefore:

$$C_{tot} = 750 + 14375 + 20.125 + 8000 = 43.250 \text{ € and then } 43,25 \text{ €/piece}$$

The resulting estimate is indicative, but it allows us to estimate the order of magnitude of the component's production cost. The unit cost could decrease with larger production batches, since the cost of the dies would be spread across a greater number of pieces.

7. INTRODUCTION OF THE COMPONENT: CAP (N.10)

7.1 Description of the piece

The cap is the component that closes the engine block at the front and allows for the support and correct positioning of the crankshaft. Furthermore, through the holes in the external flange, it allows for attachment to the engine block using screws and nuts.

From a geometric point of view, the component consists of an external circular flange, a central hub and a series of radial ribs that connect the two parts, ensuring adequate structural rigidity while keeping the overall weight of the piece low.

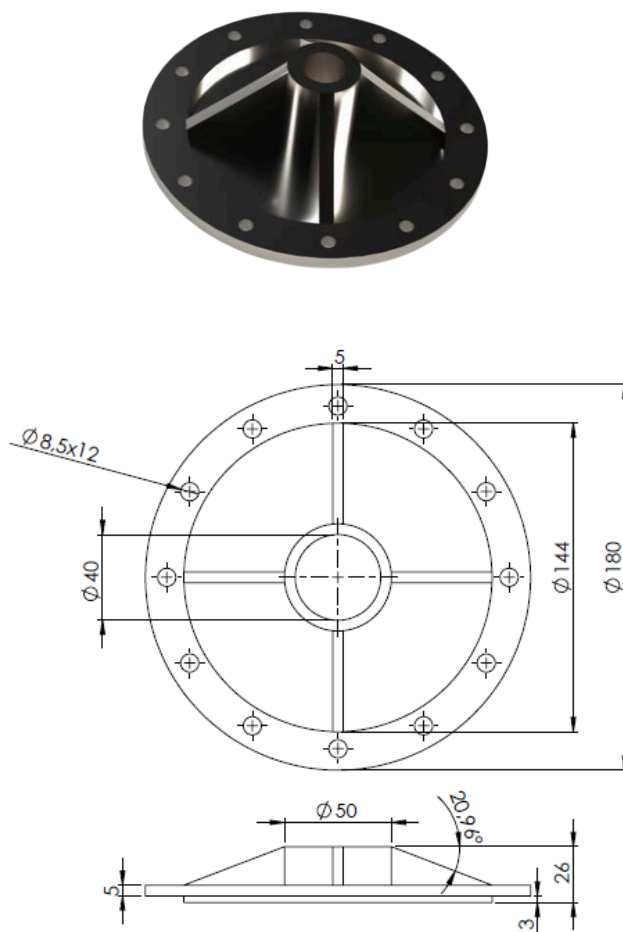


(Fig. 33)

In the original assembly, the cap was modeled as a single component. However, since welding was one of the required processes for the project, and none of the assembly's components naturally require a welded joint, it was decided to adopt an alternative construction configuration for the cap.

In particular, the component is hypothetically divided into three distinct elements:

- an external annular flange;
- a basic disk;
- a central hub complete with connecting ribs.

The three elements are then assembled by welding, obtaining a final component that is geometrically equivalent to the one present in the initial assembly.

This solution allows you to study and apply the welding process required by the project without altering the mechanical function of the component inside the engine.

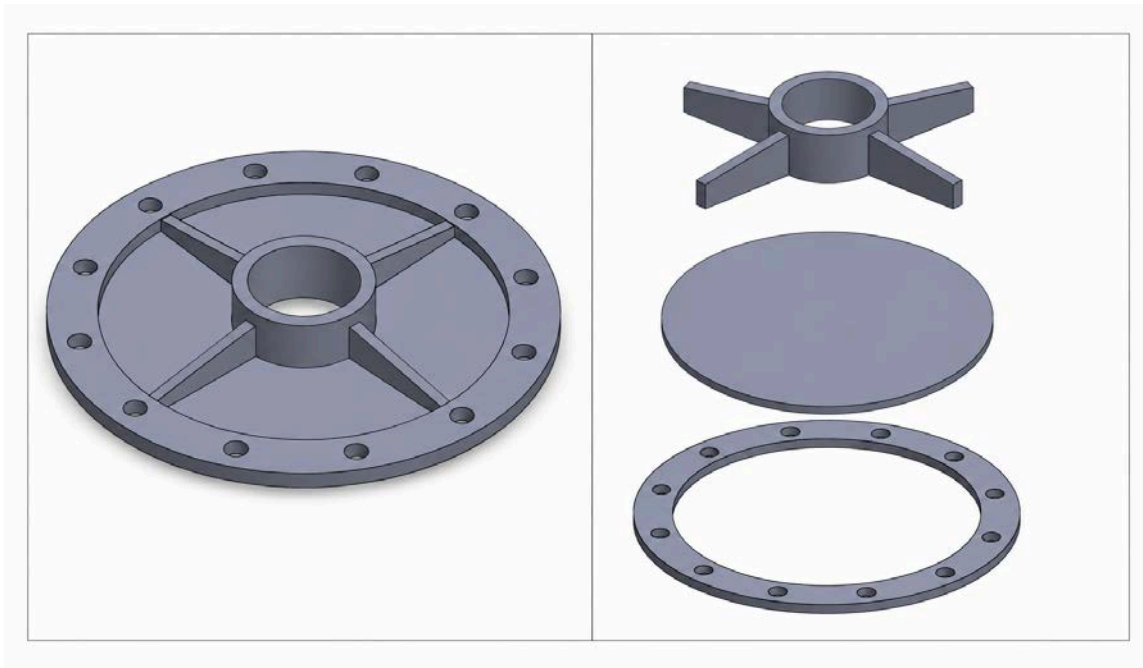


[Fig. 34] Final component and diagram of the subdivision of the cap into the parts to be assembled by welding.

7.2 Choice of processing technique

Welding was chosen to produce the cap. In the original model, the component is made of a single piece; however, for the purposes of studying the production process, it was considered dividing it into multiple parts, subsequently assembled using welded joints.

The adopted configuration involves the separate production of the external flange, the base disk, and the assembly consisting of the central hub and the four stiffening ribs. Once the individual elements are obtained, they are assembled by welding to obtain the final component.

Among the main welding processes available, we considered: coated metal arc welding (SMAW), MIG/MAG welding, brazing, and TIG welding. To identify the most suitable technique, the following comparison was performed.

Processes	Advantages	Disadvantages	Assessment
Coated electrode welding (SMAW)	The process is economical and simple to perform. Inexpensive equipment.	Lower bead quality, presence of slag to be removed, lower precision for small components	Not chosen because it does not guarantee the required precision.
MIG/MAG welding	High execution speed, good productivity and ease of automation.	Higher heat input and greater risk of deformations on small components.	Not chosen because it prioritizes productivity over precision.
TIG welding	High bead quality, excellent control of the weld pool, reduced deformations and high precision.	Longer execution times than MIG/MAG and slightly higher costs.	Most suitable process to obtain a precise, resistant and reliable joint.

After comparing the main welding processes, the final choice fell on **TIG welding**, as it guarantees the best compromise between joint quality, dimensional precision and mechanical resistance.

The process uses an infusible tungsten electrode and an inert gas, usually argon, which shields the weld pool from the surrounding atmosphere. This results in clean, oxidation-free weld seams with excellent mechanical characteristics.

The use of TIG technology also ensures better control of the heat input, reducing the risk of deformations and allowing the dimensional tolerances required by the component to be maintained.

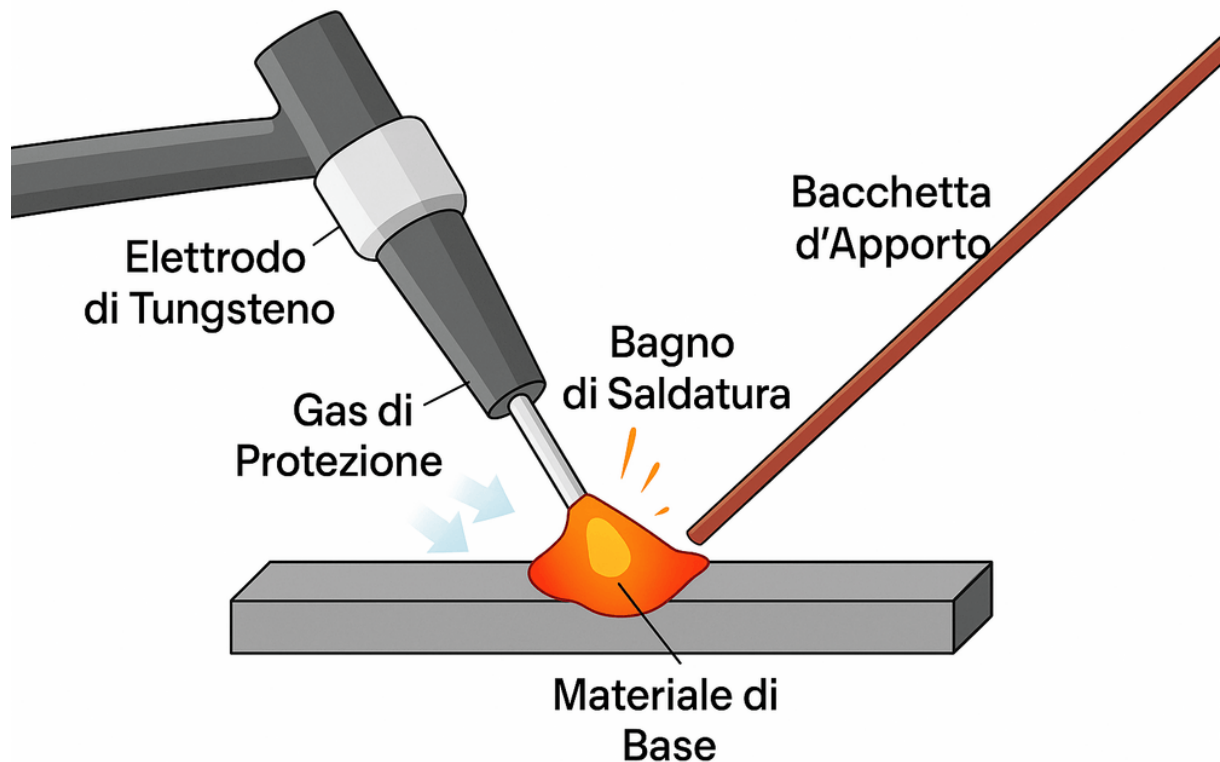


[Fig. 35] Schematic representation of the TIG welding process adopted for the assembly of the cap.

7.3 Choosing the machine

For the execution of the welding operations a **TIG (Tungsten Inert Gas) welding machine in direct current (DC)**, particularly suitable for the creation of high-quality joints on small-sized components with relatively complex geometries.

The TIG process generates an electric arc between a non-consumable tungsten electrode and the base metal. During the process, the weld area is protected by a flow of inert gas, usually argon, which prevents the weld pool from coming into contact with the outside atmosphere, preventing oxidation and contamination.

The choice of this machine is motivated by the need to obtain precise and clean joints between the different parts that make up the cap, limiting thermal deformations to a minimum and ensuring a good surface finish of the final component.

The main features of the TIG welder are:

- high stability of the electric arc;
- excellent control of heat input;
- high quality of the welding bead;
- reduced splash formation;
- possibility of welding small thickness components;
- good precision in making joints.

The use of TIG technology is therefore particularly suitable for the assembly of the cap, allowing for the production of a final component with adequate mechanical and dimensional characteristics.



[Fig. 36] Example of a direct current TIG welder used to create the joints between the parts making up the cap.

7.4 Welding parameters

After selecting the TIG process and the corresponding machine, it is necessary to define the main operating parameters that influence the quality of the joint. The choice of these parameters depends on the material to be welded, the thickness of the components, and the mechanical characteristics required of the final piece.

In the case of the cap, since it is made up of elements of relatively small dimensions and limited thicknesses, it is advisable to use moderate current values, in order to limit thermal deformations and ensure correct execution of the welding.

The parameters adopted for the process are shown in the following table.

Parameter	Value
Welding process	TIG (GTAW)
Base material	42CrMo4 steel
Current type	Continued (DC)
Polarity	DCEN (negative electrode)
Shielding gas	Pure Argon
Gas flow rate	8 - 10 l/min
Filler material	ER80S-D2
Tungsten electrode diameter	1,6 mm
Current intensity	70 - 90 A
Arc voltage	10 -14V
Feed rate	80 – 120 mm/min

The use of argon as a shielding gas allows the weld pool to be isolated from the surrounding atmosphere, preventing oxidation and ensuring better metallurgical quality of the joint. Polarity DCEN (*Direct Current Electrode Negative*) is the most used in welding steels because it allows a greater concentration of heat on the piece, ensuring good penetration of the bead.

The choice of the above parameters allows for a stable and high-quality weld, reducing the risk of defects such as porosity, inclusions or deformations and guaranteeing the required mechanical characteristics of the final component.

7.5 Processing phases

To produce the cap using TIG welding, it is necessary to follow a precise sequence of operations that guarantees the correct assembly of the various parts and the final quality of the joints.

The main processing stages are described below.

1. Production of individual components

In the first phase, the three elements that make up the cap are produced separately: the external annular flange, the base disc and the group composed of the central hub and the four stiffening ribs.

2. Surface preparation

The surfaces to be welded are carefully cleaned to eliminate any traces of oxide, grease, oil or other impurities that could compromise the quality of the joint.

3. Positioning and locking

The three components are positioned using special assembly equipment and then locked to ensure correct alignment during welding.

4. Preliminary pointing

Before the final welding, some localized tack welding is performed to keep the various elements in position and avoid movements due to thermal expansion.

5. Performing TIG welding

We then proceed to create the welding seams along the contact surfaces between the base disc, the external flange and the hub-rib group, until the complete component is obtained.

6. Component cooling

Once the process is complete, the piece is left to gradually cool to room temperature, limiting the formation of residual stresses and unwanted deformations.

7. Final inspection

The final phase consists of a visual inspection of the weld seams and a dimensional check of the component, verifying the absence of surface defects and compliance with the dimensions required by the project.

7.6 Production times and costs

7.6.1 Processing times

To estimate the time required to produce the cap using TIG welding, all the main operations of the production process were considered, from the preparation of the components to the final inspection of the assembled piece.

In particular, the time required for positioning and clamping the parts, preliminary spot welding, execution of the welding seams, cooling of the component and final checks were taken into account.

It is estimated that the average time required to complete a cap is approximately **12 minutes**.

Considering a production of **1000 pieces**, the total processing time is:

$$T_{tot} = 1000 \cdot 12 = 12.000 \text{ min} = 200 \text{ h}$$

Therefore, for the production of the entire batch approximately **200 hours of work**.

7.6.2 Processing costs

For the calculation of costs, an hourly cost of the specialized operator equal to **25 €/h** and an hourly cost of the TIG welder, including energy consumption and ordinary maintenance, equal to **15 €/h**.

The overall hourly cost of the process is therefore:

$$C_h = 25 + 15 = 40 \text{ €/h}$$

Multiplying this value by the total processing time previously calculated, we obtain the overall production cost:

$$C_{tot} = 200 \cdot 40 = 8000 \text{ €}$$

The unit cost of processing is therefore equal to:

$$C_u = \frac{8000}{1000} = 8 \text{ €/piece}$$

The resulting cost is compatible with medium-scale production and justified by the quality of the TIG welding joint. This process allows for the creation of a component with good mechanical characteristics, high dimensional precision, and reduced thermal deformation, ensuring the cap's proper functioning within the assembly.

